



SCUOLA INTERNAZIONALE SUPERIORE DI STUDI AVANZATI
INTERNATIONAL SCHOOL FOR ADVANCED STUDIES
Elementary Particle Theory Sector
Statistical Physics Curriculum

Phase transitions on heterogeneous random graphs: some case studies

Thesis submitted for the degree of
Doctor Philosophiæ

ADVISOR:
Prof. Matteo Marsili

CANDIDATE:
Daniele De Martino

30th September 2010

Contents

Introduction	v
1 Statistical mechanics of queuing networks	1
1.1 The Internet	1
1.2 Models of network traffic dynamics	4
1.2.1 queuing network theory	4
1.2.2 The congestion phase transition	6
1.3 Statistical mechanics of congestion	7
1.3.1 Network Ensemble calculations and results	11
1.3.2 Conclusions	19
2 Dynamical arrest on disordered structures	21
2.1 Main experimental features of the glass transition	22
2.1.1 Other-than-molecular glass formers	25
2.2 Theoretical views on the glass transition	27
2.2.1 The Frederickson-Andersen model	28
2.3 The heterogeneous FA model	32
2.3.1 Conclusions	38
3 Inverse phase transitions on heterogeneous graphs	39
3.1 Experimental inverse transitions	39
3.2 A simple model for inverse phase transition	41
3.3 Topology-induced inverse phase transition	43
3.4 Conclusions	48
4 Volatility and evolution of social networks	53
4.1 Complex social networks	53
4.2 Models of co-evolving networks	56
4.3 Node-based volatility	59
4.3.1 $\alpha > 1$: The symmetric solution	62
4.3.2 $\alpha < 1$: The asymmetric solution	63
4.3.3 The critical region: $\alpha \approx 1$	66
4.3.4 Conclusions	67

Introduction

It is possible to say that the research in statistical mechanics is in an historical phase akin to that one in quantum mechanics at the beginning of the last century[1]. There is a lot to be studied and discovered, both in fundamentals and in applications. One fundamental point is in fact the range of application of the theory itself. Methods and concepts from statistical mechanics are starting to be currently used in scientific fields as different as e.g. biology[2], economy[3], information theory[4] and traffic engineering[5]. Statistical mechanics, in fact, naturally proposes itself as a general framework to connect microscopic mechanisms and macroscopic collective behaviors. In condensed matter physics, quantitative physical laws can be seen as emerging out of a statistical description of the dynamics of the microscopic units that form the system, or even out of that one of a simpler, coarse grained version of it. Nowadays, simple lattice models are widely used to gain a qualitative and often deeper understanding of physical phenomena.

However, when a statistical mechanics perspective is adopted in fields different from physics, an interesting point comes out. In many contexts, the structure of the interactions among the microscopic units can be often heterogeneous nor embedded in a real dimensional space, and moreover, it can evolve in time. Thanks to the recent development of the numerical calculus power and of the memory resources in information technology, recent analysis show that the topology of graphs as different as social networks (friendship patterns, scientific collaboration networks, etc.) food webs in ecology, critical infrastructure like the Internet and so on, is truly heterogeneous and very complex (see [6] and ref. therein). If the analysis of the structure of such complex networks requires statistical methods, the study of the dynamical processes occurring *on* them can get useful insights from statistical mechanics[7].

A good example is provided by the study of epidemic models in heterogeneous networks[8]. The real networks on which these processes are taking place are in fact very heterogeneous, i.e. they are *scale free*. The dynamics of these processes in heterogeneous graphs can be ruled by the tails of the degree distribution. They can be in practice always in the infectuous phase and this is true e.g. for the spreading of viruses in large scale informatic systems. Interestingly, the paradigmatic Ising model has a dependence of this kind on the heterogeneity of the graph[9].

The general study of how the underlying topology affects the collective statis-

tical behavior of model systems is at the core of research in statistical mechanics. However, up to recent times this study was almost limited to homogeneous, or at least symmetrical structures of interactions, typically d -dimensional or bethe lattices. The heterogeneity calls at identifying general mechanisms and unifying schemes in the dynamics of cooperative models on general heterogeneous graphs, since they can show truly different behaviors with respect to regular lattices. The focus of this thesis is about statistical mechanics on heterogeneous random graphs, i.e. how such heterogeneity can affect the cooperative behavior of model systems, but it is not intended as a general review on it. Rather, I will show more practically how this question emerges naturally and can give new insights for specific instances, in both physics and interdisciplinary applications, for equilibrium and out of equilibrium issues as well.

The first chapter is devoted to the study of the congestion phenomena in networked queuing systems, like sub-networks of the Internet. After a brief introduction on the workings of the Internet, we will review the classic results of the queuing network theory, and the recent numerical results on congestion phenomena on complex networks. Then, I will show how to combine them within a minimal model that in practice extends queuing network theory in the congested regime[14]. With the use of network ensemble calculation techniques, it is possible to study the dependence of the traffic dynamics on the topology of the graph and on the level of traffic control as well, up to the possibility of drawing a mean field phase diagram of the system. We find many results. In particular, we find that traffic control is useful only if the network has a certain degree of heterogeneity, but, in any case, it can trigger congestion in a discontinuous way. Then, the second chapter is about the nature of the dynamical crossover in glass forming systems. After a brief review on the experimental phenomenology of the glass transition, we will do a short review on the theoretical perspectives on it. Then, I will show, within the framework of a simple facilitated spin model, how the question of the heterogeneity of the underlying spatial structure is crucial[53]. The dynamical arrest can change from a bootstrap percolation scenario to a simple one considering an heterogeneous lattice (e.g. diluted). This helps to shed lights on analogies and differences between the jamming of supercooled liquids and more heterogeneous systems, like polymer blends or confined fluids. The third chapter is on a general relationship between models and the underlying topology: how some specific features of the graph can induce inverse phase transitions in tricritical model systems. After a brief review on inverse phase transitions, we will discuss the simplest model that reproduces this behavior, i.e. the Blume-Capel model with high degeneracy of the interacting states. I will show that tricritical model systems have this behavior if sparse subgraphs are crucial for the connectivity[70]. Within this framework, I will work out many results for the Blume-Capel model and give some insights about the fact that the random field ising model shares the same phenomenology. Finally, the subject of the fourth chapter is on the co-evolving models of social networks. We will give a brief introduction to the field of social networks. The interesting point is that here the graph itself is subject to a dynamical evolution that can lead in turn to different states, with different connectivity properties.

The evolution of the network can be coupled to the dynamics defined on top of it, i.e. a so called co-evolution mechanism. I will show how the volatility, i.e. the rate at which nodes and/or links disappears, affects this evolution with a simple model[91]. Many results are found, in particular high node volatility can definitively suppress the emergence of an ordered, connected phase.

In the conclusions there is a review of the results and I will point out a general insight about the statical mechanics of models on heterogenous random graphs, supported by specific examples took out from the cases we dealt with.

Chapter 1

Statistical mechanics of queuing networks

The Internet[10] is perhaps the most complex engineering system created in the human history. Its exponential growth has played a pivotal role in the recent surge of interest in the study of complex networks. It is not a static system, rather it evolves according to a self-organized and decentralized dynamics. The structure[11] and the properties of traffic dynamics[12] it supports show a very rich phenomenology. The basic theory to analyze traffic dynamics of information processing networks, queuing network theory, relies on the simplifying hypothesis of stationarity. This theory is mainly used to investigate single cases of small systems whose structure does not change. Statistical mechanics can extend this theory, allowing the investigation of congested states and the general study of the effects of topology and of traffic control on the traffic dynamics. In this chapter, after a brief introduction on the structure and traffic dynamics of the Internet, I will review the main results of queuing network theory[13] and the recent results in congestion phenomena on complex networks(see table 6 in[12]). Then, in the final paragraph, I will show how to combine them together within the framework of a minimal model, that allows the study of congestion in queuing network systems up to the possibility of drawing mean-field phase diagrams[14]. We find many general results, both theoretical, e.g. I will show analitically the presence of a dynamical phase transition in queuing networks , and of practical importance, e.g. I will show that traffic control is useful only in heterogeneous networks.

1.1 The Internet

The Internet was originally conceived for experimental reasons within a military project in the '60 of the last century. This network of networks of computers

has nowadays a worldwide extension, connecting hundreds of millions of *hosts*¹, through which users can communicate in real time, sell and buy goods, exchange and share music, videos, informations, etc. The handling of the information flows is the result of a complex interplay of different rules, protocols and devices acting at different levels. These levels go from the physical one (the transport of electrical signals along wires or optical fibers) to that one of applications (e.g. the standard SMTP protocol to forward e-mail), usually without common standards all along the network.

The Internet is a network of networks: hosts are joined together by *switches* in LAN (local area network) or WAN (wide area network), and the exchange of information among these networks is provided by specific devices called *routers*, forming a network that represents the physical connectivity of the Internet. Routers are themselves grouped together in *autonomous systems* (AS), i.e. independently administered domains. The traffic at the network (routers) level is ruled by the TCP/IP (transmission-control protocol/Internet protocol), perhaps the only common standard protocol in the Internet:

- The information is framed in discrete units, called IP *packets*. The packet has a part devoted to the addresses of source and destination. There is a common address space for all the network.
- All the packets are routed independently by the routers. Each router has a list of paths, i.e. a kind of coarse-grained map of the network. It sends packets to its neighbors along the shortest path.
- Routers exchange continuously informations on the topology of the network, signaling damages, outages, etc.
- Each single transmission between neighbouring routers is ruled by the TCP protocol through the exchange of check and confirmation signals (ACK acknowledgements signals). A delay of ACK signals induces an halving of the packets' sending rate along that line of transmission (window-based congestion control mechanism).

The overall structure, at each level, is self-organized and evolving. The network of routers changes continuously, the nodes and the links being removed or added according to the reasons (mainly of economical nature) of single *providers* and not by a central authority. Therefore, it is hard to monitor the topology of such a graph, that is still partially unknown.

Fig.1.1 shows the degree distribution of a sub-network of the Internet monitored within the CAIDA project[15]. The curve is well fitted by a power-law with an exponent between 2 and 3. For a power law distribution $P(x) \propto x^{-\gamma}$, we have $\frac{d \log P(x)}{d(\log x)} \propto -\gamma$, independently of y , and moreover, if $\gamma < 3$ the error on $\langle x \rangle$ is not defined. The networks with a power law degree distribution with an exponent $\gamma < 3$ are thus called *scale free*. Dynamical processes defined on

¹An host is a device connected to the Internet, with its own address, that can inter-operate with other hosts

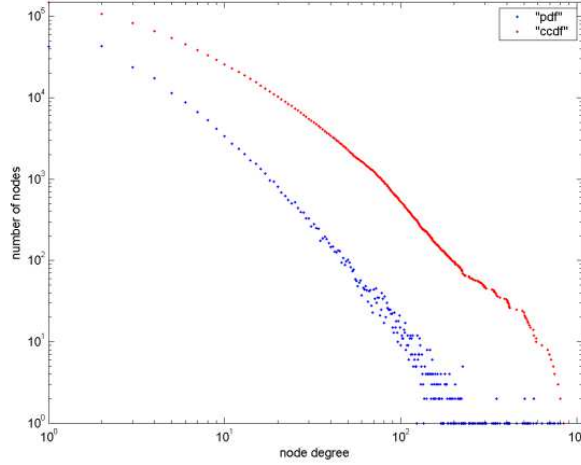


Figure 1.1: Degree distribution and complementary cumulative distribution of a subnetwork of the Internet at routers level monitored within the CAIDA project[15]

them can show qualitative change with respect to homogeneous networks[7], as we will point out later in this chapter about congestion phenomena. It seems that the scale-free degree distribution characterizes the Internet graphs at many scales, from the routers to the AS level[11]. This finding has attracted many research efforts on the Internet structure[16].

There are few stylized facts about traffic dynamics, the main being the *self-similarity* of inter-arrival time signals[17]. Looking at the temporal evolution $y(t)$ of the time spent by a signal to travel along a given path in the network under controlled conditions it is found that the self correlation function

$$C(\tau) = \frac{\langle (y(t)y(t+\tau)) \rangle - \langle y \rangle^2}{\langle y^2 \rangle - \langle y \rangle^2} : \quad (1.1)$$

- is unsummable $\sum_i |C(i)| \rightarrow \infty$
- and has a power-law tail $C(\tau) \propto \tau^{-\nu}$.

Moreover:

- The scaling of the variance of the coarse-grained signal over intervals M times larger $y_M(t) = \frac{1}{M} \sum_{i=t-M}^{t+M} y(i)$ is not normal, i.e. $\sigma_M^2 = \frac{\sigma^2}{M^\beta}$

There are many different ways to define and measure these features. They seem to be independent of the path, the time of measure and the level of traffic. There are many ways to interpret them. The robustness of these features

has attracted several modeling efforts to interpret it as a signature of the fact that the network is working at criticality between a free and a congested phase through a self-organized mechanism of some kind, as we shall see in the next paragraph. But self-similarity is even too robust for this mechanism at work: it is still present even for low level of traffic load, far out from the congested regime. Therefore, the most accepted explanation for the self-similarity of inter arrival times signals relies on the heterogeneity and strong correlation in time of the demand itself[18]. In fact, many packets can belong to the same request, with a distribution of the flows' size ² that is heterogeneous itself.

Apart from this, even if this network mostly works in the free regime, time delays and packets' loss continue to threaten Internet practitioners, because some parts of the network can be sometimes in the congested regime. However, congestion events are difficult to monitor and study, and a clear phenomenological picture is still missing. This calls for a theoretical understanding of what happens above the threshold at which a queuing network system can work.

1.2 Models of network traffic dynamics

1.2.1 queuing network theory

The classical framework used to study performances of information processing and/or service delivering networked systems is queuing network theory (QNT)[13]. Its applications range from the study of costumers forming queues in banks and offices, to the study of data traffic in packet switching networks of routers in communication systems.

The main model is the Jackson or open queuing network[19], consisting of N nodes such that:

- each node i is endowed with a FIFO (first-in first out) queue with unlimited waiting places (it can be arbitrary long).
- The delivery of a packet from the front of i follows a poisson process with a certain frequency r_i (service rates), and
 - the packet exits the network with some probability μ_i , or
 - it goes on the “back” of another queue j with probability q_{ij} .
- Packets are injected in each queue i from external sources by a Poisson stream with intensity p_i .

The state of the system is specified by the vector $\mathbf{n} = (n_1, \dots, n_N)$, where n_i is the i 's queue length. If we indicate with \mathbf{i} the vector with all components equal to zero, apart from the i^{th} that is equal to one, we have the expressions

²A flow is a group of packets within the same request

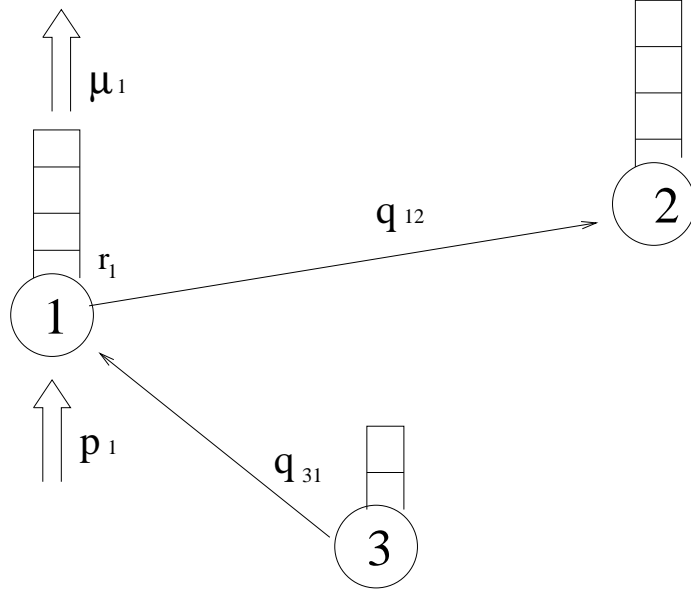


Figure 1.2: queuing network: p_i creation rates, r_i service rates, μ_i absorbing rates, q_{ij} routing probabilities

for the transition rates³:

$$W(\mathbf{n} \rightarrow \mathbf{n} + \mathbf{i}) = p_i \quad (1.2)$$

$$W(\mathbf{n} \rightarrow \mathbf{n} - \mathbf{i}) = r_i \mu_i \quad (1.3)$$

$$W(\mathbf{n} \rightarrow \mathbf{n} - \mathbf{i} + \mathbf{j}) = r_i (1 - \mu_i) q_{ij}. \quad (1.4)$$

The master equation for the probability distribution of states $P(\mathbf{n})$ reads:

$$\dot{P}(\mathbf{n}) = \sum_{\mathbf{n}'} W(\mathbf{n}' \rightarrow \mathbf{n}) P(\mathbf{n}') - \sum_{\mathbf{n}'} W(\mathbf{n} \rightarrow \mathbf{n}') P(\mathbf{n}). \quad (1.5)$$

QNT studies the stationary state, assuming it exists: $\dot{P} = 0$. How we see next, the probability distribution factorizes $P(\mathbf{n}) = \prod_i p_i(n_i)$. By using this form of the distribution as an ansatz to solve the master equation, we find:

$$p_i(n) = (1 - x_i) x_i^n, \quad (1.6)$$

where $x_i = \lambda_i / r_i$. Here the coefficients λ_i , the average packet flow towards node i , can be found on specific networks solving the set of linear equations:

$$\lambda_i = p_i + \sum_j q_{ji} (1 - \mu_j) \lambda_j. \quad (1.7)$$

³In the second and third equations $n_i > 0$

The framework of QNT can easily accomodate modifications. For instance, it is possible to think of finite size capacity for the queues, queue length state dependent service rates and/or transition probabilities. It is possible to study closed instances, with a given number of packets K that are not generated neither absorbed. QNT has many practical applications in very different contexts, from telecommunications networks to the scheduling design of factories, hospitals, ecc, and, moreover, it can give interesting insights to theoretical research.

For instance, there was a recent debate[21] about the scaling of fluctuations of the Internet time series. Looking at the time series of the amount of bytes $x(t)$ processed by a router, it is found that $\sigma \propto \langle x \rangle^\gamma$, with $1/2 < \gamma < 1$, depending on the aggregation time, and/or crossover between these limits. This can find a nice and natural explanation within QNT. In fact, if x follows an exponential distribution, as is the case for most of the queuing networks, it is $\sigma^2 = \langle x \rangle + \langle x \rangle^2$, and $\langle x \rangle$ can vary by aggregating times, mimicking exponents between $1/2$ and 1 .

The main limitation of this theory is in the stationarity assumption. It gives for guaranteed that, given a certain external demand $\mathbf{p} = (p_1, \dots, p_N)$, we are always able to build a network such that $\lambda_i < r_i$. It basically avoids completely the study of *congested* states, in which queues can grow out of stationarity. It should be noticed that in self-organized evolving networks, like the Internet, the external demand may change on times faster than our capacity to modify the network to maintain stationarity. This can trigger *congestion phenomena*, that are interesting to study from a theoretical point of view.

1.2.2 The congestion phase transition

Apart from this theory, the recent years have witnessed the proposal of several models of interacting particles hopping on graphs, to study the interplay of topology and routing strategy on the performances of networked systems in processing information (see table 6 in[12]).

In all these models packets are injected into the network with some rate P , they have to travel between given sources and destinations, where they exit the network, and they interact by forming queues. Can all the packets reach their destinations, or, alternatively, can the network process all the incoming information (quantified by P)? If it can do it, the total number of packets $N(t)$ will be stationary in time, if it cannot, $N(t)$ will be growing in time. A good parameter to distinguish these two different phases is the average queues' growth rate divided by the average rate of incoming packets, i.e. the percentage of packets trapped in queues[22]:

$$\rho = \frac{\langle \dot{N} \rangle}{P}. \quad (1.8)$$

By studying the curves $\rho(P)$, once the network and the routing strategy are given, it is possible to distinguish two phases: $\rho = 0$ (free flow) and $\rho > 0$ (congestion), clearly divided by a point P_c . Upon approaching this point from

the free phase, the self-correlation in time of the queues' length starts to develop fat tails. This was seen as an elegant explanation of the self-similar character of real time series. However, as it was previously stated, self-similarity in a real network is present even far out of the congested regime. Anyway, all these works show the inherent presence in queuing networks of a dynamical phase transition towards congestion.

The numerical investigation of the dependence of such a transition on the structure of the graph and on the routing strategy, shows interesting phenomena. One of the most interesting is the apparent *tricritical* character of the congestion transition in queuing network systems. In [23] the authors propose the following model: onto a given network, packets arrive from external source with rate P on random nodes, each packet has its destination d , and it hops from the current node i to the neighbor j such that the quantity:

$$w_j = d_{jd}h + n_j(1 - h), \quad (1.9)$$

is minimum. There d_{jd} is the distance between j and d , n_j is the number of packets sitting on j , h is a parameter that quantifies the level of congestion control ($h = 1$, no congestion control, shortest path routing). This mimick an attempt to minimize travelling times instead of distances with the use of local information. The authors did simulations on a realistic instance, i.e. the Internet network at autonomous system level. They found that a certain level of traffic control can avoid the transition up to a certain point, after which congestion is triggered in a discontinuous way, i.e. upon decreasing h , P_c is growing, but exactly at P_c , ρ jumps from 0 to a finite value (see fig.1.3).

This approach to network traffic based on the dynamics of individual particles has the problem of not being amenable to analytic approaches. These models become analitically tractable considering a randomization of the trajectories. The reach of a destination by a particle should be mimicked in a probabilistic way, i.e. during the hoppings the particle can be absorbed with some probability. This defines a framework very similar to the QNT, that I will analize in detail in the next paragraph.

1.3 Statistical mechanics of congestion

I will review the model in ref.[14]. It consists of particles hopping randomly among the nodes of a graph such that:

- They form queues,
- They are created with a certain rate.
- They have a certain probability of being absorbed during the hoppings.

Then we will mimick a protocol of congestion control in the following way:

- The node j starts to reject particles with probability $\bar{\eta}$ once its queue is longer than n^* .

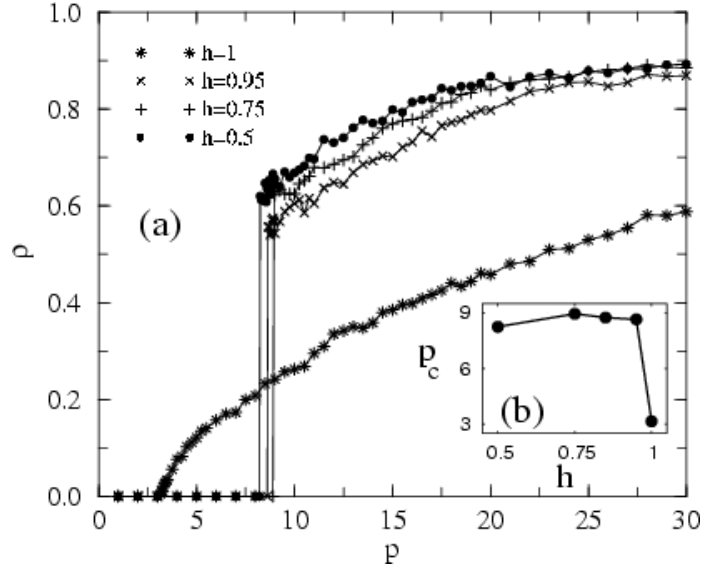


Figure 1.3: Congestion parameter curves $\rho(P)$ from simulations of a particle hopping model on the Internet at level of AS graph, from [23].

This model of particles corresponds to a queueing network such that:

- The hopping probability from node i to node j is $q_{ij} = \frac{1-\bar{\eta}\theta(n_j-n^*)}{k_i} a_{ij}$ ⁴
- A certain set of values r_i, p_i, μ_i for the service rate, demand and adsorbing probability of the node i , respectively, is given.

Here a_{ij} is the adjacency matrix of the graph⁵ and k_i the degree of the node i . The important difference from the Jackson framework is that packets have to *move* to be absorbed. They are absorbed during the hoppings and not when they are stored in the queues. Within this new framework, it is possible to extend QNT beyond stationarity. There are two phases (see fig.1.4): as the demand increases the system pass from a free phase, in which the number of particles is stationary, to a congested phase, where it is growing.

There is a phase transition between them, whose nature depends on the topology of the graph and on the level of traffic control. This is shown in fig.1.5, which reports simulations on homogeneous and heterogeneous graphs, with low and high level of traffic control. The curves $\rho(p)$ suggest that an high level of traffic control trigger the transition in a discontinuous way and can displace the transition point to higher values of p only in the heterogeneous case.

In order to study the generality of such results, I will exploit the QNT formalism, combined with the use of techniques from statistical mechanics. The

⁴ $\theta(x)$ is the step function, i.e. it is 1 for $x \geq 0$, 0 otherwise

⁵ a_{ij} is 1 if i and j are connected by a link, 0 otherwise

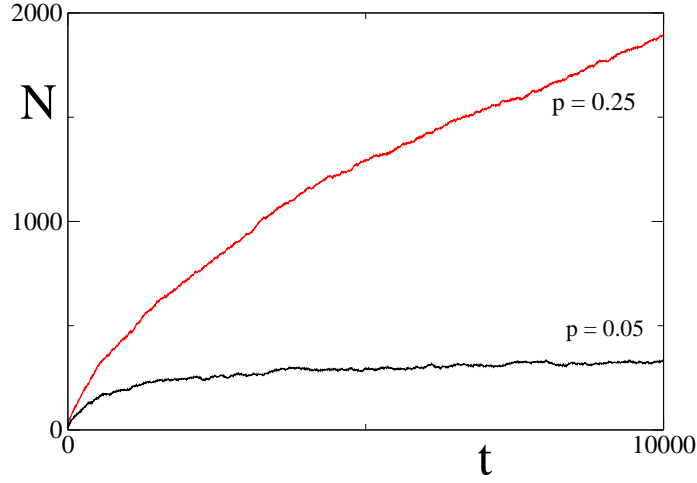


Figure 1.4: Number of packets as a function of time for an homogeneous network of 10^3 nodes, degree $K = 4$, without routing procol ($\bar{\eta} = 0$), with homogeneous condition $r_i = 1$, $\mu_i = \mu = 0.2$, in the free ($p_i = p = 0.05$) and congested phase ($p = 0.25$).

transition rates are:

$$W(\mathbf{n} \rightarrow \mathbf{n} + \mathbf{i}) = p_i \quad (1.10)$$

$$W(\mathbf{n} \rightarrow \mathbf{n} - \mathbf{i}) = r_i \sum_j \frac{\mu_j (1 - \bar{\eta} \theta(n_j))}{k_i} a_{ij} \quad (1.11)$$

$$W(\mathbf{n} \rightarrow \mathbf{n} - \mathbf{i} + \mathbf{j}) = \frac{r_i (1 - \mu_j) (1 - \bar{\eta} \theta(n_j))}{k_i} a_{ij}. \quad (1.12)$$

We work with the approximation of a factorized form for the probability distribution function $P(\mathbf{n}) \simeq \prod_i p_i(n_i)$ ⁶.

Imposing detailed balance $p_i(n_i)W(n_i \rightarrow n_i + 1) = p_i(n_i + 1)W(n_i + 1 \rightarrow n_i)$, we can express the single point distributions $p_i(n_i)$ in terms of the the two local quantities $q_i = p_i(0)$ and $\chi_i = \text{Prob}(n_i \geq n^*)$. We have

$$W(n_i \rightarrow n_i + 1) = p_i + (1 - \mu_i) \sum_j r_j q_j \frac{1 - \bar{\eta} \theta(n_i - n^*)}{k_j} a_{ij} \quad (1.13)$$

$$W(n_i + 1 \rightarrow n_i) = \frac{r_i}{k_i} \sum_j (1 - \bar{\eta} \chi_j) a_{ij}. \quad (1.14)$$

⁶It works exactly for $\bar{\eta} = 0$ because this is equivalent to the Jackson network. See appendices in the second reference of ref.[14] for a discussion about the extension of its validity.

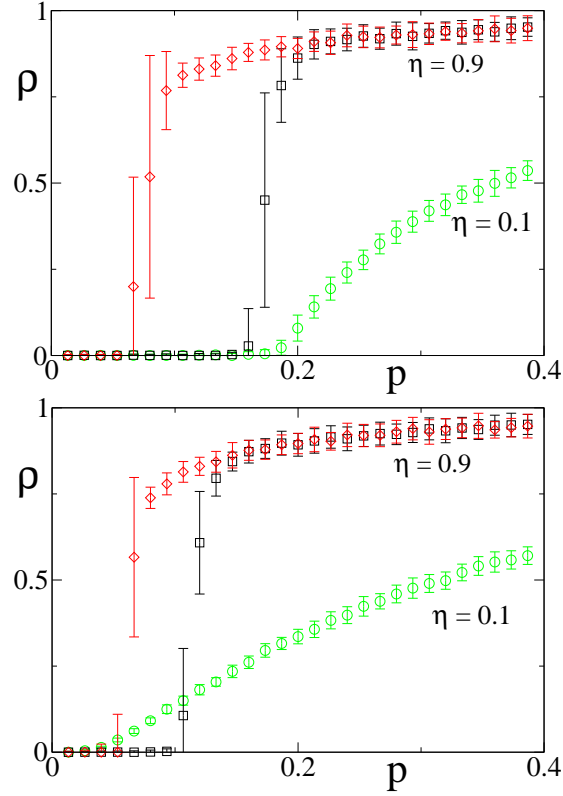


Figure 1.5: Top: Transition curves $\rho(p)$ for a random regular graph of size $N = 10^4$, $\mu = 0.2$, $\bar{\eta} = 0.1$, $\bar{\eta} = 0.9$. Bottom: Transition curves $\rho(p)$ for an uncorrelated scale free graph with $\gamma = 3$, $k_{min} = 2$ of $N = 3 \cdot 10^3$ nodes, $\mu = 0.2$, $\bar{\eta} = 0.1$, $\bar{\eta} = 0.9$ for $n^* = 10$. For $\eta = 0.9$ the system shows *hysteresis* in both the homogeneous and heterogeneous case.

Then, the average growth of the queue length of node i is:

$$\langle \dot{n}_i \rangle = p_i + (1 - \mu_i)(1 - \bar{\eta}\chi_i) \sum_j a_{ij} \frac{r_j(1 - q_j)}{k_j} - \frac{(1 - q_i)r_i}{k_i} \sum_j (1 - \bar{\eta}\chi_j) a_{ij}. \quad (1.15)$$

The equations for the q_i, χ_i come from:

- The normalization conditions $\sum_{n_i} p_i(n_i) = 1$.
- The stationarity of queues' length $\langle \dot{n}_i \rangle = 0$.

If the second condition gives not physical results, we have that $q_i = 0$, $\chi_i = 1$, from which we can calculate $\langle \dot{n}_i \rangle$. This can be summarized in terms of the linear

set of equations

$$\chi_i = \max\{0, \min[1, C_i(\vec{\chi}, \vec{q})]\} \quad (1.16)$$

$$q_i = \max\{0, \min[1, Q_i(\vec{\chi}, \vec{q})]\}, \quad (1.17)$$

where

$$Q_i(\vec{\chi}, \vec{q}) = 1 - \frac{p_i + (1 - \mu_i) \sum_j a_{ij} r_j (1 - q_j) / k_j}{p_i - r_i / k_i \sum_j a_{ij} \bar{\eta} \chi_j} \quad (1.18)$$

$$C_i(\vec{\chi}, \vec{q}) = \frac{1}{\bar{\eta}} \left[1 + \frac{p_i - r_i / k_i \sum_j a_{ij} \bar{\eta} \chi_j}{(1 - \mu_i) \sum_j a_{ij} r_j (1 - q_j) / k_j} \right]. \quad (1.19)$$

For sake of simplicity we consider from now on $p_i = p$, $r_i = 1$ and $\mu_i = \mu$.

1.3.1 Network Ensemble calculations and results

We consider an uncorrelated random graph with a given degree distribution $P(k)$. This is a graph taken from the ensemble of all the graphs with a given degree distribution, all with equal statistical weights. If we have N nodes $i = 1 \dots N$, it is possible to build a graph of this kind along these lines (configuration model[24]):

- We extract the degree k_i of each node i randomly according to the desired distribution $P(k)$.
- Each node i has k_i stubs dangling from it. We randomly match these stubs, taking care to avoid tadpoles and double links⁷.

A typical network of this ensemble has locally the structure of a tree, such that dynamical processes defined onto it can be successfully approximated with the use of mean field techniques. In particular, for our model, we will make the hypothesis that all the nodes with the same degree have the same statistical dynamical features.

The mean field rates for the queue length of a node with degree k are ⁸:

$$\begin{aligned} w_k(n \rightarrow n+1) &= p + (1 - \mu)(1 - \bar{q}) \frac{k}{z} (1 - \bar{\eta} \theta(n - n^*)) \\ w_k(n \rightarrow n-1) &= \theta(n)(1 - \bar{\chi}), \end{aligned} \quad (1.20)$$

where z is the average degree, $\bar{q} = \sum_k q_k P(k)$ and $\bar{\chi} = \sum_k \frac{k}{z} \chi_k P(k)$. The average queue length $\langle n_k \rangle$ follows the rate equation

$$\langle \dot{n}_k \rangle = p + (1 - \mu)(1 - \bar{q}) \frac{k}{z} (1 - \chi_k) - (1 - q_k)(1 - \bar{\chi}). \quad (1.21)$$

Note that summing over k and dividing by p we obtain a measure of the order parameter $\rho(p)$.

⁷This can introduce undesired correlation, see[24]

⁸We have absorbed for sake of simplicity the $\bar{\eta}$ in the definition of the χ

Since \dot{n}_k depends linearly on k , high degree nodes are more likely to be congested, therefore, for every p , there exists a real valued threshold $k^*(p)$ such that all nodes with $k > k^*$ are congested whereas nodes with degree less than k^* are not congested. Congested nodes ($k > k^*$) have $q_k = 0$ and $\chi_k = \bar{\eta}$. The probability distribution for the number of particles in the queue of free nodes with degree $k < k^*$ can be extracted by calculating the generating function $G_k(s) = \sum_n \mathcal{P}_k(n_k = n) s^n$ from the detailed balance condition $w_k(n_k + 1 \rightarrow n_k) \mathcal{P}_k(n_k + 1) = w(n_k \rightarrow n_k + 1) \mathcal{P}_k(n_k)$. The generating function takes the form

$$G_k(s) = q_k \left\{ \frac{1 - (a_k s)^{n^*}}{1 - a_k s} + \frac{(a_k s)^{n^*}}{1 - (a_k - b_k) s} \right\} \quad (1.22)$$

corresponding to a double exponential, where $a_k = [p + (1 - \mu) \frac{k}{z} (1 - \bar{q})] / [1 - \bar{\chi}]$ and $b_k = \bar{\eta} [(1 - \mu) \frac{k}{z} (1 - \bar{q})] / [1 - \bar{\chi}]$. From the normalization condition $G_k(1) = 1$ and the condition $\dot{n}_k = 0$, we get expressions for q_k , χ_k ,

$$q_k = \left[\frac{1 - a_k^{n^*}}{1 - a_k} + \frac{a_k^{n^*}}{1 - a_k + b_k} \right]^{-1} \quad (1.23)$$

$$\chi_k = 1 + \frac{p - (1 - q_k)(1 - \bar{\chi})}{(1 - \mu)(1 - \bar{q}) \frac{k}{z}} \quad (1.24)$$

and, finally, for \bar{q} , $\bar{\chi}$.

The value k^* is self-consistently determined imposing that nodes with $k = k^*$ are marginally stationary, i.e. $\dot{n}_{k^*} = 0$ with $q_{k^*} = 0$, $\chi_{k^*} = \bar{\eta}$, that translates into the equation

$$k^* = \frac{1 - p - \bar{\chi}}{(1 - \mu)(1 - \bar{\eta})(1 - \bar{q})} z. \quad (1.25)$$

The set of closed equations for \bar{q} , $\bar{\chi}$ can be solved for any degree distribution $P(k)$ and $\rho(p)$ can be computed accordingly.

Homogeneous networks

The equations for \bar{q} and $\bar{\chi}$ simplifies to a single equation when all nodes have the same properties, and in particular the same degree ($k_i = K$, $\forall i$). On these networks, the mean-field behavior can be trivially studied for any value of n^* , but we consider as an illustrative example the limit $n^* \rightarrow \infty$. Only two solutions of the equation relating \bar{q} and $\bar{\chi}$ are possible: the free-flow solution ($\rho = 0$) with $\bar{q} = 1 - p/\mu$ and $\bar{\chi} = 0$ that exists for $p \leq \mu$, and congested-phase solution, where all nodes have $n_i \rightarrow \infty$, i.e. $\bar{\chi} = \bar{\eta}$ and $\bar{q} = 0$. The latter solution has $\rho = \dot{n}/p = 1 - (1 - \bar{\eta})\mu/p$ and exists for $p \geq (1 - \bar{\eta})\mu$. The behavior of the congestion parameter with both the continuous and discontinuous transitions to the congested state is plotted in Fig. 1.6 for $\bar{\eta} = 0.25, 0.75$. The corresponding phase diagram, reported in the inset of Fig. 1.6, shows that in the interval $p \in [(1 - \bar{\eta})\mu, \mu]$ both a congested- and a free-phase coexist. We find an hysteresis cycle, with the system that turns from a free phase into a congested one discontinuously as p crosses μ . It reverts back to the free phase only at

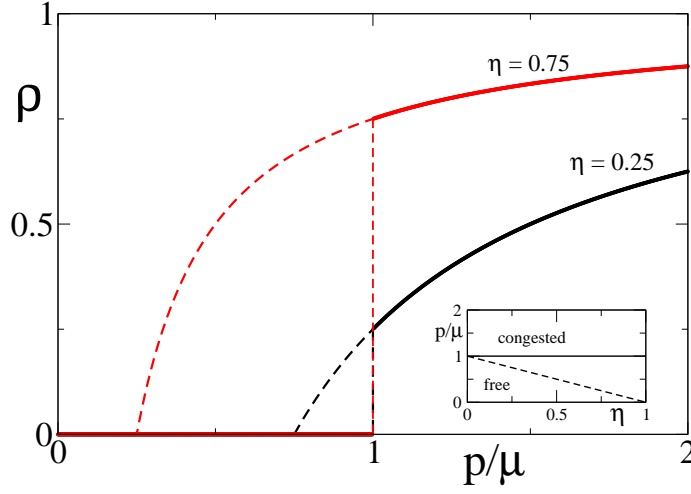


Figure 1.6: Behavior of the congestion parameter $\rho(p/\mu)$ for a random regular network for $\eta = 0.25, 0.75$. Inset: phase diagram for the same graph.

$p = (1 - \bar{\eta})\mu$ as p decreases. It is interesting to observe that in the homogeneous case the transition is always discontinuous until there is traffic control $\bar{\eta} > 0$.

Heterogeneous networks

In the case of heterogeneous networks the equations for \bar{q} and $\bar{\chi}$ have to be solved numerically. For instance, in Fig. 1.7 we compare the theoretical prediction (full line) for $\rho(p)$ in a scale-free network with results of simulations (points). The agreement is good, the theoretical prediction at the ensemble level confirming the scenario already observed in the simulations. The curves are obtained for $\mu = 0.2$ and $n^* = 10$, but the behavior does not qualitatively change for different values of these parameters. The dependence on $\bar{\eta}$ brings instead qualitative changes. Increasing $\bar{\eta}$ from 0.1 to 0.9, the transition becomes discontinuous and p_c increases.

The main difference with respect to homogeneous networks is that not all nodes become congested at the same time. The rate p at which a node becomes congested depends on its degree, the hubs being first. The process governing the onset of congestion and the effects of the rejection term can be understood in the limit $n^* \rightarrow \infty$, that simplifies considerably the calculations without modifying the overall qualitative behavior for sufficiently large n^* . We have to solve in the limit $n^* \rightarrow \infty$ the self-consistent equations for $\bar{\chi}$ and \bar{q} . In this limit, uncongested nodes have $a_k < 1$, hence $\chi_k \rightarrow 0$ and $q_k = 1 - a_k$. All nodes with degree $k < k_F$, where $k_F = \max(k^*(1 - \bar{\eta}), k_{min})$, are free from congestion. Congested nodes have $q_k \rightarrow 0$ and $\chi_k = \bar{\eta}$ (for $k \geq k^*$). In addition there are also fickle nodes, which are those with $k_F \leq k < k^*$ and $\chi_k = 1 - \frac{k_F}{k}$. Using

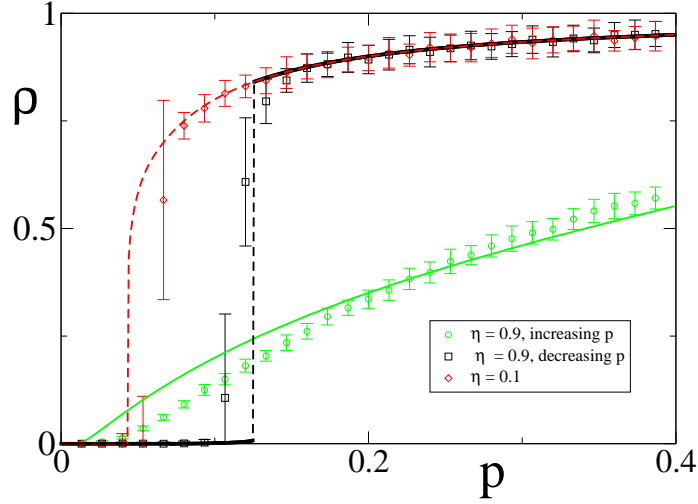


Figure 1.7: $\rho(p)$ for an uncorrelated scale-free graph ($P(k) \propto k^{-3}$, $k_{min} = 2$, $k_{max} = 110$, $N = 3000$), $\mu = 0.2$, $n^* = 10$ and $\bar{\eta} = 0.1$ and $\bar{\eta} = 0.9$, from both simulations (points) and theoretical predictions (lines). Hysteresis is observed increasing (black curve and points) and then decreasing (red curve and points) p across the transition.

this classification, we get a first expression for $\bar{\chi}$, i.e.

$$\bar{\chi}_1 = \sum_{k=k_F}^{k^*} \left[1 - \frac{k_F}{k} \right] \frac{k}{z} P(k) + \bar{\eta} \sum_{k=k^*}^{k_{max}} \frac{k}{z} P(k). \quad (1.26)$$

Eq. (1.25) provides a further relation between \bar{q} , $\bar{\chi}$ and k^* . We eliminate \bar{q} using its definition which leaves us with another expression for $\bar{\chi}$,

$$\bar{\chi}_2 = 1 - \frac{1}{2A} \left\{ 1 + Ap - B + [(1 + Ap - B)^2 + 4ABp]^{1/2} \right\} \quad (1.27)$$

where $A = z/[k^*(1 - \bar{\eta})(1 - \mu)]$ and $B = \sum_{k=k_{min}}^{k_F} \left[1 - \frac{k}{k_F} \right] P(k)$. To determine $\bar{\chi}$ we have to solve the implicit equation $\bar{\chi}_1 = \bar{\chi}_2$.

In Fig. 1.8 we plot the difference $\Delta\chi = \bar{\chi}_1 - \bar{\chi}_2$ vs. k^* , for $\bar{\eta} = 0.1$ (left) and 0.9 (right) and different values of p on a scale-free graph. The zeros of $\Delta\chi(k^*)$ correspond to the only possible values assumed by k^* . For small rejection probability ($\bar{\eta} = 0.1$ in Fig. 1.8), there is only one solution $k^*(p)$, which decreases from $+\infty$ when increasing p from 0. The value p_c at which $k^*(p_c) = k_{max}$ is the critical creation rate at which largest degree nodes become congested. At larger p , $k^*(p)$ decreases monotonously until eventually all nodes are congested when $k^*(p) = k_{min}$. Hence for low values of $\bar{\eta}$, the transition from

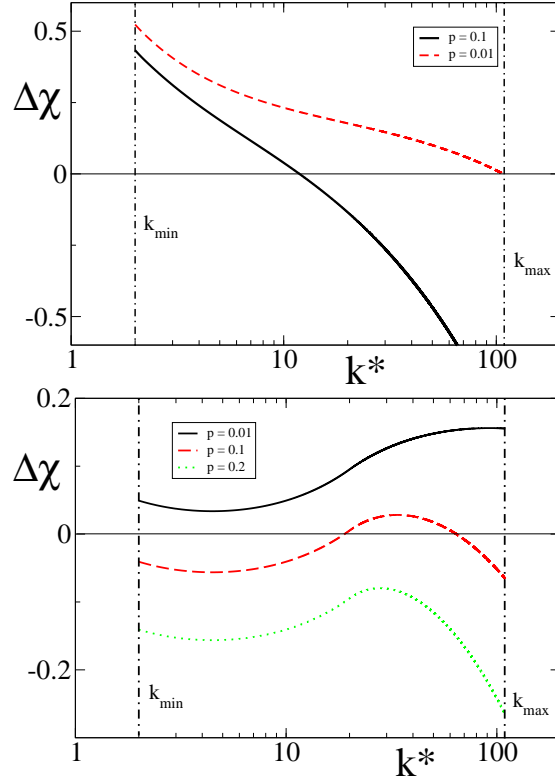


Figure 1.8: The zeros of $\Delta\chi(p)$ vs. k^* define the threshold degree for the onset of congestion in a network. The picture refers to a scale-free random network with $\gamma = 3.0$, $k_{min} = 2$ and $N = 3000$ ($k_{max} = 110$), and different values for $\bar{\eta} = 0.1$ (left) and 0.9 (right) and p . The solution $k_1^*(p)$ in the right panel falls outside the plot.

free-flow to the congested phase occurs continuously at the value of p for which $k^*(p) = k_{max}$.

At large $\bar{\eta}$ ($\bar{\eta} = 0.9$ in Fig. 1.8), the scenario is more complex. Depending on p , the equation can have up to three solutions, $k_1^*(p) \leq k_2^*(p) \leq k_3^*(p)$. It is easy to check that only k_1^* and k_3^* can be stable solutions. For $p \ll 1$ there is only one solution at $k_3^*(p) \gg k_{max}$, corresponding to the free phase. This is thus the stable solution for p increasing from zero. As p increases, another solution $k_1^*(p) < k_3^*(p)$ can appear, and $k_3^*(p)$ moves towards lower degree values. Three situations may occur:

- i. The solution $k_3^*(p)$ disappears before reaching k_{max} . Then $k_1^*(p)$ becomes the stable solution, and the congested phase appears abruptly. However, given the shape of the function $\Delta\bar{\chi}$ (see Fig. 1.8), when this happens

$k_1^*(p) \rightarrow 0$ and in particular we expect $k_1^*(p) < k_{min}$, so that above the transition the whole network is congested and follows the law $\rho(p) = 1 - (1 - \bar{\eta})\frac{\mu}{p}$.

- ii. The solution $k_3^*(p)$ crosses k_{max} and exists until it reaches k_{min} . Then the congested phase emerges continuously and the network is only partially congested (i.e. only the nodes with $k \geq k_3^*(p)$). The order parameter grows until it reaches the curve of complete congestion $\rho(p) = 1 - (1 - \bar{\eta})\frac{\mu}{p}$ ($k_3^*(p) < k_{min}$).
- iii. The solution $k_3^*(p)$ crosses k_{max} but disappears before reaching k_{min} , and k_1^* becomes the stable solution. In this case the congested phase appears continuously (only high-degree nodes are congested), but at some point another transition occurs that brings the system abruptly into the completely congested state.

In general, the exact phenomenology observed in the mean field and simulations depends strongly on the tail of the degree distribution, i.e. on the graph ensemble considered.

Note that in case of discontinuous transitions, the presence of an hysteresis phenomenon is associated to the stability of the two solutions $k_1^*(p)$ and $k_3^*(p)$. For instance, in case *ii* or *iii*, we start from the free-phase at low p , the system selects the solution $k_3^*(p)$ and follows it upon increasing p until the solution $k_3^*(p)$ disappears. On the contrary, starting from the congested phase (large p) the system selects the solution $k_1^*(p)$ and remains congested until this solution disappears (see inset of Fig. 1.7).

In Fig. 1.9 we can see the solution $k^*(p)$ for the same graph of Fig.1.7, with $\bar{\eta} = 0.7$: at p_1 , when $k^* = k_{max}$, the system becomes congested in a continuous way, at p_3 there is a discontinuous jump to higher values of congestion, while above p_4 the network is fully congested and finally, coming back to p_2 there is a jump to a less congested state. Between p_2 and p_3 there is coexistence of high and low congested states with hysteresis.

In summary, the system can show a sort of hybrid transition: a continuous transition to a partially congested state followed by a discontinuous one to a (almost) completely congested one (see Fig.1.10).

On heterogeneous random graphs, the behavior of the system in the plane $(\bar{\eta}, p)$ depends in a complex way on its topological properties, such as the degree cut-off and the shape of the degree distribution. For this reason the precise location of the critical lines, separating different phases, can be determined only numerically using the methods exposed in the previous section. In the following, we give a qualitative description of the general structure of the phase diagram in the limit $n^* \rightarrow \infty$, then we substantiate the analysis reporting an example of phase diagram obtained numerically for the same networks ensemble of Fig. 1.7.

A first important region of the space of parameters is the one in which a completely free solution exists, i.e. $k_{max} \leq k_F$. This solution is characterized

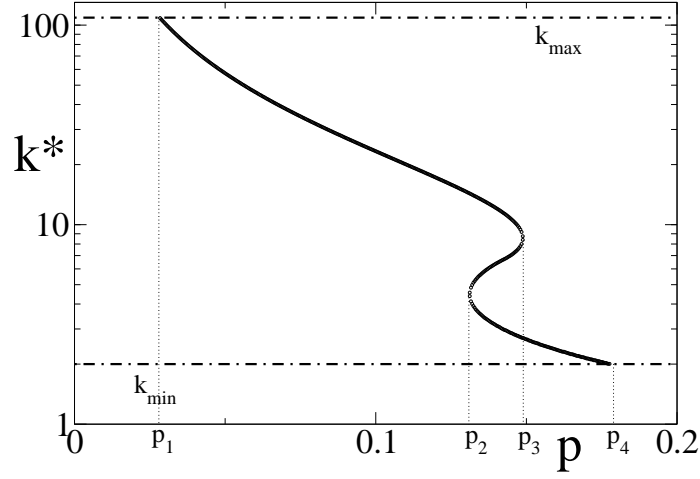


Figure 1.9: The solution $k^*(p)$ for the scale-free graph of Fig.1.7, with $\bar{\eta} = 0.7$. At p_1 , $k^* = k_{max}$, and the system becomes partially congested in a continuous way. Between p_2 and p_3 there are three solutions, two of them are stable. Increasing p , the system jumps suddenly to a more congested state at p_3 , whereas decreasing p , the system jumps to a less congested state at p_2 . Above p_4 the system is completely congested.

by $\bar{q} = 1 - p/\mu$, $\bar{\chi} = 0$ and $\rho = 0$. From the expression for $\dot{n}_k = 0$ computed in k_{max} we find that this happens as long as $p \leq p_{c0}$ with

$$p_{c0} = \frac{\mu}{\mu + (1 - \mu) \frac{k_{max}}{z}}. \quad (1.28)$$

Note that this region does not depend on the rejection probability $\bar{\eta}$, because rejection affects only congested nodes.

The transition takes place when the maximum degree nodes first become congested, i.e. $k^* = k_{max}$. Since $\dot{n}_{k^*} = 0$, $q_{k_{max}} = 0$ and $\chi_{k_{max}} = \bar{\eta}$, we get from Eq. 1.21 a first expression for $p_c = 1 - \bar{\chi} - \frac{k_{max}}{z}(1 - \mu)(1 - \bar{\eta})(1 - \bar{q})$. Now computing ρ averaging Eq. 1.21 and imposing $\rho = 0$, we find a second expression for $p_c = \mu(1 - \bar{q})(1 - \bar{\chi})$. Eliminating \bar{q} from these two equations, we find the critical line

$$p_c(\bar{\eta}) = \frac{(1 - \bar{\chi})^2}{1 - \bar{\chi} + \frac{k_{max}}{z}(1 - \bar{\eta}) \frac{1 - \mu}{\mu}} \quad (1.29)$$

where $\bar{\chi} = \sum_{k \geq k_F} \frac{kP(k)}{z} \left(1 - \frac{k_{max}(1 - \bar{\eta})}{k}\right)$. Below this line (dotted line in Fig. 1.11) the system is not congested ($\rho = 0$), even if in the region $p_{c0} \leq p \leq p_c(\bar{\eta})$ higher-degree nodes are unstable ($k_F \leq k_{max} \leq k^*$).

It is possible to show that $p_c(\bar{\eta})$ attains its maximum in $\bar{\eta}_c = 1 - \frac{k_{min}}{k_{max}}$ where

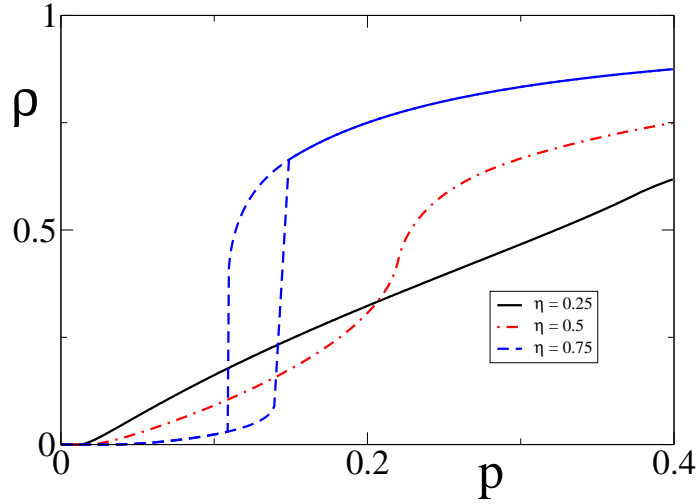


Figure 1.10: Increasing $\bar{\eta}$, the congestion parameter $\rho(p)$ develops a discontinuous transition. Here we report the case of the graph of Fig.1.8. For $\eta = 0.75$, we have first a continuous, then a discontinuous transition.

$p_{cmax} = \mu \frac{k_{min}}{z}$, where $k_F = k_{min}$ and so above this point the curve is constant $p_c(\bar{\eta} > \bar{\eta}_c) = p_c(\bar{\eta}_c)$.

The transition line $p_c(\bar{\eta})$ corresponds to the point p_1 in Fig. 1.9, calculated for all values of $\bar{\eta}$. We can calculate the two curves $p_2(\bar{\eta})$, $p_3(\bar{\eta})$ as well, in order to get the points at which there are discontinuous jumps in the congestion parameter $\rho(p)$.

Looking at Fig. 1.11 we can distinguish three points A, B, C dividing the phase diagram into different regions:

- i. Below $\bar{\eta}_A$ we have a continuous transition to a congested state increasing p above p_1 .
- ii. Between $\bar{\eta}_A$ and $\bar{\eta}_B$ the transition is continuous at p_1 . Then, increasing p above p_3 , there is a discontinuous jump to a more congested state. Coming back to lower values of p , there is a discontinuous jump to a less but still congested state at p_2 , and the system eventually becomes free below p_1 in a continuous way.
- iii. Increasing p in the region between $\bar{\eta}_B$ and $\bar{\eta}_C$, there is a continuous transition from free-flow to a congested state at p_1 , and a sudden jump to a more congested phase at p_3 ; but, this time, by decreasing p from the congested state, the transition to the free phase is discontinuous and located in p_2 .
- iv. For $\bar{\eta} > \bar{\eta}_C$ the transition is a purely discontinuous one with transition points p_2 and p_3 .

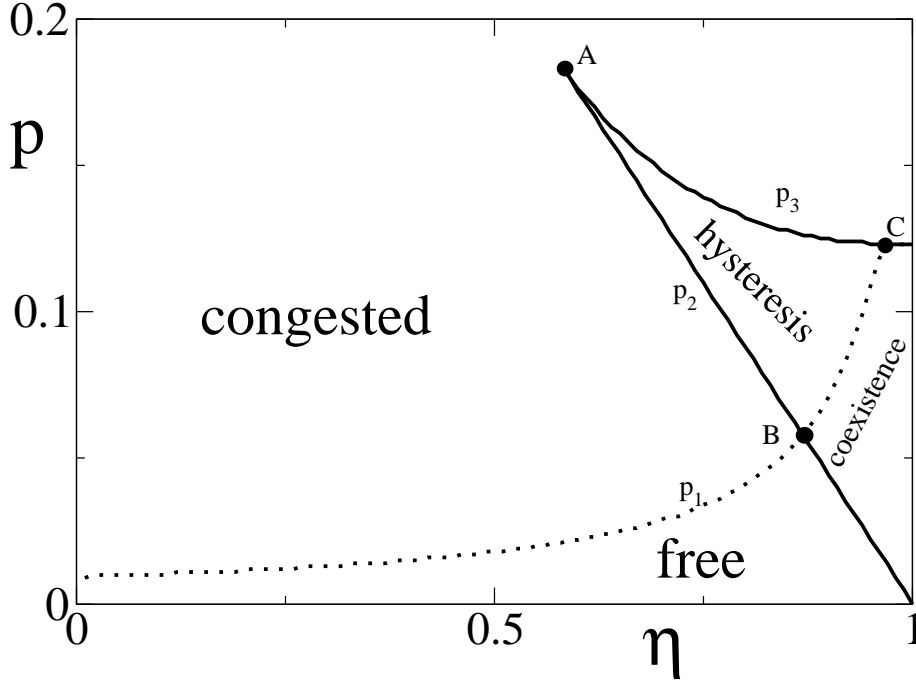


Figure 1.11: $(\bar{\eta}, p)$ phase diagram for the uncorrelated scale-free graph of Fig. 1.7.

Increasing p above the transition, at some point $p_{c_1}(\bar{\eta})$ the system becomes completely congested. For $p \geq p_{c_1}(\bar{\eta})$, the order parameter follows the curve $\rho = 1 - \mu(1 - \eta)/p$. This happens for $p \geq p_{c_1}(\bar{\eta}) = (1 - \bar{\eta})(1 - (1 - \mu)k_{min}/z)$, where $k^* \leq k_{min}$, $q = 0$, $\chi = \bar{\eta}$.

These calculations show that the phase diagram crucially depends on the tail of the degree distribution. In scale-free networks k_{max} scales with the network's size N as $N^{\frac{1}{\omega}}$ with $\omega = 2$ (structural cut-off) or $\omega = \gamma - 1$ (natural cut-off). Accordingly the critical line depends on the system's size, $p_c \propto N^{-\frac{1}{\omega}}$. The only region that does not depend on k_{max} is the one for $\bar{\eta} \geq \bar{\eta}_C$.

1.3.2 Conclusions

The model discussed above, inspired by the recent literature on congestion on complex networks, basically extends the classic framework of Jackson queuing networks along three lines:

- It goes beyond stationarity, exploring *congested* regimes, where the queues can grow.
- It accounts for congestion control protocols and this requires that the

absorption of packets takes place during the hoppings and not within the queue.

- It exploits graph ensemble calculation techniques, allowing the study of how traffic is affected by the general features of the underlying network.

Within this framework it is possible to obtain transition curves and phase diagrams at analytical level for the ensemble of uncorrelated networks and numerically for single instances. We found that traffic control improves global performance, enlarging the free-flow region in parameter space only in heterogeneous networks. In very heterogeneous networks, e.g. with scale-free degree distribution, its role should be crucial, since for low enough traffic control the critical packets insertion rate per node goes to zero with the system size. Traffic control introduces non-linear effects and, beyond a critical strength, may trigger the appearance of a congested phase in a discontinuous manner. This work can be extended in several interesting directions. First, it should be interesting to study how the dynamics change once considering a bias in the random routing, e.g. an hopping probability proportional to the betweenness centrality of the neighbouring nodes⁹, to better mimic shortest path routing. The possibility of solving the model on a given network with realistic parameters could provide both specific predictions for the robustness of the network to traffic overloads and important hints for the design of systems less vulnerable to congestion. The dynamical environment created within this model could be also exploited as a framework for testing the statistical properties of single particle dynamics under more complex routing schemes, like the study of tracking particles in hydrodynamics. Finally, it would be interesting to model the complex adaptive behavior of human users in communication networks, such as the Internet, by introducing variable rates of packets production in response to network performances. It is known that users face the social dilemma of maximizing their own communication rates, maintaining the system far from the congested state [25]. In such a situation, the presence of a continuous transition may allow the system to self-organize at the edge of criticality, whereas a discontinuous transition may have catastrophic consequences.

⁹The betweenness centrality of the node i is $\sum_{j \neq i, k \neq i} \frac{n(j, k, i)}{n(j, k)}$, where $n(j, k)$ is the number of shortest paths between j and k , and $n(j, k, i)$ is the number of them that pass through i .

Chapter 2

Dynamical arrest on disordered structures

"The deepest and most interesting unsolved problem in solid state theory is probably the theory of the nature of glass and the glass transition. This could be the next breakthrough in the coming decade. The solution of the problem of spin glass in the late 1970s had broad implications in unexpected fields like neural networks, computer algorithms, evolution and computational complexity. The solution of the more important and puzzling glass problem may also have a substantial intellectual spin-off. Whether it will help make better glass is questionable".

P.W.Anderson, Science (1995).

Fifteen years have passed since this statement, and the dramatic slowing down of the dynamics of glass forming systems is still puzzling us[26]. Its study requires a deep reasoning on the fundamentals of statistical mechanics, and methods and concepts developed in this field are likely to become paradigms for the study of complex systems in general. In this chapter I will show how a certain degree of fixed heterogeneity, e.g. in the underlying spatial structure, can change the character of the jamming transition in glass forming systems. In glass science a great deal of efforts is devoted to understanding the dynamical properties of supercooled liquids. Relaxation and transport properties of such a state are subject to a dynamical crossover upon decreasing temperature. There is an anomalous relaxation with heterogeneous patterns in space and time that are the signature of strongly cooperative effects. At a mean-field level, this crossover becomes a true phase transition. After a brief introduction on the phenomenology of glass forming systems, we will review the theoretical perspectives on it, from thermodynamical to purely dynamical approaches. In particular I will expand on the spin facilitated model by Frederickson and Anderson. Within the framework of this model it is possible to recast the dynamical jamming transition in terms of a bootstrap percolation scenario. Then, I will show how a certain degree of fixed heterogeneity, being it encoded as a simple dilution of the underlying lattice, or as a distribution in mobilities, can

dramatically change the collective behavior from bootstrap to simple percolation scenario. This can give insights on analogies and differences among the jamming of supercooled liquids and more heterogeneous systems, like polymer blends and confined fluids.

2.1 Main experimental features of the glass transition

If we cool a liquid fast enough, it can avoid crystallization entering in a metastable, *supercooled* state [27]. The typical timescales of the relaxation and transport properties of such a state dramatically increase once we further cool it. Fig 2.1 shows the shear viscosity of some supercooled liquids as a function of the temperature, divided by the temperature at which it becomes of the order of $10^{14} P$. This temperature T_g is called glass transition temperature and it is weakly dependent on the cooling rate.

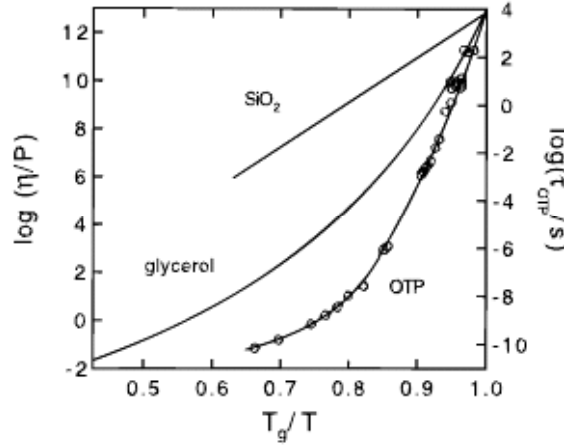


Figure 2.1: Viscosity as a function of reduced inverse temperature for three liquids: SiO_2 , glycerol and *o*-terphenyl. For the *o*-terphenyl are also shown the typical time of reorientation of molecules. From [28]

All these curves are fitted well by the Vogel-Fulcher-Tamann law (VFT):

$$\eta \propto e^{\frac{A}{T-T_k}} \quad (2.1)$$

It is possible to distinguish *strong* and *fragile* behaviors. The former is consistent with $T_k = 0$, and A can have in this case the meaning of an energy activation barrier. The latter has a true divergence at $T_k > 0$, and the typical energy scale to relax continuously increases upon decreasing temperature.

Near T_g the typical timescale to relax at equilibrium exceeds the experimental one and the system is practically out of equilibrium.

In these range of temperatures there is a drop of the specific volume and of the specific heat towards the same value of the crystal (see fig.2.2). It is possible to calculate the entropy of the supercooled liquid and to extrapolate it below T_g : at a certain point T'_k its value equals that one of the crystal[29]. There are

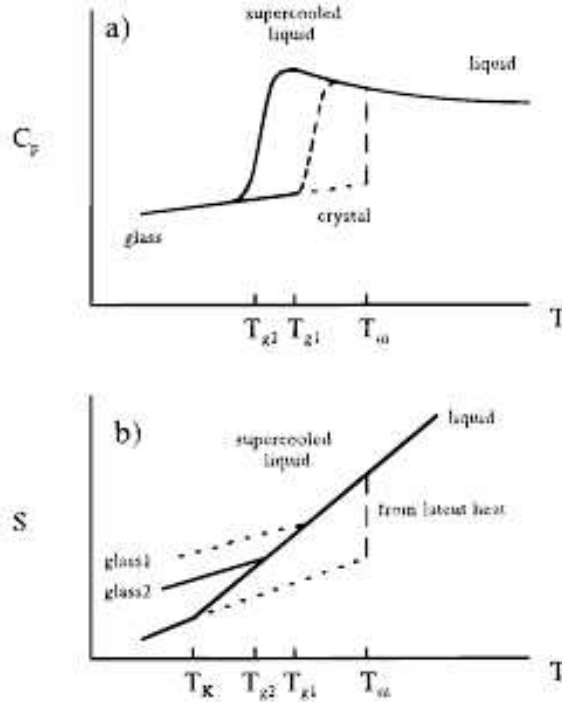


Figure 2.2: Top: a schematic plot of the temperature dependence of the specific heat for a liquid. Avoiding the melting point doesn't change its fate: at a certain point (cooling-rate dependent) there is a drop towards a solid-like dependence. Bottom: The extrapolated entropy of a supercooled liquid below the glass transition point equals the entropy of the crystal

strong empirical evidence in favour of the fact that $T_k = T'_k$ [30]. Therefore T_k should represent an infinite cooling rate limit of T_g , where there should be concomitantly a thermodynamic singularity and a divergence of the relaxation time. Hence, is it possible to speak of the glass transition in terms of a truly thermodynamic phase transition? Unfortunately, the density-density correlation function, or its fourier transform, the structure factor¹, $F(\vec{k}) = \langle \sum_i e^{i\vec{k} \cdot \vec{r}_i} \rangle$ does not show any interesting change when decreasing the temperature. On the

¹This quantity can be directly measured through scattering experiments.

other hand, the relaxation of its time-dependent version $F(\vec{k}, t)$, the intermediate scattering function, shows very interesting features upon approaching T_g from the supercooled phase, with heterogeneous patterns in space and time.

Therefore, even if the static structure of the system doesn't show when decreasing the temperature any interesting change, from the dynamical point of view, interesting phenomena are taking place.

The relaxation of $F(\vec{k}, t)$ at low temperatures is indeed not exponential, rather it proceeds by two steps (see fig2.3). First it approaches a plateau, the β relaxation, and then it departs from it towards the equilibrium value, the α relaxation. The height of the plateau starts discontinuously from a value larger than zero at a certain temperature. This is usually related to the microscopic

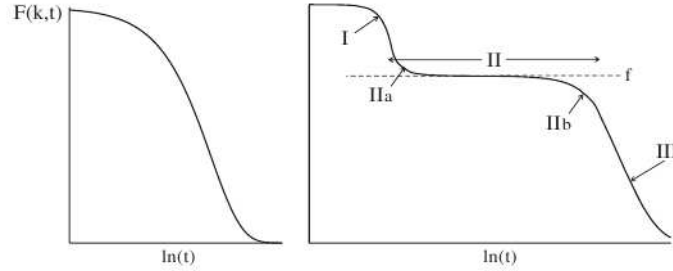


Figure 2.3: A schematic plot of the relaxation in time of the intermediate scattering function. Left: high temperature, liquid phase, exponential relaxation. Right: at lowering temperature the function relaxes in two steps, first towards a plateau, the β step, and then, after a while, to zero, the α step.

motion of the particles of the system. If we follow the average displacement in time (see fig2.4) of particles, at high temperature we have a sharp crossover from a ballistic ($d \propto t$) to a diffusive regime ($d \propto \sqrt{t}$). At low enough temperature this two regimes are separated by a plateau. This means that a particle is trapped for a while by the cage formed by its neighbours, where it vibrates. A picture confirmed by numerics and experiments as well[31]. The motion within the cage is related to the β step, the rearrangement of the cages should be related with the α one. Finally, the α step itself is not exponential, being fitted by a stretched exponential formula $\exp^{-(t/\tau)^\beta}$. This last trend is usually ascribed to a certain degree of dynamical heterogeneity: different parts of the same system can have different relaxation patterns, this causing in turn a deviation from the exponential. The microscopic resolution of the dynamics with numerical simulations has shown strong correlation patterns, like e.g. the clustering of more mobile particles (see [26] and ref therein). The fluctuations of the intermediate scattering function, i.e. the dynamical susceptibility, develops a maximum in time whose height increases upon decreasing the temperature. This maximum is related with the typical size of the correlated regions, thus defining a dynamical correlation length that diverges together with the relaxation time[26].

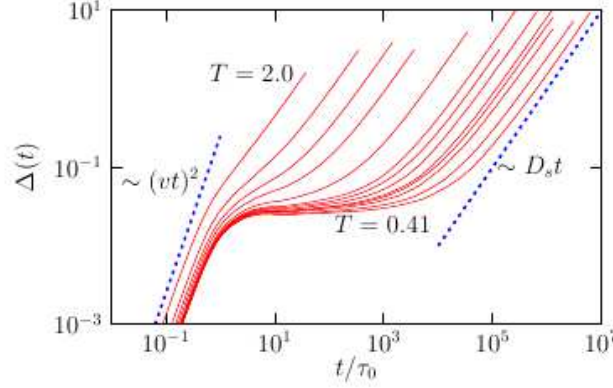


Figure 2.4: Average displacement in time of particles by simulations of Lennard-Jones spheres for several temperature. Upon decreasing temperature, the division between short-time ballistic regime and long-time diffusive one is given by a plateau. From [26]

2.1.1 Other-than-molecular glass formers

One interesting point, from a statistical mechanics perspective, is about the generality of such phenomenology. Interestingly enough, the same phenomenology, with a dramatic slowing down of the dynamics and complex patterns of relaxations in space and time, is shared by systems whose interacting units are of different scales from the molecular ones like colloidal suspensions, granular media and polymer solutions.

Colloidal suspension[33] consist of big particles in a solvent, with typical sizes of 1 – 500 nm. The continuous scattering events with the much smaller particles of the solvent renders the dynamics of such particles brownian, with diffusion time of the order of 1 ms. They can be modeled as hard spheres, with an interaction potential that is infinite below a certain distance $2R$ and zero otherwise. In this case the temperature has the only role of rescaling times and what matters is the density ρ , or alternatively, the packing fraction $\Phi = 4/3\pi R^3\rho$. At increasing Φ the viscosity and/or the relaxation times of the system dramatically increases, and at $\Phi_g \simeq 0.58$ the relaxation times exceed the experimental ones and the system is jammed. The system is now an elastic amorphous solid, the gel. All this remember the already seen phenomenology of the glass transition, and, in fact, it is found that a VFT formula is a good fit for the dependence of relaxation times on density, the dynamics of the correlation function has a two step relaxation and there is a certain degree of spatial dynamical heterogeneity. Another kind of systems that show jamming are granular media[34]. They consist of large ($N = 10^2$ - 10^6) assembly of macroscopic particles, from powder (10^{-5} m) to rocks (10 m). Because of their macroscopic

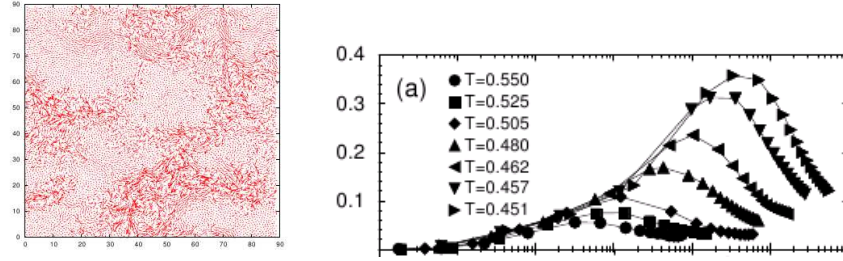


Figure 2.5: Left: spatial map of single particle displacements from simulations of a bidimensional Lennard-Jones system. It is possible to recognize qualitatively different mobilities and the presence of non trivial correlations in the motion. From [26] Right: The dynamical susceptibility develops a maximum in time whose height increases upon decreasing temperature, from simulations of a Lennard-Jones system in[32]

scales, the thermal energy has no role and they have to be vibrated, sheared, etc, by an external source to explore the phase space. Therefore, there should be a continuous injection of energy that is continuously dissipated by friction, a force that play a key role in these systems. Their phenomenology is very rich. In particular, depending on the strength of the driving force, their properties can be seen as similar to that one of the usual phases of matter, with transition among them. That's why it is common to speak of granular gases, liquids and solids[35]. An interesting point comes up: when the grains are in the “solid” phase they are usually not arranged in a regular and/or crystalline structure. The solid is amorphous and the transition from the fluid phase is a dynamical arrest with a complex relaxation pattern, as can be seen e.g. in compaction-by-vibration experiments[36]. Interestingly enough, also polymer solutions have a jamming transition. When decreasing the temperature/increasing the density, the dynamics of these systems is slowed down with a dramatic increase of the viscosity, till the system becomes an elastic solid, a gel[37]. There is clear dynamical crossover with the intermediate scattering function showing a stretched exponential decay. However, at odds with simple liquids, this sol/gel phase transition is well known. When decreasing the temperature/increasing the density, the polymers stick together, forming a network that at a certain point can span the whole system, a process that is called *percolation*. The study of such phenomenon opened the huge field of percolation theory, a kind of general and geometrical view on phase transitions[38]. In the simplest percolation scenario we have a lattice, whose bonds can be either empty or occupied with some probability p . At low p , the lattice is disconnected in clusters of finite size. Upon increasing p , at a certain point p_c , there is a continuous transition by which one of the clusters span the whole lattice, that is now connected. The average clusters' size defines in this case naturally a correlation length[39]. It is interesting to notice that there are numerical evidences that this simple perco-

lation scenario for a dynamical arrest seems to be present even in super-cooled liquids once we confine them[40].

2.2 Theoretical views on the glass transition

As we pointed out before, an intriguing qualitative difference in the dynamics of the supercooled liquid, that should give insights about mechanisms underlying the dramatic slowing down, is the anomalous two steps relaxation of correlation functions. A picture by Goldstein[41] tries to explain it in terms of a dynamics in the phase space ruled by activated processes. In a certain range of temperatures the energy landscape visited by the system is composed of many local minima. The dynamics should consist of vibrations within one minimum, the β step, and then jumps among minima, the α step.

On the other hand, it is possible to write down equations for the correlation function, and by means of suitable approximations to solve them. This is the framework of the mode coupling theory (MCT)[42], that gives many interesting insights and experimentally proved results for the high temperature regime of supercooled liquid[43]. It predicts quantitatively the features of the relaxation of correlation functions, with a two step relaxation, the development of a plateau in a discontinuous way and increasing fluctuations. But, at odds with the real liquid, at a certain point T_c the correlation function sticks to that plateau. Hence, the main drawback of this theory is the wrong prediction of a singularity in the dynamics with a power law divergence of the relaxation time at $T_c > T_g$.

Interestingly, the approximated equations of this theory are exactly the same of a mean-field model of spin glass: the p-spin spherical model[44]. Spin glasses are disordered materials whose magnetic properties show interesting behaviors that resemble very close that ones of glasses. They are usually modeled by classical spins on lattice, whose interactions can be both antiferromagnetic and ferromagnetic. These model systems are characterized by the phenomenon of frustration. It is impossible or extremely hard to satisfy all the interaction terms in the Hamiltonian, and this gives rise to a very complex energy landscape, full of minima and saddles. This is often a distinctive feature of complex systems in general, and concepts and methods used for spin glasses are currently used in fields as different as biology (neural networks) and information theory (algorithmic complexity)[45]. In the p-spin spherical model N continuous spins σ_i interact by p-body terms, the hamiltonian being:

$$H = - \sum_{i_1, \dots, i_p} J_{i_1, \dots, i_p} \sigma_{i_1} \cdots \sigma_{i_p} \quad (2.2)$$

where the J are quenched² random variables with a gaussian probability distribution of zero mean, and the spins are subject to the spherical constraint

²The interaction terms are slowly changing with respect to the spin variables, i.e. they are fixed once for all. In the thermodynamic limit, the average over all the possible configurations of interactions of extensive quantities, like the free energy, should give the same result of a given single instance.

$\sum_i \sigma_i^2 = N$. Most of these model systems in general, and the p-spin model in particular, are subject, upon lowering T , to a dynamical phase transition and moreover they have a truly thermodynamic singularity, the replica symmetry breaking phase transition³. The first, corresponding exactly to the singularity of the MCT, it is an extreme case of the already mentioned Goldstein scenario. The dynamics is ruled by activated processes, i.e jumps among local minima of the energy, whose number is exponential in the system size. This crossover becomes a truly phase transition because, at mean field level, the barriers among minima are infinite in the thermodynamic limit. The second is static and it is characterized by ergodicity breaking.

The phenomenology of the p-spin model seems to give a good metaphor for the dynamics in phase space of structural glasses. Therefore, it has recently inspired replica-based approaches for Lennard-Jones fluids[46] and hard-sphere systems[47]⁴. However spin glasses are different from structural glasses, the main difference being the presence of quenched disorder.

An alternative approach is to look at glassiness from a pure dynamical perspective, without recurring to a complex energy landscape scenario. This approach is based to the study of lattice models with simple hamiltonian and trivial equilibrium behavior, but whose dynamics is subjected to some kinetic constraints, such that they can show glassy relaxation patterns[48]. These models can give deep and useful insights about the microscopic mechanisms of the first step of the glass transition, the dynamical crossover. It should not be forgotten that the equilibrium dynamical properties of the supercooled system around this crossover are accessible to experiments. Below it, the experimental investigation of the thermodynamic properties requires exceedingly large times. In particular, within their framework the question of how the underlying spatial topology affects the dynamics can be directly addressed and easily analyzed, as we shall see soon for a particular case.

2.2.1 The Frederickson-Andersen model

One of the first kinetically constrained model was introduced by Frederickson and Andersen (FA)[49]. On top of each site i of a lattice there is a classical 1/2 Ising spin s_i that can be 1 or -1 . The spins are uncoupled and there is a global magnetic field of strenght 1 pointing up, the Hamiltonian being simply $H = -\sum_i s_i$. The static properties are very simple and the stationary probability distribution function of the spin configurations factorizes $P(s_1, \dots, s_N) = \prod_i p_i(s_i)$. The dynamics is characterized by an additional constraint: a spin can flip if at least f of its neighbours are down. Down spins should represent region with high mobility such that they trigger the relaxation of their neighbours. This rule doesn't violate detailed balance but it can trigger a dynamical arrest. Upon decreasing the temperature, at a certain point, the

³A replica is a copy of the system with exactly the same realization of quenched disorder, if any. Actually replicas were first introduced as a trick for calculations.

⁴However, in finite dimension the scenario is even more complex: different parts of the same system could be in different minima, with a characteristic size ξ for these domains

system cannot relax because a finite fraction of the spins doesn't flip anymore, i.e. they are frozen. A good parameter to characterize this transition is thus the fraction of blocked spins Φ as a function of the temperature.

It is possible to analyze this model at a mean field level onto a bethe lattice of degree z [50]. This lattice can be seen as the infinite size limit of a Cayley tree, i.e. the graph obtained starting to branch from a seed node with a constant branching $k = z - 1$, or of a random regular graph, i.e. a graph taken from the ensemble of all the graphs whose nodes have degree z , all with equal statistical weight. The first is a tree but it has strong boundary effects, the second is locally a tree, having loops whose length scales with the logarithm of the system size.

Let us call $B = P(A)$ the probability of the event A : the spin at the end of a random link is in the state -1 , or it can flip to this state by rearranging the k sites above it. B verifies the iterative equation:

$$B = (1 - p) + p \sum_{i=0}^{k-f} \binom{k}{i} B^{k-i} (1 - B)^i \quad (2.3)$$

where $p = \frac{1}{1+e^{-1/T}}$ is the probability that the spin is $+1$ at equilibrium. The term $1 - p$ on the rhs is the probability that the spin is already in the state -1 . The other term is the probability that the spin is in the state $+1$ (p) and that it can flip by rearranging the neighbours (the sum). The sum is thus the probability that the event A is not verified for at most $k - f$ out of k neighbours, i.e. that A is verified at least for f of them, that is, the constraint is satisfied. There is always a solution $B = 1$. For $f = 1$ it is the only solution. For $f > 1$, the so-called cooperative cases, we can have a fixed point $B < 1$. We define $x = 1 - B$ that verifies the equation:

$$x = p \sum_{i=0}^f \binom{k}{i} x^{k-i} (1 - x)^i \quad (2.4)$$

The parameter that distinguish jammed from free phases is the fraction of spins permanently frozen Φ :

$$h = \sum_{i=0}^{f-2} x^{k+1-i} (1 - x)^i \quad (2.5)$$

$$\Phi = p \sum_{i=0}^{f-1} x^{k+1-i} (1 - x)^i + (1 - p) \sum_{i=0}^{f-1} (ph)^{k+1-i} (1 - ph)^i \quad (2.6)$$

The two contributions are the probability that a spin is frozen in the $+1$ or -1 state, respectively.

Let's analyze the case $f = 2$, $k = 3$. We have the trivial solution $x = 0$ and $1 = px(3 - 2x)$. The critical value at which the transition takes place is $p_c = 8/9$, or $T_c \simeq 0.48$, where Φ jumps discontinuously from 0 to $\Phi_c \simeq 0.67$, such that $\Phi - \Phi_c \simeq (T_c - T)^{1/2}$. The dynamics of relaxation at equilibrium is

analyzed in terms of the persistence function $\phi(t)$, i.e. the fraction of spins that do not flip till time t . This is a measure of the self correlation of the system and $\lim_{t \rightarrow \infty} \phi(t) = \Phi$. Looking at the temporal trends of ϕ in fig.2.6, left, we can see how effectively, it has an exponential behavior at high T , then it deviates from it, starting to develop a plateau upon lowering T , till T_c , where it sticks to the plateau coincident with the value of Φ . The integral of ϕ gives an estimate of the typical relaxation time, that diverges at T_c with exponent $\gamma \simeq 3$ (see fig., right).

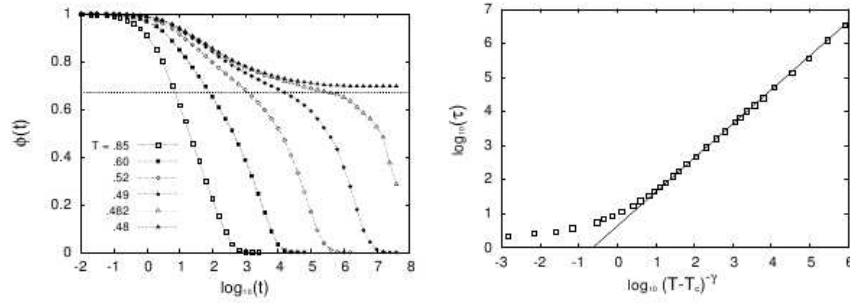


Figure 2.6: left: Time trends of the persistence function $\phi(t)$. Upon decreasing temperature, it has a two step relaxation, developing a plateau in a discontinuous way. The straight line is calculated analitically. Right: Power law divergence of the integral relaxation time as a function of the temperature at T_c . Simulations from[50]

The fluctuations of $\phi(t)$ show critical behavior upon approaching the T_c . Fig 2.7 shows the dynamical susceptibility $\chi(t) = N(\langle \phi(t)^2 \rangle - \langle \phi(t) \rangle^2)$ that develops a maximum whose height is diverging at T_c .

This dynamical phase transition is thus called *hybrid*, because the parameter Φ jumps discontinuously at the transition point to a finite value, but it has critical fluctuations and a well defined exponent for the value of $\Phi - \Phi_c$ upon approaching the T_c .

Even if an exact mapping is still missing, this jamming scenario is in very good agreement with the dynamical phase transition of the simplest MCT and of the p-spin spherical model.

The bootstrap percolation problem

The FA model can be mapped onto the bootstrap percolation (BP)[51] problem. In BP, each site is first occupied with a particle with probability p , then, particles with less then m neighbouring particles are removed. Iterating the procedure, we can end up with a remaining m-cluster of particles or not, depending on p , the initial density. This model can be analyzed exactly on a Bethe lattice of degree z . We let R be the probability that an occupied site i is not connected

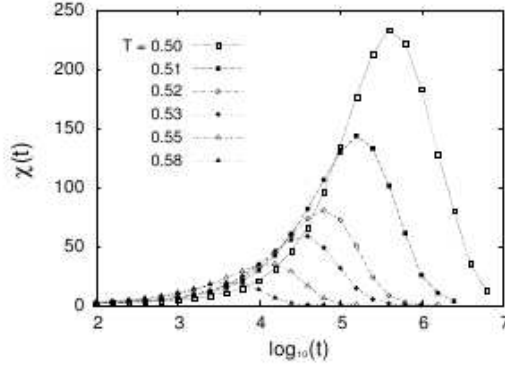


Figure 2.7: Time trends of the dynamical susceptibility. A maximum is developing, whose height increases at decreasing temperature. Simulations from [50]

to an infinite m -cluster containing its nearest neighbor j . It can be so if j is not occupied (w.p. $1 - p$) or if less than $m - 1$ of the other neighbors of j are also not in the m -cluster. Thus we find that:

$$R = 1 - p + p \sum_{i=0}^{m-2} \binom{z-1}{i} R^{z-i} (1-R)^i \quad (2.7)$$

And this is the same equation of B if

$$m = z - f + 1 \quad (2.8)$$

There is always a solution $R = 1$. Depending on p we can have a fixed point $R < 1$. The case $m = 2$ has the same equation of the ordinary percolation problem[38]. The remaining cluster in the $m = 1$ case is the same of $m = 2$ case with the adjoint of dangling bonds, i.e. the chain structures connected to the 2-cluster. Below the transition point of the $m = 2$ case, in the $m = 1$ case, there are still remaining clusters, but they are disconnected chains whose relative size decreases to zero in the thermodynamic limit. The fraction of sites in the m -cluster, or the probability that a site is part of it, P_m , has the form:

$$P_m = p \sum_{i=0}^{z-m} \binom{z}{i} R^i (1-R)^{z-i} \quad (2.9)$$

These equations can be solved along the same lines of the FA model. Fig.2.8 shows the transition curves $P_m(p)$ for a bethe lattice with connectivity $z = 6$. We have a continuous transition $P_m \propto (p - p_c)^\beta$ for $m = 1, 2$ with exponents $\beta = 1, 2$ respectively. For $m > 2$ the transition is discontinuous $P_m - P_{mc} \propto (p - p_c)^\beta$ with exponent $\beta = 1/2$.

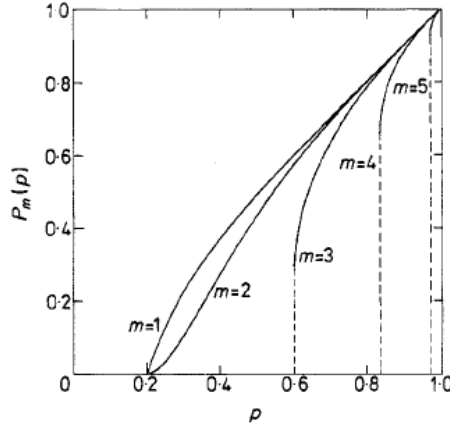


Figure 2.8: Relative size of the BP m -cluster as a function of the density $P_m(p)$, for several m for a bethe lattice of degree $z = 6$.

2.3 The heterogeneous FA model

As we have seen, it is possible on a random regular graph to recast the jamming in the FA as a bootstrap percolation transition. In particular, depending on the facilitation parameter f of the model, and on the degree z of the underlying lattice, it is possible to have a bootstrap or a simple percolation scenario, if $m = z - f + 1$ is larger or not than 2 respectively. It is possible to consider situations in which m is varying from site to site, i.e. considering different degrees and/or facilitation parameters[52]. Let us consider a diluted version of the previously analyzed lattice, i.e. a trimodal random graph with degree distribution $P(k) = u\delta_{k,2} + (q_1 - u)\delta_{k,3} + (1 - q_1)\delta_{k,4}$, the average degree is $z = 4 - q_1 - u$. Let us[53] put on top of such a lattice the FA model with facilitation parameter $f = 2$ [53]. We can extend the equation 2.3 to general heterogeneous random graphs considering the probability B_k that a spin verifies A and it has $k + 1$ neighbours,

$$B_k = (1 - p) + p \sum_{i=0}^{k-f} \binom{k}{i} B^{k-i} (1 - B)^i \quad (2.10)$$

And $B = \sum_k \frac{(k+1)P(k+1)}{z} B_k$ is the average of B_k over the degrees, that verifies the equation:⁵

$$B = (1 - p) + p \sum_{k=0}^{\infty} \frac{(k+1)P(k+1)}{z} \sum_{i=0}^{k-f} \binom{k}{i} B^{k-i} (1 - B)^i \quad (2.11)$$

⁵On a random graph with degree distribution $P(k)$, the degree distribution of a random neighbouring node is $P(k)k/z$

or, in terms of $x = 1 - B$:

$$x = p \sum_k \frac{(k+1)P(k+1)}{z} \sum_{i=0}^{f-1} \binom{k}{i} x^{k-i} (1-x)^i \quad (2.12)$$

The equations for $f = k+1$ and $f = k$ are the same, and they are the same of ordinary percolation. We have, finally (apart of the $x = 0$ solution):

$$\frac{1}{p} = a(2-x) + (1-a)x(3-2x) \quad (2.13)$$

where $a = \frac{3q_1-u}{z}$. Then we have:

$$x = \frac{3-4a + \sqrt{9-8a - \frac{8(1-a)}{p}}}{4(1-a)} \quad (2.14)$$

This solution exists if $p > p_{c1} = \frac{8-8a}{9-8a}$, and, if $a > a_c = 3/4$, it is positive until $p > p_{c2} = \frac{1}{2a}$. Below a_c , we can expand around p_{c1} , $p = p_{c1} + \epsilon$, we have

$$x \simeq A_1 + A_2 \sqrt{\epsilon} \quad (2.15)$$

where $A_1 = \frac{3-4a}{4(1-a)}$ and $A_2 = \frac{\sqrt{2(1-a)}}{2p_{c1}(1-a)}$. The transition is discontinuous with exponent 1/2 and $x_c = A_1$ at the critical point. Above a_c , expanding around p_{c2} we end up with

$$x \simeq A_3 \epsilon \quad (2.16)$$

where $A_3 = \frac{4a^2}{4-3a}$, a continuous transition with exponent 1. The crossover is at the point $a_c = 3/4$, $p_c = 2/3$.

The fraction of blocked spins Φ has the general form:

$$\Phi = p \sum_k P(k) \sum_{i=0}^{f-1} \binom{k}{i} x^{k-i} (1-x)^i + (1-p) \sum_k P(k) \sum_{i=0}^{f-1} \binom{k}{i} h^{k-i} (1-h)^i \quad (2.17)$$

where

$$h = p \sum_k \frac{(k+1)P(k+1)}{z} \sum_{i=0}^{f-2} \binom{k}{i} x^{k-i} (1-x)^i \quad (2.18)$$

that, in our case it is:

$$h = px \frac{2u + 3(q_1 - u)x + 4(1 - q_1)x^2}{4 - q_1 - u} \quad (2.19)$$

$$\begin{aligned} \Phi = & p(ux(2-x) + (q_1 - u)x^2(3-2x) + (1 - q_1)x^3(4-3x)) \\ & + (1-p)(uh(2-h) + (q_1 - u)h^2(3-2h) + (1 - q_1)h^3(4-3h)) \end{aligned} \quad (2.20)$$

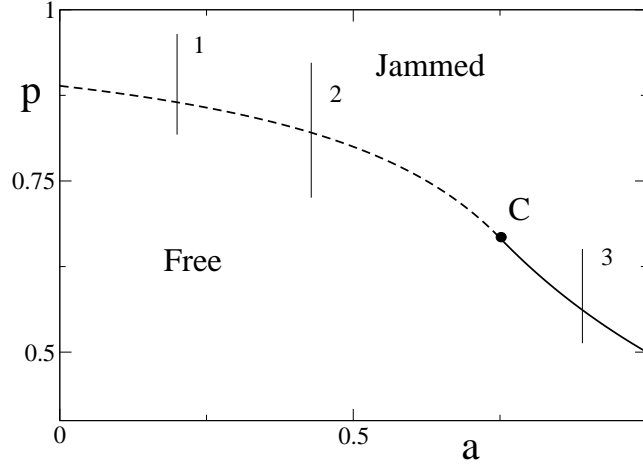


Figure 2.9: Phase diagram of the system in the (a, p) plane, at $C = (3/4, 2/3)$ the transition changes character

Below a_c we have

$$\Phi \simeq 2p_c u \left(1 + \frac{2(1-p_c)u}{4-q_1-u}\right) A_3 \epsilon \quad (2.21)$$

If $u = 0$, the leading order in the ϵ expansion is 2 (see the right part of fig.2.10):

Above a_c , we have instead:

$$\Phi - \Phi(x_c) \propto \sqrt{\epsilon} \quad (2.22)$$

In synthesis, the picture is as follows:

- If $a < 3/4$, above $p_{c1} = \frac{8-8a}{9-8a}$ there is a discontinuous jamming transition with exponent $1/2$
- If $a > 3/4$, above $p_{c2} = \frac{1}{2a}$ there is a continuous transition with exponent 1

We will consider from now on three lines in the phase diagram, fig.2.9: $q_{11} = 0.25$, that can be considered a perturbation with respect to a random regular graph; $q_{12} = 0.7$, where the transition is still discontinuous but closer to the point C , and $q_{13} = 0.85$, in the region with continuous transition. Fig.2.10 shows the transition curves $\Phi(T)$ along these three lines. We have, respectively, the critical temperatures $T_1 = 0.5386$, $T_2 = 0.9362$ and $T_3 = 2.0843$.

Fig.2.11 shows the persistence $\phi(t)$, i.e. the fraction of spins that do not flip until time t , by simulations. Upon decreasing T , the system starts to relax in a non-exponential way and then, it falls out of equilibrium, developing a plateau in the persistence, i.e the fraction of blocked spins $\phi(\infty) = \Phi$. As predicted from analytics, the plateau starts to develop discontinuously and/or

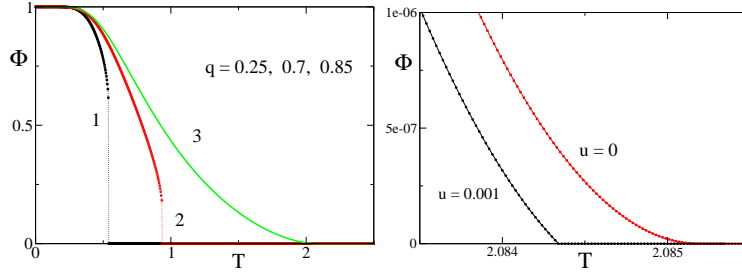


Figure 2.10: Left: Transition curves $\Phi(T)$ for $q_1 = 0.25, 0.7, 0.85$, $u = 0.001$. Right: Inserting a small fraction of nodes with degree 2 the transition exponent changes from 2 to 1 ($q_1 = 0.85$).

continuously from the transition point, depending on the connectivity of the underlying graph (controlled by q_1). Nearby the transition temperature T_c , we can verify that there is a scaling law for the persistence of the type $\phi(t, T) = \phi(t/\tau(T))$, where τ is the integral time, i.e. simply the integral over time of the ϕ . This anomalous relaxation can be solved microscopically, looking at the distribution of persistence times $P(\tau)$, i.e. the time for the first spin-flip to occur. In fig.2.12 we can see that for both $q_1 = 0.25, 0.7$, when decreasing the temperature, the distribution starts to develop another peak, instead, for $q_1 = 0.85$, when decreasing T , the distribution starts to develop a fat tail. Then, the dependence on temperature of typical relaxation times $\tau(T)$, calculated as the average of the distribution is in a good agreement with a power law

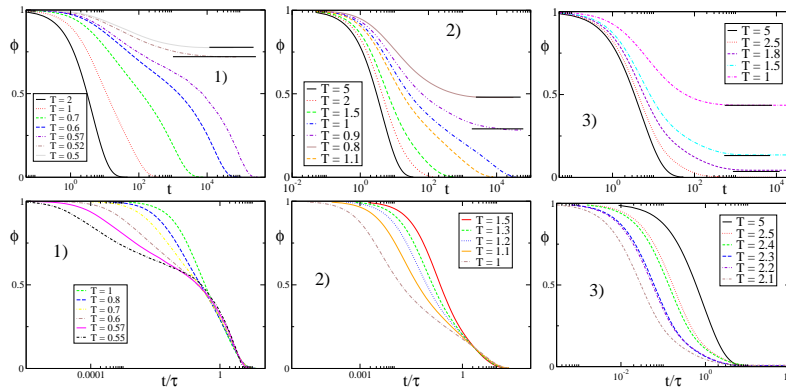


Figure 2.11: Top: persistence curves $\phi(t)$ for $q_1 = 0.25, 0.7, 0.85$ ($u = 0.001$), respectively from left to right, for several temperatures. Simulations for a graph of size $N = 5 \cdot 10^4$, averages over 10 realizations, plateaus from analytical results. Bottom: Rescaled persistence curves

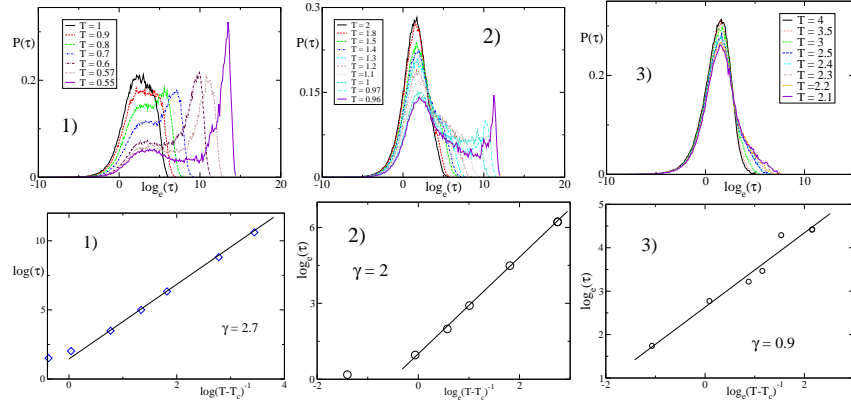


Figure 2.12: Top: distribution of persistence times $P(\tau)$ for $q_1 = 0.25, 0.7, 0.85$ ($u = 0.001$), respectively from left to right, for several temperatures. Simulations on top of a graph of size $N = 2.5 \cdot 10^5$. Bottom: Average persistence times $\tau(T)$

divergence at the critical temperature $\tau(T) \simeq (T - T_c)^{-\gamma}$, where γ depends on q_1 . Finally, we investigate the dynamical susceptibility $\chi^2(t) = N \langle (\phi(t) - \langle \phi(t) \rangle)^2 \rangle$ (see fig.2.13). This increases with time until it develops a maximum and/or a plateau, respectively for discontinuous and/or continuous transitions, whose height increases and diverges upon approaching T_c . However, it should be said

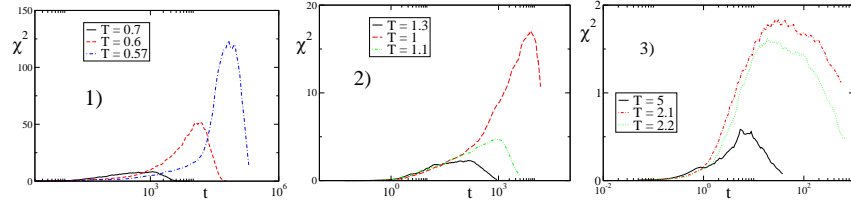


Figure 2.13: Dynamical susceptibility $\chi^2(t)$ for $q_1 = 0.25, 0.7, 0.85$ ($u = 0.001$), respectively from left to right, for several temperatures. Simulations on top of a graph of size $N = 10^4$, averages over 100 realizations

that the divergence of relaxation time in the continuous case needs further investigations.

Facilitated spin mixtures on homogeneous graph

An interesting point is that it is possible to obtain exactly the same results considering an homogeneous lattice and varying facilitation parameter from node to node. Lets' consider the FA model with a trimodal $f = 2, 3, 4$ distribution of

facilitation parameter in a bethe lattice with degree $z = 4$, respectively a spin can have $f = 2$ with probability $1 - q$, $f = 3$ w.p. $q - r$ and $f = 4$ w.p. r . The self-consistent equation for B , the probability that, following a link, a spin is up, or can be in the next steps moving the other spins on the top, is:

$$B = (1 - p) + p(B^3 + 3(1 - q)(1 - B)B^2) \quad (2.23)$$

We have for $x = 1 - B$, apart from the $x = 0$ solution:

$$x = \frac{3(1 - 2q) + \sqrt{9p^2 - 8p + 12qp(1 - p)}}{2p(2 - 3q)} \quad (2.24)$$

This solution exists, for $q < q_c = 1/2$, if $p > p_{c1} = \frac{4(3q-2)}{3(4q-3)}$, and, if $q > q_c = 1/2$, it is positive until $p > p_{c2} = \frac{1}{3q}$. Below q_c , we can expand around p_{c1} , $p = p_{c1} + \epsilon$, we have

$$x \simeq A_1 + A_2\sqrt{\epsilon} \quad (2.25)$$

where $A_1 = \frac{2q-1}{3q-2}$ and $A_2 = \frac{3\sqrt{2-3q}(4q-3)}{4(3q-2)^2}$. The transition is discontinuous with exponent $1/2$ and $x_c = A_1$ at the critical point. Above a_c , expanding around p_{c2} we end up with

$$x \simeq A_3\epsilon \quad (2.26)$$

where $A_3 = \frac{3q^2}{1-2q}$, a continuous transition with exponent 1. The crossover is at the point $q_c = 1/2$, $p_c = 2/3$.

The fraction of blocked spins is:

$$\phi = p(x^3(4 - 3x) + 6qx^2(1 - x)^2 + 4rx(1 - x)^3) + (1 - p)(h^3(4 - 3h) + 6qh^2(1 - h)^2 + 4rh(1 - h)^3) \quad (2.27)$$

where

$$h = p(x^3 + 3(1 - q)x^2(1 - x) + 3rx(1 - x)^2) \quad (2.28)$$

and x is the solution that we have discussed. Below q_c we have

$$\phi \simeq 4p_cr(1 + 3r(1 - p_c))A_3\epsilon \quad (2.29)$$

Above a_c , we have instead:

$$\phi - \phi(x_c) \propto \sqrt{\epsilon} \quad (2.30)$$

In synthesis, the picture is as follows:

- If $q < 1/2$, above $p_{c1} = \frac{4(3q-2)}{3(4q-3)}$ there is a discontinuous jamming transition with exponent $1/2$
- If $q > 1/2$, above $p_{c2} = \frac{1}{3q}$ there is a continuous transition with exponent 1

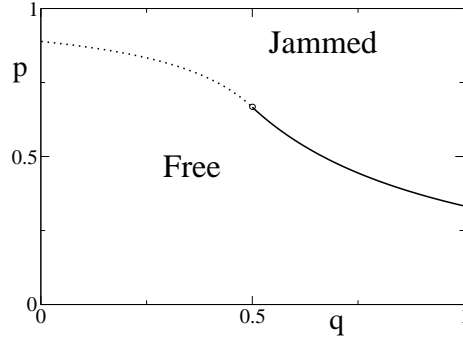


Figure 2.14: Phase diagram of the system in the (q, p) plane, at $(1/2, 2/3)$ there is a critical point

2.3.1 Conclusions

In the cooperative case, the Frederickson-Andersen model can give a good mean-field microscopic description of the anomalous relaxation and dynamical crossover of glass forming liquids in the range of temperature slightly above the crossover point. The relaxation of correlation functions proceeds by two steps, the height of the plateau starting discontinuously from a finite value. The dynamical susceptibility grows in time till it reaches a maximum whose height increases upon decreasing the temperature. At odds of real liquids and similarly to the MCT there is a power law singularity at T_c , where the system starts to be jammed. Microscopically this corresponds to a bootstrap percolation transition.

I showed that this same model can change character on a diluted, heterogeneous structures. For high enough dilution the transition becomes continuous, within the class of simple percolation. There are not two steps in the relaxation, that still shows stretched exponential dependence upon approaching the critical point. The dynamical susceptibility develops a plateau whose height is slowly increasing when approaching the singularity.

This simple percolation dynamical arrest scenario is known to be the one of the sol/gel transition in polymer blends, and recent numerical simulation studies shown that it is valid also for strongly confined fluids.

It seems that the simple ingredient of a fixed heterogeneity, being encoded in the spatial structure or in the mobilities, can change qualitatively a dynamical arrest scenario, dividing systems in two classes from this point of view.

However, more detailed numerical investigations of this model in the continuous regime are needed, but it should be important to test the universality of such a mechanism applying it to other kinetically constrained models, like the one by Kob-Andersen[54] or others[55].

Chapter 3

Inverse phase transitions on heterogeneous graphs

The relationship between model systems and the underlying topology is at the core of research in statistical mechanics. It is a common belief that the distinctive equilibrium features of simple model systems are affected only by the internal symmetries and by the dimensionality of the space. In this chapter it is shown that a certain degree of heterogeneity in the underlying structure of network of interactions can trigger inverse phase transitions in tricritical model systems.

Inverse phase transitions are striking phenomena in which an apparently more ordered phase becomes disordered by cooling. In the first paragraph there is a basic introduction to such phenomenon, with a special focus on inverse melting because of its relationship with some fundamental problems in statistical physics[56]. Then, there is a discussion about the simplest model system that shows inverse melting, i.e. the Blume-Capel model with higher degeneracy of interacting states[57]. Finally, I will show how inverse melting can emerge spontaneously in tricritical model systems if the underlying graph has certain features, i.e. if sparse subgraphs are crucial for its connectivity. I will work out many results[70] for the simple Blume-Capel model, and I will give some insights that the random field Ising model shares the same phenomenology.

3.1 Experimental inverse transitions

Inverse transitions in their most generic meaning have been detected in a number of different materials and between phases of different nature (see [57] and [58] for a review). The first experimentally seen inverse phase transition regards the miscibility properties of liquid mixtures[59]. Fig 3.1(left) shows the loop-shaped phase diagram of the solution Nicotine+ H_2O . A reentrant phenomenon is evident. The solution is mixed at a high temperature, it demixes by cooling and it gets mixed again by further cooling. Many different multicom-

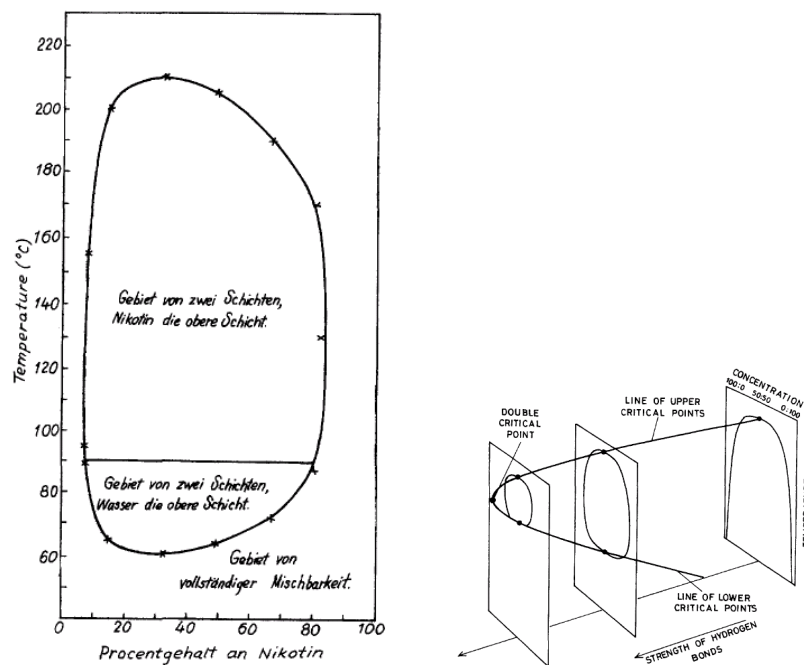


Figure 3.1: Left: experimental sketch of the looped miscibility phase diagram (T, c) of the solution Nicotine+ H_2O . From[59]. Right: sketch of the general miscibility phase diagram of a binary solution including the strenght of hydrogen bonds between unlike molecules as a third axis.

ponent solutions show this behavior[58]. The mechanism behind it relies on the strong directionality of hydrogen bonds between unlike molecules[60]. In the low temperature mixed phase, when unlike molecules interact, they form some complexes with a well defined orientation, thus freezing their internal rotational degrees of freedom. This in turn has the effect of lowering the total entropy with respect to the demixed phase. Therefore in this case demixing is basically an entropy driven process and the demixed phase is counter-intuitively more disordered.

At the beginning of the last century[62] speculations were put forward about the possibility of an *inverse melting*: a crystal that liquifies by cooling. This is confirmed nowadays experimentally on many substances, the most famous examples being the inverse melting of He_3 and He_4 at high pressures[56]. The interesting point is that in this case the standard ratio of the entropies of the solid and liquid phases is inverted, the solid being more disordered. In particular, at the point at which the inverse behavior starts, the entropies of the two phases are equal. This is a practical realization of the Kauzmann scenario[56] that I sketched in the second chapter. The specific heat of many substances in the

supercooled liquid phase is usually higher than the one of their crystalline phase. The decrease by cooling of the entropy of the supercooled liquid is steeper than the one of the crystal. Extrapolating it below the point at which the system gets out-of-equilibrium, the glass transition point, there should be a temperature at which they are equal. It should be possible that the liquid below this point has a lower entropy. This was seen as a paradox because it was believed that the ground state of a physical system made of identical objects should be a crystal. Many mechanisms were proposed to avoid this and some of them are at the core of theoretical views on the glass transition. However, the existence of inverse melting shows that in general this is not a paradox. It is true that a crystal can have an higher entropy than a less interacting phase. This can be explicitly pointed out in the polymer melts. A polymer can be in many microscopic configurations. The ground state is often unique, non-interacting and looped(see fig3.2). Thermal noise can unfold this structure, making the polymers interacting. All together they can form networks, i.e. a solid phase. A very well known case is the inverse melting of the crystal polymer made by the isotactic poly(4-methylpentene-1), P4MP1 (see fig3.2[63]).

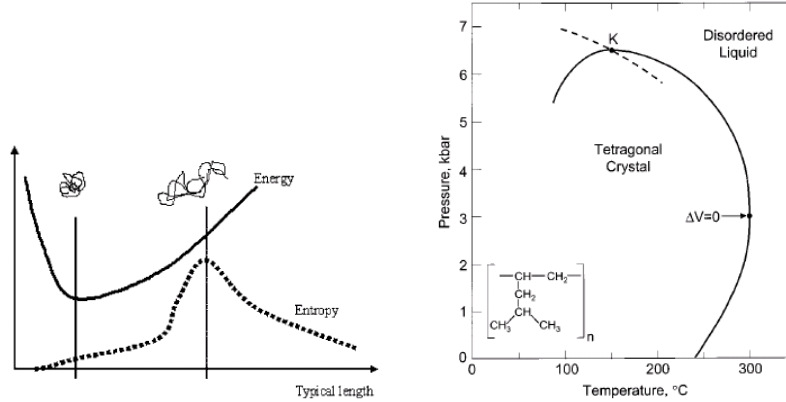


Figure 3.2: Left: Sketch of the energy and entropy of a polymer chain as a function of the length. Right: Sketch of the melting curve in the (T, p) plane for the polymer P4MP1.[63]

3.2 A simple model for inverse phase transition

Many mathematical models were proposed to explain how a phase transition can be inverted (see [57] and [61] for a review). In almost all of them the most interacting configuration of the units that made the system has by construction an higher degeneracy. The simplest model that can encode this feature is the Blume-Capel model. At first proposed to explain the occurrence of a first order

magnetic transition in the UO_2 [64], it became the representative of tricritical systems. It consists of N ferromagnetic interacting 1-spins $s_i = \pm 1, 0$ that have a cost in energy to be present, i.e a chemical potential Δ , the hamiltonian being:

$$H = - \sum_{\langle i,j \rangle} s_i s_j + \Delta \sum_i s_i^2 \quad (3.1)$$

Where the first sum is over the bonds of a given lattice. Inspired by the already seen phenomenology of inverse transition in polymer melts we can think of the interacting phase as having more degeneracy than the non-interacting one[57]. That is, we imposed by hand that the states with $s_i = \pm 1$ are $r \geq 1$ times more present of the ones with $s_i = 0$. We can recur to a mean field approximation, i.e. no spatial structure, by which every couple of spin is interacting. We rescale the interaction by $2N$. Using standard gaussian integral techniques it is possible to find the expression of the free energy:

$$\beta f = \frac{\beta m^2}{2} - \log(1 + 2r \cosh(\beta m) e^{-2\beta \Delta}) \quad (3.2)$$

Where m is the order parameter, the average magnetization, that can be found by minimizing f . This requires to solve the self consistent equation:

$$m = \frac{2r \sinh(\beta m)}{e^{\beta \Delta} + 2r \cosh(\beta m)} \quad (3.3)$$

There is always a solution $m = 0$. We can expand in powers of m :

$$m = Am + Bm^3 + \dots \quad (3.4)$$

When $A = 1$, another solution starts to occur, i.e. when

$$\beta = 1 + \frac{1}{2r} e^{\beta \Delta} \quad (3.5)$$

And the solution $m = 0$ becomes unstable, i.e. a maximum for f . The equation 3.5 defines thus consistently a curve of second order, continuous critical points, till $B < 0$. When B changes sign, at $T_c = \frac{1}{3}$, $\Delta_c = \log 4T_c$ there is a tricritical point, after which the transition becomes discontinuous. However, the eq.3.5 after this point continues to be the line of stability of the $m = 0$ solution, i.e. the spinodal curve of the paramagnets. It is possible to study numerically the stability of the other solution, thus defining the spinodal curve of the ferromagnetic solution. In the region between the two spinodal curves both the paramagnetic and ferromagnetic solutions are minima of the free energy. The transition is thus characterized by coexistence and hysteresis phenomena in this region. It is possible to compare the free energies of both solutions to characterize which one is stable (absolute minimum). In particular the Clasusius-Clapeyron equation is valid along the equilibrium curve :

$$\frac{d\Delta}{dT} = \frac{S_m - S_p}{\rho_m - \rho_p} \quad (3.6)$$

Where S is the entropy, $\rho = \langle s^2 \rangle$, and the labels m, p refers to the ferromagnetic and paramagnetic phase respectively. This equation shows that $\frac{d\Delta}{dT} > 0$ implies $S_m > S_p$. In fig 3.3 the phase diagram in the (Δ, T) plane is shown for $r = 6$. There it is possible to see clearly the emergence of a reentrant phenomenon with respect to the normal case ($r = 1$, in the inset) Inverse phase transitions can

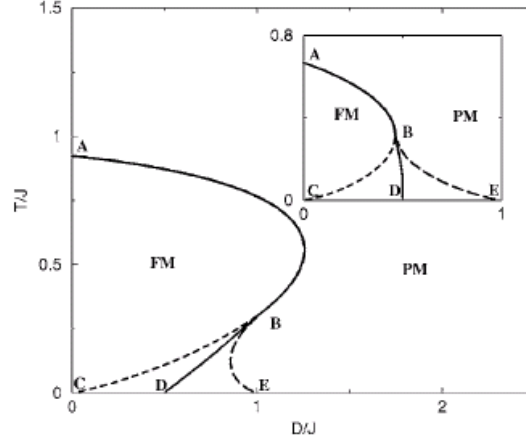


Figure 3.3: Phase diagram of the Blume-Capel model in the (Δ, T) plane with higher degeneracy of the interaction state $r = 6$. Inset: the same for the normal case $r = 1$.

emerge also *spontaneously* in tricritical model systems, without the assumption of an higher degeneracy of the interacting states. For instance, the spin glass version of the Blume Capel model, with ferromagnetic and *antiferromagnetic* couplings, shows inverse *freezing* [66] between glassy and fluid phases.

I will show in the next paragraph that inverse phase transitions can emerge spontaneously also in the normal, ferromagnetic, Blume-Capel model on heterogeneous structures.

3.3 Topology-induced inverse phase transition

Let's consider the Blume-Capel model now on a general heterogeneous graphs[70]. For random graphs of given degree distribution $P(k)$ it is possible to set up the following approximation scheme (Curie-Weiss). We consider the following Hamiltonian function:

$$H = -\frac{1}{2N} \sum_{i \neq j} h_i h_j s_i s_j + \Delta \sum_i s_i^2 \quad (3.7)$$

Where the h_i are independently identically distributed quenched random variables according to the distribution $P(k)$. This is equivalent to consider the

model on a fully connected geometry with link weights $a_{ij} = \frac{h_i h_j}{2N}$. The calculation follows along the lines sketched in the previous paragraph. Finally, we come up with self consistent equations for m , m_v , i.e. respectively the average magnetization of a randomly chosen node and that one of a node reached following a randomly chosen link:

$$m_v = \sum_k \frac{kP(k)}{z} \frac{2\sinh(\beta k m_v)}{e^{\beta\Delta} + 2\cosh(\beta k m_v)} \quad (3.8)$$

$$m = \sum_k P(k) \frac{2\sinh(\beta k m_v)}{e^{\beta\Delta} + 2\cosh(\beta k m_v)} \quad (3.9)$$

Where z is the average degree. The continuous critical line depends on the ratio between $\langle k^2 \rangle$ and z :

$$\beta \frac{\langle k^2 \rangle}{z} = 1 + \frac{1}{2} e^{\beta\Delta} \quad (3.10)$$

Then, at $T_c = \frac{1}{3} \frac{\langle k^2 \rangle}{z}$, $\Delta_c = \log 4T_c$ there is the tricritical point, after which the transition becomes discontinuous. We can define rescaled variables $\delta = \Delta \frac{\langle k \rangle}{\langle k^2 \rangle}$, $\tau = T \frac{\langle k \rangle}{\langle k^2 \rangle}$, such that the λ -line collapses on a master function:

$$\delta = \tau \log[2(1/\tau - 1)] \quad (3.11)$$

After the tricritical point, the line of first order phase transitions shows a striking difference between the homogenous and heterogeneous case, with the appearance of a reentrant phenomenon in the latter.

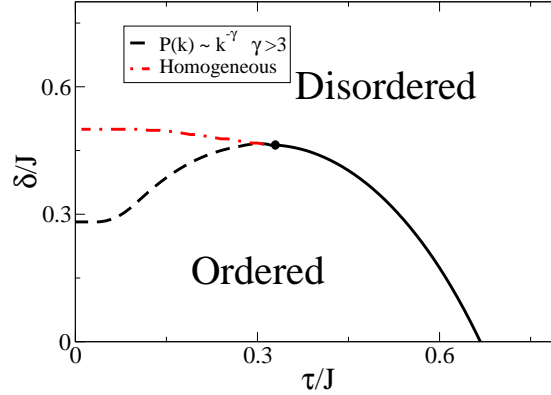


Figure 3.4: Phase diagram (δ, τ) of the Blume-Capel model within the Curie-Weiss approximation. The first order branch can be reentrant for heterogeneous networks

However, this approximation is not exact. But given the tree-like nature of random graphs it is possible to set up a better approximation (Bethe-Peierls).

In fact, we can write the partition function in a recursive way. Let's select one node and write the partition function as a function of the ones of the sub-branches from that node. The approximation relies in the factorised form, that is, independent sub-branches (no loops).

$$\mathbb{Z} = \sum_{s_0} e^{-\beta \Delta s_0^2} \prod_{j \in N_0} g_{0j}(s_0) \quad (3.12)$$

$$g_{ij}(s_i) = \sum_{s_j} e^{\beta(s_i s_j - \Delta s_j^2)} \prod_{k \in N_j, k \neq i} g_{jk}(s_j) \quad (3.13)$$

writing $g_{ij}(s_i) = A_{ij} e^{\beta(u_{ij}s_i - v_{ij}s_i^2)}$, we can solve for the u_{ij} , v_{ij} from the equations

$$x = \sum_{k \neq i} u_{jk}$$

$$y = \Delta + \sum_{k \neq i} v_{jk}$$

$$-2\beta v_{ij} = \log \frac{(1 + e^{-\beta y} 2 \cosh(\beta(x+1)))(1 + e^{-\beta y} 2 \cosh(\beta(x-1)))}{1 + e^{-\beta y} 2 \cosh(\beta x)} \quad (3.14)$$

$$2\beta u_{ij} = \log \frac{1 + e^{-\beta y} 2 \cosh(\beta(x+1))}{1 + e^{-\beta y} 2 \cosh(\beta(x-1))} \quad (3.15)$$

and get the magnetization per node

$$m_i = \frac{2 \sinh(\beta \sum_i u_{0i})}{e^{\beta(\Delta + \sum_i v_{0i})} + 2 \cosh(\beta \sum_i u_{0i})} \quad (3.16)$$

These equations can be solved for specific instances¹. Fig.3.5 shows for an heterogeneous random graph the transition curves $m(T)$ and the phase diagram as well, from both simulations and BP approximation scheme. The agreement is very good and the picture sketched previously by the CW is correct. A certain degree of heterogeneity for the graph can be responsible for reentrant phenomena and inverse phase transition in this model.

Is it possible to better characterize this “certain degree of heterogeneity”? Fig.3.5 also shows how a change in the exponent of the degree distribution can suppress this inverse phase transition.

Once again we can turn to the CW approach to get useful insights. The zero-temperature self consistent equation takes the form

$$m_v = \sum_k \frac{k}{z} P(k) \theta(k m_v - \Delta) \quad (3.17)$$

¹At low temperatures is convenient to observe that $T \log(1 + 2 \cosh(\beta x) e^{-\beta y}) \rightarrow f(x, y)$, where $f(x, y) = 0$ if $|x| < y$, $f(x, y) = |x| - y$ otherwise

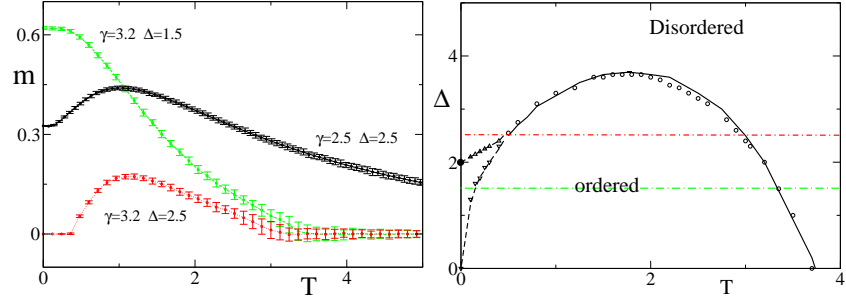


Figure 3.5: Inverse phase transition and reentrant phenomena in a heterogeneous random graph of size $N = 10^4$, with degree distribution $P(k) \propto k^{-\gamma}$, $\gamma = 3.2$ and $k_{min} = 2$. Left: Transition curves $m(T)$. For large enough Δ there is a reentrant phase transition, that is dumped for a different exponent $\gamma = 2.5$. Right: Phase diagram. From Monte carlo simulations (points) and BP numerical calculations (lines).

It is interesting to observe that in this approximation there is a degree $k^* = \frac{\Delta}{m_v}$ such that nodes with connectivity $k > k^*$ have $m_k = 1$, while for the others $m_k = 0$. The fact that nodes with different connectivities can be in different phases can be easily checked for a bimodal random graph. Fig. 3.6 shows the transition curves $m(T)$ at $\Delta = 3$ of the components of a bimodal random graph with connectivity distribution $P(k) = 0.2\delta_{k10} + 0.8\delta_{k2}$. The nodes with degree 2 show a reentrant phase transition, while the high degree nodes go to a value slightly less than 1 at zero temperature.

This suggests that the reentrant phenomenon can be ascribed to a mechanism by which low degree nodes are “turned off” at low temperature because they are frozen in the $s_i = 0$ state by the effect of the chemical potential Δ . This in turn can lower the connectivity of their neighbours, with a cascade effect that can disconnect some parts of the graph. For nodes of degree 2 this argument can be worked out rigorously. The effective interaction transmitted by a node of degree 2 between its ends depends on the temperature and it can be calculated with the use of the simplest renormalization group scheme:

$$2\beta J_{eff} = \log\left(\frac{1 + 2e^{-\beta\Delta} \cosh(2\beta)}{1 + 2e^{-\beta\Delta}}\right) \quad (3.18)$$

Fig 3.7 shows its non-monotonous behavior for $\Delta > 2$.

This argument suggests that also the role of degree-degree correlations of the graph can be crucial for the collective behavior of such model system. The degree correlations of a network can be quantified by the assortativity:

$$r = \frac{\langle kk' \rangle_l - \langle (k + k')/2 \rangle_l^2}{\langle (k^2 + k'^2)/2 \rangle_l - \langle (k + k')/2 \rangle_l^2} \quad (3.19)$$

Where $\langle \rangle_l$ denotes an average over the links, and (k, k') denotes the degree of

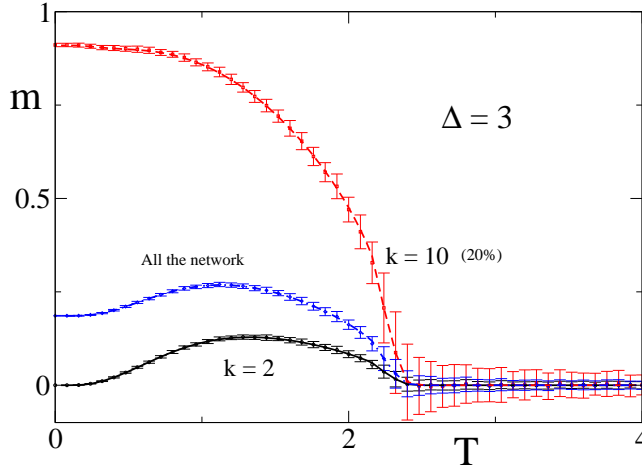


Figure 3.6: Transition curves $m(T)$ for the different components of a bimodal random graph. From Monte carlo simulations(points) and BP numerical calculations(lines).

the nodes at either end of links.

It is possible to obtain a graph with a given degree distribution and assortativity r along the lines of the following exponential random graph model[65]. Let's Suppose that we want to construct a network model specified by an observable x . We can think of an ensemble in which the probabilistic weight of a given network G is $P(G) \propto e^{-H(G)}$, where $H(G) = \theta x(G)$ and θ should be such that x is equal to the desired value. Then a suitable monte-carlo scheme has to be adopted to sample the network ensemble. In our case $x = r$ and $H = -\theta/2 \sum_{\langle i,j \rangle} k_i k_j$, if the degree distribution is fixed. We can think of the following mixing procedure (see fig3.8). Two links are randomly drawn (a, b) and (c, d) and are substituted by the new links (a, c) and (b, d) with probability $P = \min\{1, \exp(-\theta(k_a - k_d)(k_c - k_b))\}$. This update rule verifies the detailed balance and doesn't change the degree of the nodes. The effects of this procedure are shown graphically in 3.8 for a small network.

Fig.3.9 shows the transition curves $m(T)$ at $\Delta = 3$ of the different components of the previous bimodal graph after this mixing procedure ($\theta = -1$, disassortative mixing). This time the fact that the low degree nodes are turned off at decreasing temperature is enough to disconnect the whole graph of interactions, tuning a reentrant phase transition. This mechanism for reentrance based on the freezing of sparse subgraphs can give an explanation of the different behaviors observed in the left part of fig.3.5. It is the case that random graphs with a power law degree distribution have qualitatively different structures if the value of the exponent γ is above or below 3. In fact, the number of short loops in a network with $\gamma < 3$ is big. These networks are more clustered and

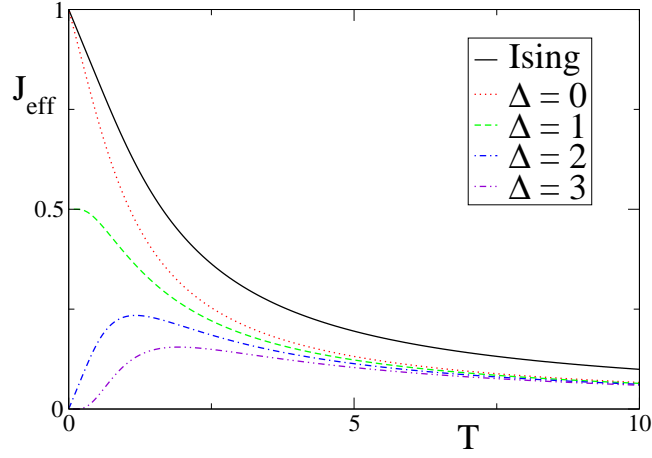


Figure 3.7: Effective interaction $J_{eff}(T)$ between the ends of a node of connectivity 2 as a function of the temperature for several Δ .

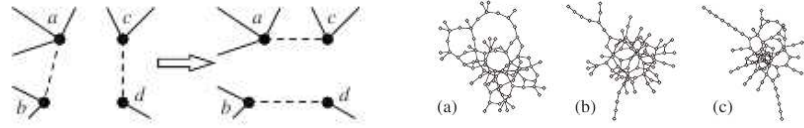


Figure 3.8: Left: a sketch of the rewiring procedure. Right: Its application onto a network of 100 nodes. a is disassortative ($\theta = -1$), b uncorrelated and c is assortative ($\theta = 1$). From [65].

sparse subgraphs should not be crucial for their connectivity, as it should be the case if $\gamma > 3$ [67].

3.4 Conclusions

In this chapter I showed how an inverse phase transition can emerge spontaneously in the Blume-Capel without recurring to an higher degeneracy of the interacting state. I showed a mechanism that trigger this phenomenon, based on the freezing of sparse subgraphs. If they are crucial for the connectivity, the overall graph of interactions can be disconnected by cooling. It should be the case that this picture is correct in general for tricritical model system and I will give some hints about this mechanism at work also for the random field ising model.

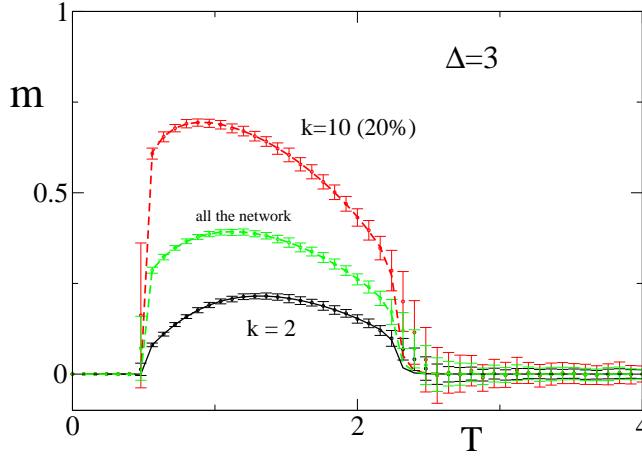


Figure 3.9: Transition curves $m(T)$, $\Delta = 3$ onto a disassortative bimodal random graph of size $N = 10^4$. From Monte carlo simulations(points) and BP numerical calculations(lines).

The random field ising model

In this model, ferromagnetic interacting Ising spins $s_i = \pm 1$ are subject to local quenched fields, the hamiltonian being:

$$H = - \sum_{\langle i,j \rangle} s_i s_j + \sum_i h_i s_i \quad (3.20)$$

The h_i are i.i.d. random variables, distributed in a bimodal fashion $p(h_i) = 1/2(\delta_{h_i,h} + \delta_{h_i,-h})$. This model was introduced to study disordered magnets and it is the minimal model to describe phase transition in systems that show *crackling noise*[68]. The response of this model to time-varying external field has three regimes:

- At high h the system responds as a paramagnet, i.e. its magnetization follows the external field in a continuous way.
- At low h the system responds as a magnet. It responds as a paramagnet for high T and as a ferromagnet for low T , i.e. the magnetization jumps discontinuously depending on the sign of the external field.
- At intermediate h the magnetization follows the external field with little jumps. The spin flip dynamics is characterized by avalanche events whose size in scale free[69].

The dynamics of each spin is the result of a possible competition between the local field and the effective field coming from the interaction with the neighbors.

The study of the model on a general random graph with degree distribution $P(k)$ follows the same lines of the Blume-Capel model. Hence, in the Curie-Weiss scheme, we have the self consistent equations for m , m_v , i.e. respectively the average magnetization of a randomly chosen node and that one of a node reached following a randomly chosen link:

$$m_v = \frac{1}{2} \sum_k \frac{kP(k)}{z} (\tanh(\beta(km_v + h)) + \tanh(\beta(km_v - h))) \quad (3.21)$$

$$m = \frac{1}{2} \sum_k P(k) (\tanh(\beta(km_v + h)) + \tanh(\beta(km_v - h))) \quad (3.22)$$

In general, expanding in power of m_v the rhs, we can find the critical second order λ -line $\beta \frac{\langle k^2 \rangle}{z} = \cosh^2(\beta h)$, until $\tanh^2(\beta h) < \frac{1}{3}$. Then, at $T_c = 2/3 \frac{\langle k^2 \rangle}{z}$, $h_c = T_c \tanh^{-1}(1/\sqrt{3})$ there is a tricritical point, after which the transition becomes first-order. Again, for a power law degree distribution a reentrant phase diagram is found (fig.3.10, left).

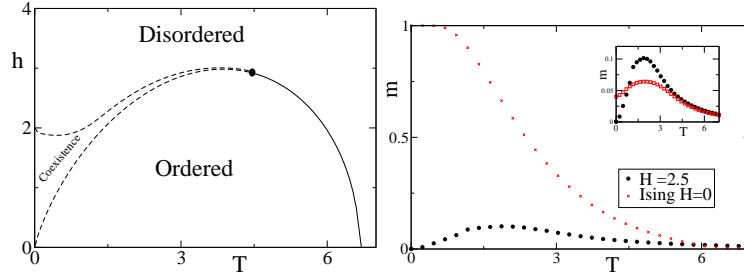


Figure 3.10: Left: phase diagram (T, h) for the random field Ising model on a random graph with degree distribution $P(k) \propto k^{-3.2}$, $k_{min} = 2$ $k_{max} = 100$. From CW approximation. Right: transition curves from BP calculations. The inset shows $m(T)$ ($H = 2.5$) for different microscopic realizations of the quenched local fields.

It is possible to set up a BP approach to improve this approximation. We have the recursive equations for the partition function:

$$\mathbb{Z} = \sum_{s_0} e^{\beta h_0 s_0} \prod_{j \in N_0} g_{0j}(s_0) \quad (3.23)$$

$$g_{ij}(s_i) = \sum_{s_j} e^{\beta(s_i s_j + h_j s_j)} \prod_{k \in N_j, k \neq i} g_{jk}(s_j) \quad (3.24)$$

Then we can write $g_{ij}(s_i) = A_{ij} e^{\beta u_{ij} s_i}$ and we have the equations:

$$2\beta u_{ij} = \log\left(\frac{\cosh(\beta(1 + h_j + \sum_{k \neq i} u_{jk}))}{\cosh(\beta(-1 + h_j + \sum_{k \neq i} u_{jk}))}\right) \quad (3.25)$$

from which we can get the magnetization per node $m_0 = \tanh(\beta(h_0 + \sum_i u_{0i}))$. Fig.3.10 (right) shows the transition curves $m(T)$ for a random graph with degree distribution $P(k) \propto k^{-3.2}$, $k_{min} = 2$, $N = 10^4$. At $H = 2.5$ there is a weak reentrant phenomenon, but the form of the curves $m(T)$ is strongly dependent on the microscopic realization of the quenched local fields(inset). However the phase diagram of this model has a complex structure of singularities even on homogeneous graph[71] and further investigations are needed.

Chapter 4

Volatility and evolution of social networks

The idea of applying methods and concepts from natural science, in particular statistical physics, to the study of social systems has a long history[72].

Many social and economic phenomena have an inherent network dimension[73]. The question of embedness of such phenomena in *social networks* has been addressed directly only in recent times, because of the recent technological development in storing and handling large dataset of informations.

Social networks have complex structures that are evolving in time. In particular, the same kind of network can show qualitatively different structures, sparse and disconnected *vs* dense and connected.

After a brief introduction on the structure and evolution of social networks, we will present the mechanism of coevolution to model their formation through a class of models proposed by G.Ehrhardt et al[90]. In these, the evolution of the network is coupled with the dynamics defined on top of it. A feedback effect can trigger the appearance of different phases, disordered and disconnected in clusters or ordered and connected, respectively, in a discontinuous way.

Within the simplest model of this class, I will show how the kind of volatility, i.e. the rate at which nodes and/or links disappear, affects the evolution of the network[91]. It is found that when the volatility is mostly node-based the emergence of an ordered phase is definitively suppressed.

4.1 Complex social networks

The recent surge of interest of the worldwide public opinion on social networks perhaps has its motivations in the spreading of virtual settings like Facebook. Anyway, the network dimension is important in many concrete aspects of social and economic life. Examples range from informal contacts in labour market [75] and peer effects in promoting (anti-)social behaviors [83] to inter-firm agreement for R&D [85]. This issue of embeddedness was addressed in early times[80],

but only recently it is possible to deal with it in practice thanks to the recent technological development in informatics.

Let's consider as an example the question of the social dimension in science research. Some insights about it can be gained from the study of coauthorship networks. Here the nodes are scholars, that are connected by a link if they wrote a paper together. Ref.[76] reports on the analysis of:

- A network of coauthorship of papers in the Medline bibliographical database from 1995 to 1999. Medline is a widely used and compendious database for covering biomedical research.
- A networks of coauthorships of physicists assembled from papers posted on the widely used Physics E-print archive at Cornell university between 1995 and 1999.
- A collaboration network of mathematicians compiled from databases maintained by the journal *Mathematical Reviews*, covering the period from 1940 to the present without break, from [77].

	Biology	Physics	Mathematics
Number of authors	1,520,251	52,909	253,339
Number of papers	2,163,923	98,502	—
Papers per author	6.4	5.1	6.9
Authors per paper	3.75	2.53	1.45
Average collaborators	18.1	9.7	3.9
Largest component	92%	85%	82%
Average distance	4.6	5.9	7.6
Largest distance	24	20	27
Clustering coefficient	0.066	0.43	0.15
Assortativity	0.13	0.36	0.12

decade	1970s	1980s	1990s
total authors	33770	48608	81217
average degree	.894	1.244	1.672
standard deviation of degree	1.358	1.765	2.303
size of giant component	5253	13808	33027
—as percentage	.156	.284	.407
second largest component	122	30	30
isolated authors	16735	19315	24578
—as percentage	.496	.397	.303
clustering coefficient	.193	.182	.157
average distance in giant component	12.86	11.07	9.47
standard deviation of distance in giant component	4.03	3.03	2.23

Figure 4.1: Top: statistical features of the coauthorship networks analyzed in [76]. Bottom: Evolution of the statistical features of the coauthorship networks of economists analyzed in [84]

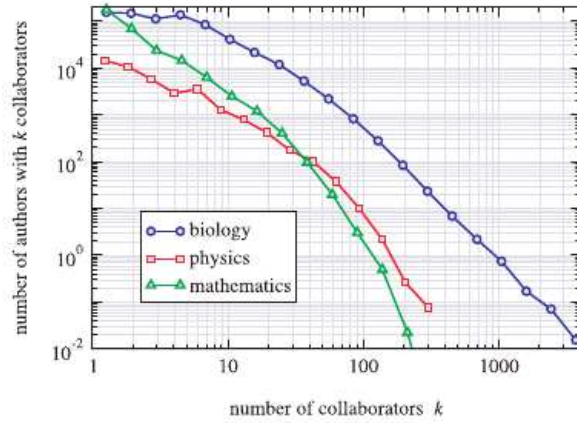


Figure 4.2: Distribution of the number of collaborators per scientists in the coauthorship networks analyzed in [76]

A summary of the basic statistics of these networks is given in table 4.1¹. These reveal many interesting features about academic communities. All the three communities have a largest connected component that cover the great part of the graph, with rather small average distances and diameters. The statement of scientific research as a common and collective enterprise immediately comes up in a graphical way. The average number of authors per paper and the average number of collaborators is bigger in biology and smaller in mathematics, with physics in between. This should be presumably a result of different methods of research. Biological research in fact consists mostly of experimental work by large groups of laboratory scientists. Mathematical research instead consists of theoretical work done primarily by individuals alone or by pairs of collaborators. Physics should be a combination of the two. The distribution of collaborators per scientists is shown in fig.4.2. They all show fat-tails, showing the presence of few scientists with a lot of collaborations and probably having in them a leading role. The average clustering coefficients, i.e. the probability that two collaborators of a researcher are collaborators themselves are also rather different in different fields. This is very high in physics 0.43, and quite low in biology 0.06. The finer details of these networks show moreover interesting community structures[78](see e.g. fig 4.3).

Finally, these networks are subject to a dynamical evolution. The evolution of the coauthorship networks of economists from the Econlit database is analyzed in [84]. The basic statistical features are shown again in fig.4.1(bottom). The largest connected component is growing, with emerging features similar to the previous cases, and the authors state of the research in economy as an *emerging*

¹There are no precise data about the number of papers in the mathematics database. However, according to [77] they should be around 1.6 million.

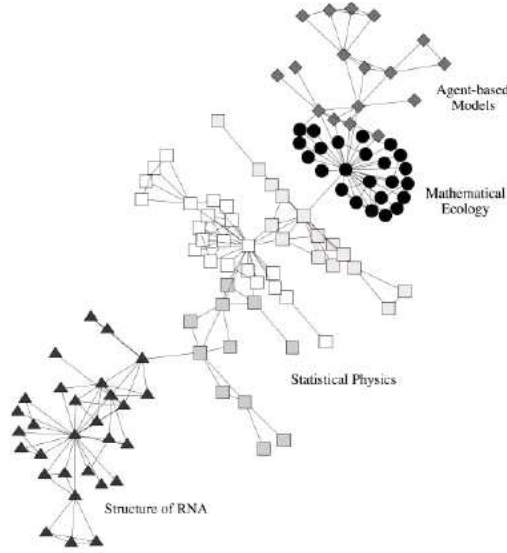


Figure 4.3: The largest component in the network of collaborations in the Santa Fe institute. From[78]

small world, as it is called a compact network, whose diameters and average distances are small with respect to the size.

If the analysis of the structure of large and complex social networks needs statistical methods, the analysis of their evolution can gain insights from statistical mechanics modeling.

4.2 Models of co-evolving networks

The competition between order and disorder is by no means restricted to physics[79]. Also economies and societies – as systems of many interacting individuals – organize themselves in different (macroscopic) states, with different degrees of order – informally interpreted as coordination on social norms, compliance with laws or conventions [74]. Besides all its inherent complexity, one important element of additional richness is that the relation between the degree of order in a society and the cohesion of the underlying social network is not unidirectional as in physics, where the topology of interactions is fixed. The structure of the networks in these phenomena is dynamically shaped by incentives of agents (nodes), be they individuals or organizations, who establish bilateral interactions (links) when profitable. In addition, this interplay typically takes place in a volatile environment. That is, the favourable circumstances that led at the same point to the formation of a particular link may later on deteriorate,

causing the removal or rewiring of that link. This combination of factors raises a number of interesting issues in statistical physics, as the collective behavior of the interacting degrees of freedom may radically change when they are coupled to the dynamics of the network they are defined on.

I will review here the results of ref.[90]. In all the models defined there, the feedback between nodes and networks dynamics arises from assuming that the formation of a link requires some sort of similarity or proximity of the two parties. This captures different situation. For example, in cases where trust is essential in the establishment of new relationships (e.g. in crime or trade networks), linking may be facilitated by common acquaintances or by the existence of a chain of acquaintances joining the two parties. In other cases (e.g. in R&D or scientific networks) a common language, methodology, or comparable level of technical competence may be required for the link to be feasible or fruitful to both parties. This class of models reveals a generic behavior characterized by a discontinuous transition from an uncoordinated state characterized by a sparse network, to a coordinated state on a dense network. As discussed in Ref. [90], this agrees with anecdotal evidence on the observation of sharp transitions[84],[85] and resilience properties[86],[87] of some social networks. However, our focus here will be mostly on the statistical phenomenon, than on its interpretation in socio-economic terms, given that the phenomenology bears a formal similarity with the liquid-gas transition.

Consider a population of N agents. They form the nodes $i = 1, \dots, N$ of a network that is described by an undirected graph. The formation and destruction of links proceeds by the following steps:

- Each node i attempts to establish a new link with a randomly chosen node j at rate η .
- Given a notion of a *social distance* d_{ij} between nodes i and j , if $d_{ij} \leq \bar{d}$ the link is formed, otherwise it is formed with probability ϵ .
- Links are destroyed at rate λ

It is possible to set up a mean field approximation. It consists in neglecting degree correlations between neighbouring nodes, i.e. we approximate the network with a random graph. Random graphs are characterized only by their degree distribution $P(k)$. We make the hypothesis that the $p(k)$ satisfies a master equation whose rates are:

$$w(k \rightarrow k-1) = \lambda k \quad (4.1)$$

$$w(k \rightarrow k+1) = 2\eta(\epsilon + (1-\epsilon)P(d_{ij} \leq \bar{d})) \quad (4.2)$$

The factor 2 comes because each node can either initiate or receive a new link. The definition of the social distance should depend upon the specific phenomena we are looking at.

A first simple specification can be with d_{ij} being the geodetic distance on the graph, and $\bar{n} = N - 2$. This describes a situation in which the formation

of new links is strongly influenced by proximity on the graph. If i and j are in different components the rate of link formation is $2\epsilon\eta$, otherwise is 2η . In the large N limit the latter only occurs if the graph has a giant component with a finite fraction γ of the nodes. For random graphs (see e.g. [73]) $\gamma = 1 - \phi(u)$, where $\phi(s) = \sum_k p(k)s^k$ is the generating function, and u is the probability that a link, followed in one direction, does not lead to the giant component. This latter satisfies

$$u = \phi'(u)/\phi'(1) \quad (4.3)$$

Hence u^k is the probability that an agent with degree k is not in the giant component, and then

$$w(k \rightarrow k+1) = 2\eta(\epsilon + (1-\epsilon)\gamma(1-u^k)) \quad (4.4)$$

The stationary state condition brings the equation for ϕ :

$$\lambda\phi'(s) = 2\eta(\epsilon + (1-\epsilon)\gamma)\phi(s) - 2\eta(1-\epsilon)\gamma\phi(us) \quad (4.5)$$

which can be solved numerically to the desired accuracy. The solution of this equation is summarized in fig.4.4. Either one or three solutions are found, depending on the parameters. In the latter case the intermediate solution (dashed line in fig.4.4) is unstable and it separates the basins of attraction of the two stable solutions within this mean field approach. The solution is exact when there is no giant component, and numerical simulations show that the approach is very accurate away from the phase transition.

Next let's consider a setup in which d_{ij} reflects the proximity of nodes in terms of some continuous, non negative attributes h_i . In short, the attributes could represent the level of technical expertise of two firms involved in a R&D partnership, or the competence of two researchers involved in a joint project. Each agent updates his attribute h_i with a rate ν , that we suppose much larger than λ and η . Let's explore a setting of *best practice* imitation (BP) where individuals aim at improving in the direction of increasing h_i by on site efforts and by learning from their neighbors. We posit that $h_i(t^+) = \max_{N_i}\{h_j(t)\} + \eta(t)_i$, where η_i are i.i.d. gaussian random variables with zero mean and variance Δ , that capture idiosyncratic change of expertise due to i 's own (say research) efforts. We set the distance $d_{ij} = |h_i - h_j|$. Fig 4.5 reports typical results of simulations of this model. As in the previous model, there is a discontinuous transition between a sparse and dense network state, characterized by hysteresis effects. In the stationary state $h = \langle h_i \rangle$ grows linearly in time with velocity v . Notably the growth is much faster in the dense state than in the sparse one. This model exhibits an interplay between the process on the network, i.e. the dynamics of the h_i and the network evolution. It is this interdependence and the corresponding positive feedback that produces the discontinuous transition and phase coexistence.

The last specification I consider is such that link formation requires some form of coordination or compatibility. For example, a profitable interaction may fail to occur if the two parties do not speak the same language and/or do not

adopt compatible technologies or standards. We can characterize each agent i with a variable σ_i which represents the social norm (convention or technological standard) adopted. There are q possible social norms, i.e. $\sigma_i \in \{1, \dots, q\}$. I will call them colors. We impose that the formation of a new link between i and j requires that $\sigma_i = \sigma_j$. The color of a node is updated with rate ν to the color of any of its neighbors, unless the node is isolated. In the latter case the nodes takes a random color. In terms of statistical physics, the model can be thought of as a q state Potts model defined on a graph of N nodes, with $T = 0$, that evolves in a coupled fashion to the dynamics of the system. This model is solved exactly in [90], but given its simplicity, we will see in the next paragraph how to generalize it to take into account the possibility of agents' turnover, i.e. a node-based volatility.

4.3 Node-based volatility

Indeed, the effect of volatility was up to now limited to link removal, but the turnover of agents (i.e. node removal and arrival) may be an important factor in many real systems. In order to investigate this question, we concentrate

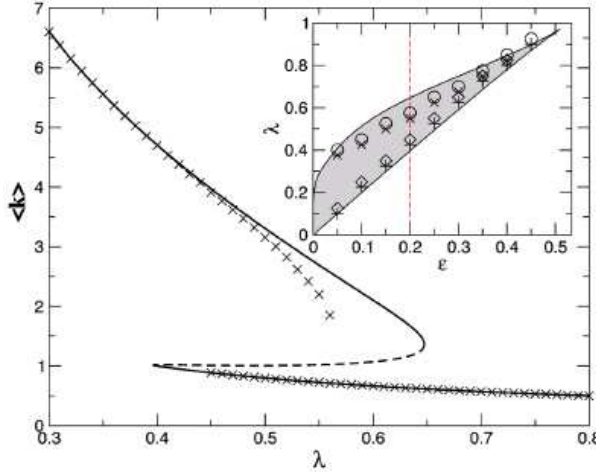


Figure 4.4: Mean degree $\langle k \rangle$ as a function of λ for $\epsilon = 0.2, \eta = 1$, when d_{ij} is the distance on the graph and $\bar{d} = N - 2$. Lines are from mean field theory, points from simulations, starting from both low and high connected phases. Inset: phase diagram from the mean field. Coexistence occurs within the shaded region, whereas above(below) only the sparse(dense) state is stable. Numerical simulation agree qualitatively. The high(low) density state is stable up (down) to the points marked with X (\diamond) and is unstable at points marked with O ($+$). From [90]

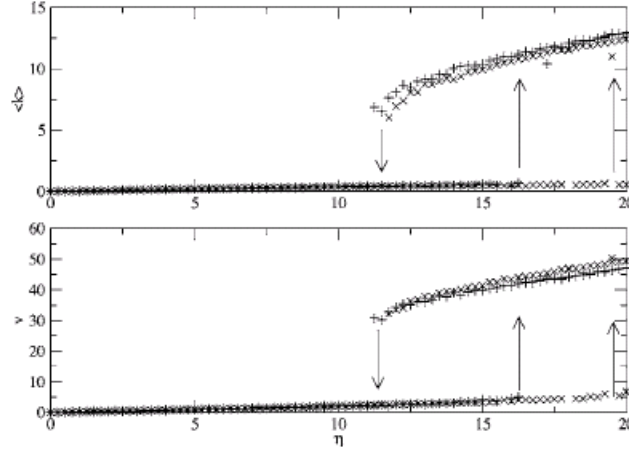


Figure 4.5: Mean degree $\langle k \rangle$ and growth rate v as a function of η from numerical simulations of the BP model. Shown are simulations with $N = 500$ (plusses) and 1000 (crosses). Arrows denote the approximate point at which the system jumps from one phase to the other. Here $\epsilon = 0.001$, $\Delta = 0.1$ and similarity threshold $\bar{d} = 2$. From [90]

on the simplest model for which a full analytic treatment is possible. In the concluding section, we argue that this qualitative change is expected in a wider class of model, and it can have much stronger effects. I consider the model of coordination sketched in the end of the last paragraph, but I generalize it, considering the possibility that with rate α all the links of a node disappear. This will show how the alternative assumptions of link or node based volatility have profound effects on the dynamics of network formation[91]. In the following I set for sake of simplicity $\lambda = 1$ and I rescale by a factor 2 the link creation rate η .

Therefore, the parameter α interpolates between two kinds of volatility. For $\alpha = 0$ volatility only affects links and for $\alpha \gg 1$ it mostly affects nodes. As observed in Ref. [90], the color update rule is effective only for isolated nodes, in the long run, and in that case the color is drawn at random. Since only links between same type agents are created, after a transient all nodes are either isolated, or connected to nodes of the same color. Therefore the particular way in which the neighbor is chosen is immaterial. For example, both a majority rule (most frequent color) or a voter-type rule (random neighbor) would give the same dynamics. The model can be generalized to a probabilistic update rule for the colors introducing a finite temperature T (see [90]). Results do not change considerably as long as T is small enough, so we shall confine ourselves to the $T = 0$ case.

Ref. [90] has shown that for $\alpha = 0$, the system shows an hysteretic transition

in η from a symmetric to an asymmetric state². The symmetric state is characterized by a sparse network, with average degree $\langle k \rangle < 1$, with a symmetric distribution of colors. In the asymmetric state, instead, a dense network with $\langle k \rangle > 1$ arises, along with a dominant color, which is adopted by agents more frequently than the others. All the colors are a priori equivalent and the fact that only one is selected is a simple example of a *spontaneous symmetry breaking*. The dominant component is selected by random fluctuations and is stabilized by the feedback mechanism between link formation (which is more frequently successful for nodes of the dominant component) and the freezing of the colors of connected nodes (akin to the ferromagnetic interaction in Potts models). In this sense, the model shows how order and disorder are intimately related with the dynamics of the social network in a volatile environment.

In what follows, we solve the model in the stationary state for $N \rightarrow \infty$, for all the values of α . We find that the $\alpha = 0$ behavior is generic for all $\alpha < 1$, but the transition is softened as α increases. For $\alpha > 1$ instead we show that the system is always in the symmetric phase. Hence, in terms of statistical mechanics, $\alpha = 1$ is a second order critical point separating a phase with spontaneously broken symmetry from a symmetric phase.

If we call $n_{k,\sigma}$ the density of nodes with k links and color $\sigma = 1, \dots, q$ we have the following rate equations:

$$\begin{aligned} \dot{n}_{k,\sigma} = & (k+1)n_{k+1,\sigma} - kn_{k,\sigma} - \alpha n_{k,\sigma} + \\ & + x_\sigma(n_{k-1,\sigma} - n_{k,\sigma}) \end{aligned} \quad (4.6)$$

$$\begin{aligned} \dot{n}_{0,\sigma} = & \alpha \sum_{k>0} n_{k,\sigma} + n_{1,\sigma} - x_\sigma n_{0,\sigma} + \\ & + \frac{\nu}{q} \sum_{\sigma'=1}^q (n_{0,\sigma'} - n_{0,\sigma}) \end{aligned} \quad (4.7)$$

where, for future convenience, we have introduced the dynamical variables

$$x_\sigma = \eta \sum_{k=0}^{\infty} n_{k,\sigma}. \quad (4.8)$$

Making the sum over all k of these equations and multiplying by η we find

$$\dot{x}_\sigma = \frac{\eta\nu}{q} \sum_{\sigma'=1}^q (n_{0,\sigma'} - n_{0,\sigma}) \quad (4.9)$$

which implies that, in the stationary state, each component has the same fraction $n_{0,\sigma} = n_0/q$ of disconnected ($k=0$) nodes. it is straightforward to derive an equations for the characteristic functions $\pi_\sigma(s)$ of the degree distribution $p_\sigma(k) = n_{k,\sigma} / \sum_q n_{k,\sigma}$ of the component σ . In the stationary state this reads:

$$(1-s) \frac{d\pi_\sigma}{ds} = [\alpha + x_\sigma(1-s)]\pi_\sigma(s) - \alpha. \quad (4.10)$$

²I will recover it as a special case

The stationary solution is found by direct integration:

$$\pi_\sigma(s) = \alpha \int_0^1 dz z^{\alpha-1} e^{-x_\sigma(1-s)(1-z)} \quad (4.11)$$

It is easy to see that this interpolates between a Poisson distribution, $\pi_\sigma(s) = e^{x_\sigma(s-1)}$ for $\alpha \rightarrow 0$, which coincides with the result of Ref. [90], and an exponential distribution $\pi_\sigma(s) = \alpha/[\alpha + x_\sigma(1-s)]$ for $\alpha \rightarrow \infty$. The latter limit is derived upon changing variables to $y = z^\alpha$ in Eq. (4.11) and expanding $1 - y^{1/\alpha} \simeq -\frac{1}{\alpha} \log y$ in the argument of the exponential. Notice also that the average degree in component σ is $\langle k \rangle_\sigma = \pi'_\sigma(1) = x_\sigma/(1+\alpha)$. This is precisely what one expects from balance of link creation and destruction of links in component σ .

Observing that $\pi_\sigma(0) = \eta \frac{n_{0,\sigma}}{x_\sigma} = \frac{\eta n_0}{q x_\sigma}$ we find an equation for x_σ in the stationary state, which reads

$$G_\alpha(x_\sigma) \equiv \alpha x_\sigma \int_0^1 du u^{\alpha-1} e^{x_\sigma(u-1)} = \frac{\eta n_0}{q}. \quad (4.12)$$

Notice that the r.h.s. of Eq. (4.12) is independent of σ . The variables x_σ are determined by Eq. (4.12) and the normalization condition, which takes the form

$$\sum_{\sigma=1}^q x_\sigma = \eta. \quad (4.13)$$

The properties of the solutions of Eqs. (4.12,4.13) depend on the behavior of the function $G_\alpha(x)$, which are discussed in the appendix, and can be classified in symmetric and asymmetric solutions.

4.3.1 $\alpha > 1$: The symmetric solution

For $\alpha > 1$ the function $G_\alpha(x)$ is a monotone increasing function.

The function $G_\alpha(x)$ can be written as

$$G_\alpha(x) = \alpha \int_0^x dz \left(1 - \frac{z}{x}\right)^{\alpha-1} e^{-z}$$

For $\alpha > 1$ we have

$$\frac{dG_\alpha}{dx} = \frac{\alpha(\alpha-1)}{x^2} \int_0^x dz z \left(1 - \frac{z}{x}\right)^{\alpha-1} e^{-z} > 0$$

Hence Eq. (4.12) has a single solution and Eq. (4.13) implies that $x_\sigma = \eta/q$ for all components σ . Notice also that

$$\frac{d}{dx} \frac{G_\alpha(x)}{x} = -\alpha \int_0^1 du u (1-u)^{\alpha-1} e^{-ux}$$

i.e. $n_0 = G_\alpha(\eta/q)/(\eta/q)$ in the symmetric solution is a decreasing function of η/q . In addition $G_\alpha(x) \simeq x$ for $x \ll 1$, i.e. $n_0 \rightarrow 1$. Hence Eq. (4.12) yields the total fraction of disconnected nodes

$$n_0 = \frac{q}{\eta} G_\alpha(\eta/q)$$

as a function of the parameters q, α and η . We can analyze the stability of the symmetric solution recalling that $\eta n_{0,\sigma} = G_\alpha(x_\sigma)$. Then Eq. (4.9) becomes a dynamical equation for x_σ

$$\dot{x}_\sigma = \frac{\nu}{q} \sum_{\sigma'=1}^q [G_\alpha(x_{\sigma'}) - G_\alpha(x_\sigma)]. \quad (4.14)$$

Linear stability of the symmetric solution is addressed by setting $x_\sigma = \eta/q + \epsilon_\sigma$, with $\sum_\sigma \epsilon_\sigma = 0$. Then to linear order

$$\dot{\epsilon}_\sigma = \frac{\nu}{q} G'_\alpha(\eta/q) \sum_{\sigma'=1}^q [\epsilon_{\sigma'} - \epsilon_\sigma] = -\nu G'_\alpha(\eta/q) \epsilon_\sigma. \quad (4.15)$$

Hence, as long as $G_\alpha(x)$ is an increasing function of x , the symmetric solution is stable. This is always the case for $\alpha > 1$, as we shall see, it fails to hold for $\alpha < 1$.

4.3.2 $\alpha < 1$: The asymmetric solution

For $\alpha < 1$ the symmetric solution still exists. However the function $G_\alpha(x)$ now has a maximum for some $x_0(\alpha)$ and $G_\alpha(x) \rightarrow \alpha$ from above as $x \rightarrow \infty$. Therefore the symmetric solution becomes unstable when $\eta > \eta_+$ where

$$\eta_+ \equiv q x_0(\alpha) \quad (4.16)$$

because beyond that point $G'_\alpha(\eta/q) < 0$.

The occurrence of a maximum in G_α also implies that Eq. (4.12) admits solutions with $x_\sigma = x_- < x_0(\alpha)$ for some σ 's and $x_\sigma = x_+ > x_0(\alpha)$ for the other components. Since x_σ is related to the density of a component σ , we shall call a component dense if $x_\sigma = x_+$ and diluted if $x_\sigma = x_-$. As in Ref. [90], all solutions with more than one dense component are unstable. Indeed, by the same argument used to analyze the stability of the symmetric solution, a perturbation with $\epsilon_\sigma = 0$ for all diluted components would grow as $\dot{\epsilon}_\sigma = -\nu G'_\alpha(x_+) \epsilon_\sigma$ on all dense components. These unstable modes correspond to density fluctuations across dense components. Once one of these components acquires slightly more mass, the density of links in it increases, which makes it less likely for nodes in this component to become isolated. At the same time, this component will recruit isolated nodes at a slightly faster pace, due to its larger density. It is then intuitively clear that the initial density perturbation will grow unboundedly.

These unstable modes ($G'_\alpha(x_+) > 0$ implies $\dot{\epsilon}_+ > 0$) are clearly absent in the solution with only one dense component. These are the asymmetric solutions we shall focus on in what follows. There are q of them, depending on which color is associated with the dense component. The variables x_\pm are determined by the system of equations

$$G_\alpha(x_+) = G_\alpha(x_-) \quad (4.17)$$

$$x_+ + (q-1)x_- = \eta \quad (4.18)$$

This solution is shown in Fig. 4.6.

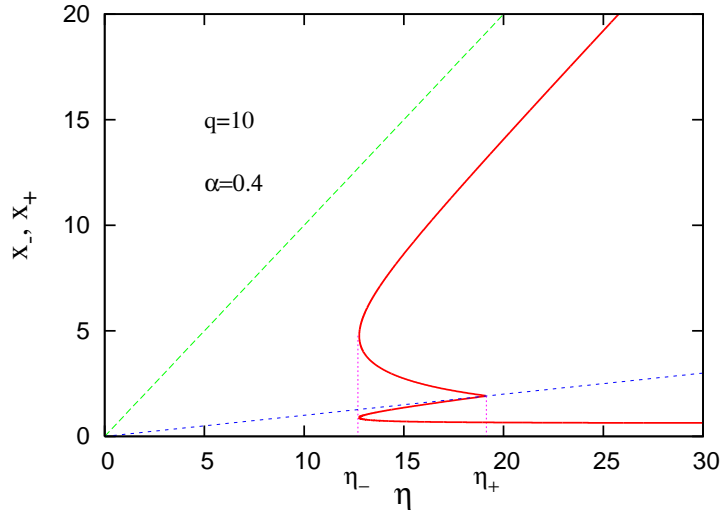


Figure 4.6: Solutions x_\pm as a function of η for $q = 10$ and $\alpha = 0.4$. The dashed line $x = \eta/q$ separating the two curves is the symmetric solution.

Actually, of the two asymmetric solutions the one with x_+ decreasing with η is clearly unphysical as this would have a connected component with an average degree $\langle k \rangle_\sigma = x_+/(1+\alpha)$ which decreases with the rate η with which links are formed. As in ref. [90], it is easy to see that only solutions with x_+ increasing in η are stable. Indeed, regarding η and x_- as functions of x_+ in Eq. (4.18) we find

$$\frac{d\eta}{dx_+} = 1 + (q-1)\frac{dx_-}{dx_+} = \frac{G'_\alpha(x_-) + (q-1)G'_\alpha(x_+)}{G'_\alpha(x_-)}.$$

Consider perturbations of the form $x_\sigma = x_+ + \epsilon$ for the dense component and $x_\sigma = x_- - \epsilon/(q-1)$ for the others. Then by a derivation analogous to that leading to Eq. (4.15), we find

$$\dot{\epsilon} = -\frac{\nu}{q} [G'_\alpha(x_-) + (q-1)G'_\alpha(x_+)] \epsilon = -\frac{\nu}{q} G'_\alpha(x_-) \frac{d\eta}{dx_+} \epsilon.$$

Given that $G'_\alpha(x_-) > 0$, this implies that on solutions with x_+ decreasing with η , the perturbation ϵ grows unboundedly.

The asymmetric solution ceases to exist for $\eta < \eta_-^3$. In the region $\eta \in [\eta_-, \eta_+]$ both the symmetric and the asymmetric solutions co-exist. The coexistence region, in the α, η plane is reported in Fig. 4.8.

The practical relevance of the results derived so far is best discussed introducing an order parameter

$$m = \frac{x_+ - x_-}{\eta} \quad (4.19)$$

which is the difference in the density of the dense and diluted components. This vanishes in the symmetric phase and is non-zero in the asymmetric one. In Fig. 4.7 where we report the behavior of the average degree of the network

$$\langle k \rangle = \sum_{k,\sigma} n_{k,\sigma} k = \frac{\eta}{1+\alpha} \frac{1+(q-1)m^2}{q}. \quad (4.20)$$

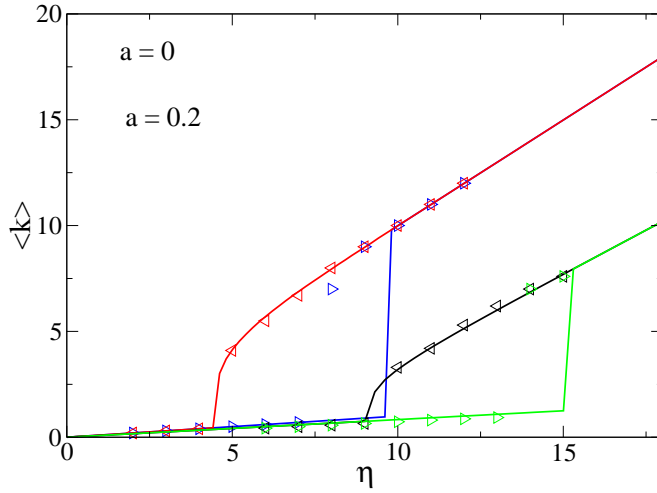


Figure 4.7: Mean degree $\langle k \rangle$ as a function of η/λ for a system with $q = 10$ colors, for $\alpha = 0$ and 0.2 , simulations are for systems of 1000 nodes.

Fig. 4.7 shows that as η sweeps through the coexistence region the system undergoes an hysteresis loop: the degree jumps from low to high values at η_+ as η is increased whereas when η decreases from large values, the network collapses back to the symmetric phase when η_- is crossed. In the case $\alpha = 0$ [90], the symmetric phase is characterized by sparse networks, with a vanishing giant

³We note, in passing, that the condition $d\eta/dx_+ = 0$ provides an equation which allows to determine η_- .

component. This is no more true when $0 < \alpha < 1$, specially close to η_+ ⁴. Numerical simulations fully confirm this picture, even though for finite systems the symmetric (asymmetric) phase is meta-stable close to η_+ (η_-) and therefore the transition occurs for lower (larger) values of η .

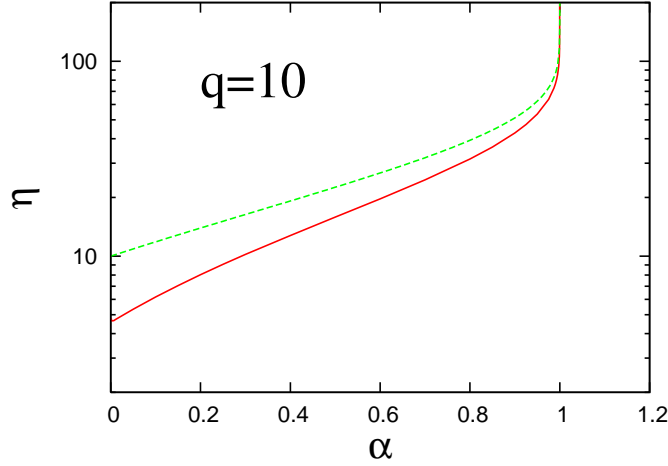


Figure 4.8: Phase diagram for $q = 10$. The symmetric phase extends below and to the right of the (full) line $\eta_-(\alpha)$ whereas above the (dashed) line $\eta_+(\alpha)$ only the asymmetric phase is stable. The coexistence region, where both phases are stable, is delimited by the two curves.

4.3.3 The critical region: $\alpha \approx 1$

The behavior of the order parameter m on the critical lines which confine the coexistence region is shown in Fig. 4.9. This shows that the transition is continuous but with a peculiar critical behavior. For $\alpha = 1 - \epsilon$ we can approximate

$$\begin{aligned} G_\alpha(x) &\simeq (1 - \epsilon) \int_0^x du \left[1 - \epsilon \log \left(1 - \frac{u}{x} \right) \right] e^{-u} \\ &= (1 - \epsilon)(1 - e^{-x} + \epsilon(E_i(x) - \gamma)) \end{aligned}$$

where $E_i(x)$ is the exponential integral function, and for $\epsilon \rightarrow 0$ we have $x_\pm \rightarrow \infty$ and $E_i(x) \simeq \frac{e^x}{x}$. Hence

$$G_\alpha \simeq (1 - \epsilon)(1 - e^{-x} + \epsilon/x)$$

Exactly at the critical point $\eta = qx_0$, where x_0 is such that $G'_\alpha(x_0) = 0$. We have $\epsilon \frac{e^{x_0}}{x_0^2} = 1$ from which we can get $x_0 \simeq -\log \epsilon + 2 \log |\log \epsilon|$.

⁴Indeed the condition for the presence of a giant component is $\langle k(k-1) \rangle_\sigma > \langle k \rangle_\sigma$ which, by a straightforward calculation, reads $\eta \geq q(1 + \alpha/2)$. At the critical point $\eta_+ = qx_0(\alpha)$ this reads $x_0(\alpha) \geq 1 + \alpha/2$ which holds true for all $\alpha > 0$.

From $G_\alpha(x_+) = G_\alpha(x_-)$ and the expressions of x_- and x_+ with respect to x_0 and m , we finally have

$$m \sim c/x_0(\alpha) \sim |\log(1 - \alpha)|^{-1}. \quad (4.21)$$

where c is given self-consistently by:

$$c = e^c(1 - e^{-qc})/q$$

In terms of the usual description of critical phenomena, where $m \sim |1 - \alpha|^\beta$, this model is consistent with an exponent $\beta = 0^+$. Indeed, the singular behavior of m is very close to that of a first order phase transition.

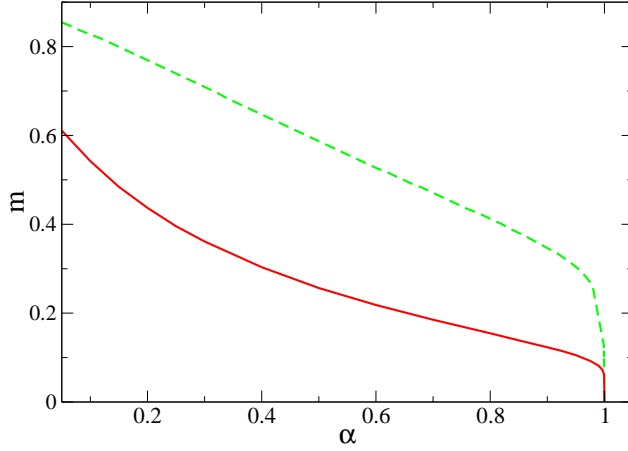


Figure 4.9: Order parameter m on the boundary of the coexistence region η_- (full line) and η_+ (dashed line) as a function of α for $q = 10$.

4.3.4 Conclusions

The introduction of node volatility, in the simple model discussed here, makes the transition from a symmetric (disordered) diluted network to an asymmetric (ordered) dense network less sharp. Indeed when node volatility dominates ($\alpha > 1$) the transition disappears altogether, and the symmetric (disordered) state prevails. The phenomenology is strongly reminiscent of that of first order phase transitions (e.g. liquid-gas or paramagnet-ferromagnet) though the critical behavior is highly non-trivial.

The virtue of the particular model studied is that it allows a detailed analytic approach which allows one to gain insight on all aspects of its behavior. This

model belongs to a general class of models which embody a generic feedback mechanism between the nodes and the network they are embedded in, which can be expressed in the following way: while the network promotes similarity or proximity between nodes, proximity or similarity enhances link formation. This feedback allows the system to cope with environmental volatility, which acts removing links at a constant rate. Interestingly, the emergence of an “ordered” state plays a key role in this evolutionary struggle. We believe the general

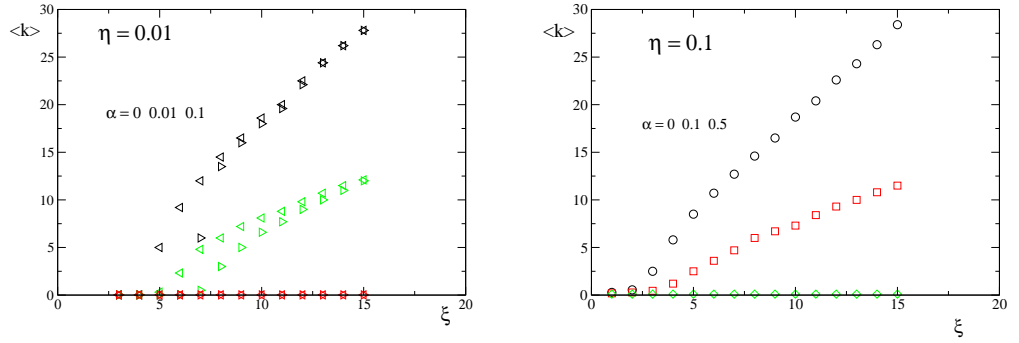


Figure 4.10: Mean degree as a function of the rate ξ of formation of links with neighbours of neighbours, for $N = 1000$ ($\lambda = 1$). Top: $\eta = 0.01$, Bottom: $\eta = 0.1$.

findings discussed here will extend to the general class of models of Ref. [90]. In particular, we expect the phase transition to be blurred by the effect of node volatility and to disappear when the latter exceed a particular threshold.

Actually, Fig. 4.10 shows that this is the case even for the model of Ref. [89]. This is a model where link creation occurs either by long distance search at rate η (as in the model discussed here) or through local search (on second neighbours) at rate ξ . Again links decay at unit rate. We refer the interested reader to Ref. [89] for further details, for the present discussion let it suffice to say that the effects of (link) volatility are contrasted by the creation of a dense network with small-world features (a somewhat similar model with node volatility has been considered in Ref. [88]). Fig. 4.10 shows that the effects of node volatility are very strong. Indeed, even a very small α reduces considerably the size of the coexistence region and the value α_c at which the latter disappears is also relatively small.

These results suggest that node volatility is indeed a relevant effect in the co-evolution of socio-economic networks, as it may affect in dramatic ways the ability of the system to reach a dense and/or coordinated state.

Chapter 5

Conclusions

In this thesis each chapter is mostly independent and self-contained. Each of them is in fact referring to a specific phenomenology. Is there something in common among phase transitions in physical materials, congestion phenomena in informatic systems and the evolution of social networks?

I studied all of them using interacting dynamical models on heterogeneous graphs with the use of statistical mechanics techniques and concepts. The wide applications of lattice models from statistical mechanics has its main reason in the fact that network based representations are widely used to describe many real complex systems.

This thesis is about how a certain degree of heterogeneity in the underlying topology can affect the collective statistical behavior of a system. It is not intended as a review on it, rather I showed practically that this question emerges spontaneously and gives insights in specific instances.

In the first chapter I showed how to give a statistical mechanics perspective to the problem of congestion in large communication networked system. This comes out from a natural extension of queuing network theory to large systems and to congested states. In order to do it, the use of statistical networks' ensembles and the concept of congestion as a phase transition were really important. In this chapter we have a specific example of the fact that the collective behavior of a system can depend crucially on the underlying structure, e.g. traffic control is ineffective in homogeneous networks.

Usually it is believed that the equilibrium distinctive features of statistical physics systems should depend on the symmetries of the internal degrees of freedom and only on the dimension of the spatial structure. However the results on congestion phenomena suggest that in out of equilibrium systems the collective behavior could depend even on the details of the structure. I showed in the second chapter through a simple model of kinetically constrained spins subjected to a dynamical arrest, how a simple dilution of the underlying graph can change completely the nature of this transition. In the context of mean field models for the dynamical glass transition we can have bootstrap or simple percolation transition on homogeneous or heterogeneous structures, respectively.

Given their general nature, the dependence of the collective properties of simple interacting models on the underlying graph is interesting per se, without referring to a specific phenomenology. In the third chapter, I showed that the equilibrium features of tricritical model systems can change dramatically if the underlying graph has a certain degree of heterogeneity. The usual entropy ratio of the ordered and the disordered phase can invert on some graphs. There is an inverse phase transition, by which tricritical model systems becomes disordered upon cooling. I showed a mechanism that trigger this phenomenon, based on the freezing of sparse subgraphs. If they are crucial for the connectivity, the overall graph of interactions can be disconnected by cooling.

Up to this point I discussed cases in which the behavior of a system is affected by the underlying structure, in particular this last is fixed. But where a given structure of interactions comes from? In social networks the graph itself changes in time with an evolution that can be coupled with the dynamics defined on top of it. In the last chapter we exploited a nice analogy with statistical physics in this context. Models of coevolving social networks show discontinuous transitions between sparse and dense structures, with hysteresis and coexistence phenomena. I showed a mechanism that dump this transition, up to a critical point like in the Van der Waals picture of the liquid-gas transition.

Then, apart from the specific insights that can be obtained from applying statistical mechanics to such specific instances, is there something *more general* that we can get?

In the introduction I gave the examples of epidemic spreading processes and of the Ising model as model systems that show a phase transition whose behavior is affected in a non-trivial way by the heterogeneity of the underlying graph. The critical point of these models scales with the system size in heterogeneous graphs in a way such that large enough systems are always in practice in the non-trivial phase. In the SIS model the nodes of a network can be susceptible (S) or infected (I), respectively. An infected node can infect its neighbors with rate ν . Infected nodes recover from the infection with rate 1. These rules define a dynamical process of spreading that, for a given ν and initial conditions, can end up in a state that can be characterized by the fraction of infected nodes ϕ_I . If $\phi_I = 0$ the spreading of the infection is stopped (this is an absorbing state). For large enough ν we have a final state $\phi_I > 0$, there is a continuous transition whose transition point, within a mean field approximation on random graphs is[8]

$$\nu_c = \frac{\langle k \rangle}{\langle k^2 \rangle}. \quad (5.1)$$

The critical temperature on random graphs[9] of the Ising model is

$$\frac{1}{T_c} = \frac{1}{2} \log\left(\frac{\langle k^2 \rangle}{\langle k^2 \rangle - 2\langle k \rangle}\right). \quad (5.2)$$

These equations show that the collective behavior of such model systems can be ruled by the tails of the degree distribution of the underlying graph.

This is not the case in general. Here, in the context of the queuing network theory and of tricritical spin models I showed an analogous parallel. For these models, that show continuous and *discontinuous* transitions, there is a rather different behavior. Different parts of the same system can be in different phases. In fact the mean field analysis on heterogenous graphs of both models is characterized by a cut-off degree such that only nodes whose degree is higher than it are in the non-trivial phase, congested or magnetized, respectively. In the range of parameters such that the transition is continuous, the behavior of the system is still ruled by high degree nodes. But, when the transition is discontinuous, their behavior is ruled by the central body of the degree distribution. In queuing network theory on random graphs, the critical inserction rate of packets per node p_c scales according to:

$$p_c \simeq \begin{cases} \frac{\mu \langle k \rangle / k_M}{\mu + (1-\mu) \langle k \rangle / k_M} & \text{continuous, low traffic control.} \\ \mu k_m / \langle k \rangle & \text{discontinuous, high traffic control.} \end{cases} \quad (5.3)$$

Where k_m and k_M are the minimum and the maximum of the degree distribution. The chemical potential at the transition point Δ_c of the Blume-Capel model on a random graph scales, within a mean field approximation, according to:

$$\Delta_c \simeq \begin{cases} 2T \log(\beta \frac{\langle k^2 \rangle}{\langle k \rangle} - 1) & \text{for the continuous branch.} \\ \langle k \rangle & \text{around } T=0. \end{cases} \quad (5.4)$$

This difference in turn can trigger highly non-trivial phenomena, like inverse phase transitions in tricritical spin models or mixed phase transitions in the queuing networks. It should be interesting to test the general validity of this picture.

Acknowledgements

I would like to thank the SISSA and ICTP institutions for their stimulating environments. I acknowledge G.Mussardo for the idea and concrete realization of this phd curriculum in statistical physics. Among the many interesting people that I met during this period, I would like to thank M.Sellitto, J.J.Arenzon, G.Bianconi and D.Helbing. I thank M.Barthelemy that accepted to be the external referees of this thesis. I thank all my colleagues and friends in SISSA and ICTP, in particular Serena, Fabio, Raffo, Elena, Pier and Jacopo . I would like to thank my boss Matteo that was always showing me the “right spirit” in doing this job. A special thank to Luca Dall’Asta for his really valuable collaboration and patience all along this period. I thank A.Barato and L.Leuzzi for partial reviews of this manuscript.

Un abbraccio ed un saluto alla mia famiglia, in particolare a Ludovica, un abbraccio ed un saluto a tutti gli amici e alla “famiglia” di Trieste ed infine, un bacio a Maya!

Bibliography

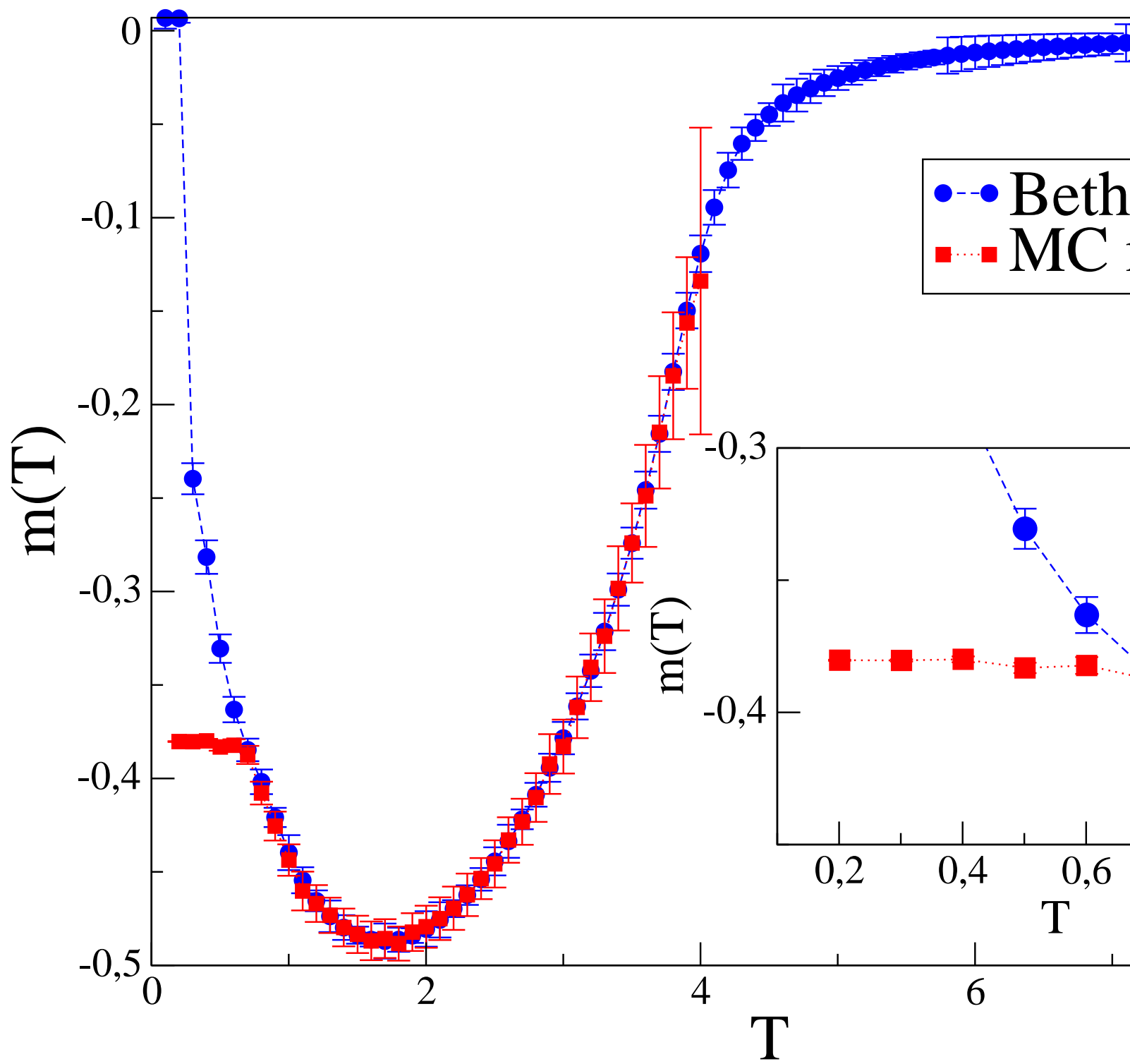
- [1] G.Gallavotti, *Enciclopedia delle scienze fisiche*, in “meccanica statistica”, ed. Treccani (2001)
- [2] K.Sneppen and G.Zocchi, *Physics in molecular biology* Cambridge University Press (2005)
- [3] R.N.Mantegna and H.E.Stanley, *An introduction to econophysics* Cambridge University Press (1999)
- [4] S.Mertens, *Computational complexity for physicists* in comp. in science and engeneering, vol 4, 3, (2002)
- [5] D.Helbing, Rev. Mod. Phys. 73, 10671141 (2001)
- [6] R. Albert, AL Barabsi, Rev. Mod. Phys. 74, 4797 (2002)
- [7] SN Dorogovtsev, AV Goltsev, JFF Mendes, Rev. Mod. Phys. 80, 12751335 (2008)
A. Barrat, M. Barthelemy, A. Vespignani, *Dynamical Processes on Complex Networks*, Cambridge University Press, 2008.
- [8] R.Pastor-Satorras and A.Vespignani, Phys. Rev. Lett. 86, 32003203 (2001)
- [9] M. Leone, A. Vzquez, A. Vespignani and R. Zecchina, Eur. Phys. Jour. B, Vol 28, N. 2, 191-197 (2002)
- [10] <http://en.wikipedia.org/wiki/Category:Internet>
- [11] A.Vespignani and R.Pastor-Satorras, *Evolution and structure of the Internet: a statistical physicists approach*, Cambridge university press (2004)
- [12] R.D.Smith, arXiv:0807.3374v3 (2008)
- [13] G.Bolch, S.Greiner, H. de Meir and K.S.Trivedi, *queuing networks and markov chains*, NY Wiley (2006)

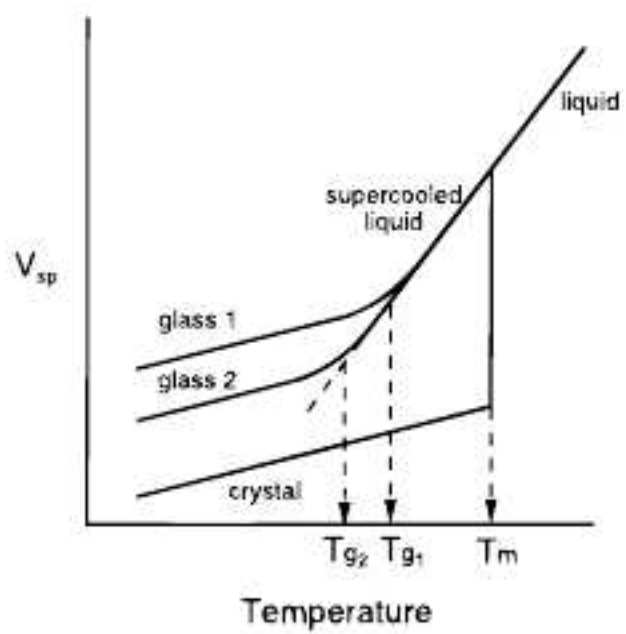
- [14] D.De Martino, L.Dall'Asta, G.Bianconi and M.Marsili, *Phys. Rev. E* **79** 015101 (2009); D.De Martino, L.Dall'Asta, G.Bianconi and M.Marsili, *J. Stat. Mech.* P08023 (2009); D.De Martino, *Proc. IEEE COMPENG010* (2010)
- [15] <http://www.caida.org/home/>
- [16] D.Krioukov, F.Chung, K.C.Claffy, M.Fomenko, A.Vespignani and W.Willinger, *The workshop on Internet topology report*, ACM SIGCOMM ComComm. Rev. **37**:1 69-73 (2007)
- [17] W.Leland,M.Taqqu,W.Willinger and D.Wilson, *Proc. ACM SIGCOMM'93* 183-193 (1993); K.Park and W.Willinger *Self similar network traffic and performance evaluation* chapt. 1, NY: Wiley (2000)
- [18] W.Willinger et al., *ACM SIGCOMM, ComComm. Rev.* **25**:4 100-113 (1995)
- [19] J.R.Jackson, *OPERATIONS RESEARCH* Vol. 5, No. 4, pp. 518-521 (1957)
- [20] M.Evans and T.Hanney, *J.Phys.A: Math.Gen.* **38** R195 (2005)
- [21] M. A. de Menezes and A.-L. Barabasi, *Phys. Rev. Lett.*, **92** 028701 (2004); Z. Eisler, J. Kertesz, S.-H. Yook and A.-L. Barabasi, *Europhys. Lett.* **69**, 664670 (2005); J. Duch and A. Arenas, *Phys. Rev. Lett.* **96**, 218702 (2006); S. Meloni, J. Gomez-Gardenes, V. Latora, and Y. Moreno, *Phys. Rev. Lett.* **100** 208701 (2008).
- [22] A.Arenas, A.Diaz-Guilera, R.Guimera, *Phys. Rev. Lett.* **86** 3196 (2001)
- [23] P.Echenique, J.Gomez-Gardenes and Y.Moreno, *Europhys.Lett.* **71** 325 (2005)
- [24] B.Bollobas, *Random graphs*, Cambridge university press (2001)
- [25] B. A. Huberman, and R. M. Lukose, *Science* **277**(5325), 535 (1997).
- [26] G.Biroli, L.Berthier, *Glasses and aging: a statistical mechanics perspective*, Enciclopedia of complexity and Systems science, Springer (2008)
- [27] A.Cavagna, *Phys. Rep.* vol. 476 (2009)
- [28] M.D.Ediger, C.A. Angell and S.R.Nagel *J.Phys.Chem* **100** 13200 (1996)
- [29] A.W.Kauzmann, *Chem. Rev.* **43**, 219 (1948)
- [30] R.Richert and C.A.Angell, *J.Chem.Phys* **108** 21 (1998)
- [31] E. R. Weeks, J. C. Crocker, A. C. Levitt, A. Schofield and D. A. Weitz, *Science* **287**, 627 (2000)

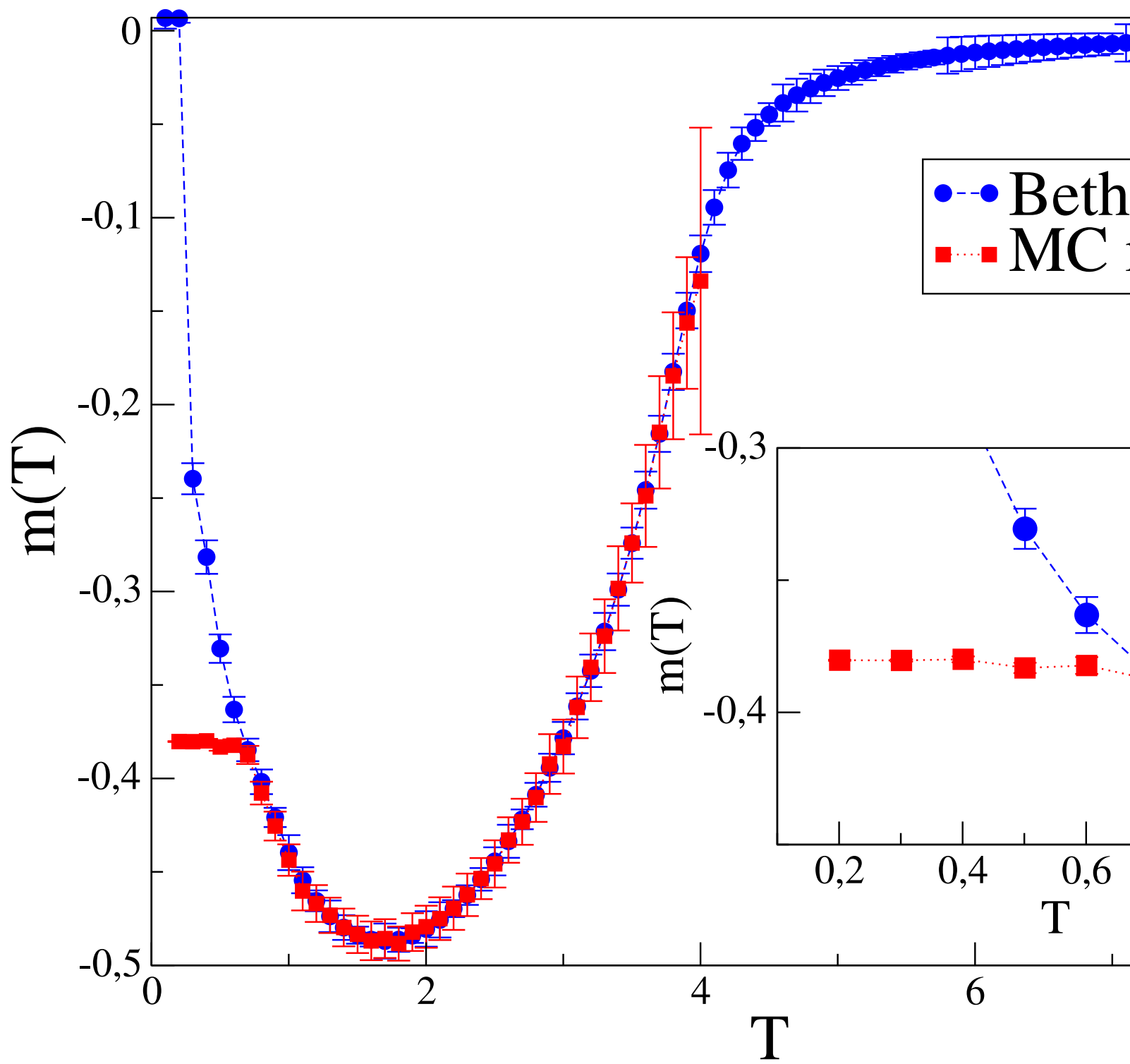
- [32] C.Donati, S.C.Glotzer, P.H.Poole, Phys. Rev. Lett **82** 25 (1999)
- [33] E.Zaccarelli, J.Phys.: cond.mat. **19** (2007)
- [34] Coniglio, A., Fierro, A., Herrmann, H. J., Nicodemi, M. (eds) Unifying Concepts in Granular Media and Glasses (Elsevier, Amsterdam, 2004)
- [35] H.M.Jaeger, S.R.Nagel and R.P.Behringer Rev.Mod.Phys. 68 (1996)
- [36] P. Richard, M. Nicodemi, R. Delannay, P. Ribire and D. Bideau, Nature Materials 4, 121 - 128 (2005)
- [37] P.De Gennes, *Scaling concepts in polymer physics*, Cornell university press (1979)
- [38] D.Stauffer, A.Aharony, *Introduction to percolation theory*, Taylor and Francis (1992)
- [39] T. Abete, A. de Candia, E. Del Gado, A. Fierro, and A. Coniglio Phys. Rev. Lett. 98, 088301 (2007)
- [40] K.Kim, K.Miyazaki and S.Saito, Europhysics lett. **88**, 3, (2009)
V.Krakoviak, Phy.rev.lett **94** 065703 (2005)
- [41] M.Goldstein J.Chem.Phys. **51** 3728, (1969)
- [42] R.Reichmann and P.Charbonneau, JSTAT P05013 (2005)
- [43] W.Gotze, J.Phys.: cond.mat 11 A1 (1999)
- [44] T.Castellani and A.Cavagna JSTAT P05012 (2005)
- [45] M Mezard, G Parisi and M Virasoro *Spin glass theory and beyond*, World Scientific Lecture Notes in Physics (1986)
- [46] M Mezard, G Parisi Arxiv preprint arXiv:0910.2838 (2009)
- [47] G Parisi, F Zamponi Reviews of Modern Physics (2010)
- [48] F. Ritort, P. Sollich, Adv. Phys. , Vol. 52, Issue 4 (2003)
- [49] GH Fredrickson, HC Andersen, Phys.Rev.Lett. **53** (1984)
- [50] M Sellitto, G Biroli, C Toninelli, Europhys. Lett. 69 496 (2005)
- [51] J Chalupa , P L Leath and G R Reich, J. Phys. C: Solid State Phys. 12 (1979)
- [52] N.Branco Jour. of Stat. Phys. Vol. 70, N. 3-4, 1035-1044 (1993)
- [53] J.J.Arenzon, D.De Martino, F.Caccioli and M.sellitto, *in preparation*
- [54] W.Kob, HC. Andersen, Phys.Rev. E 48 (1993)

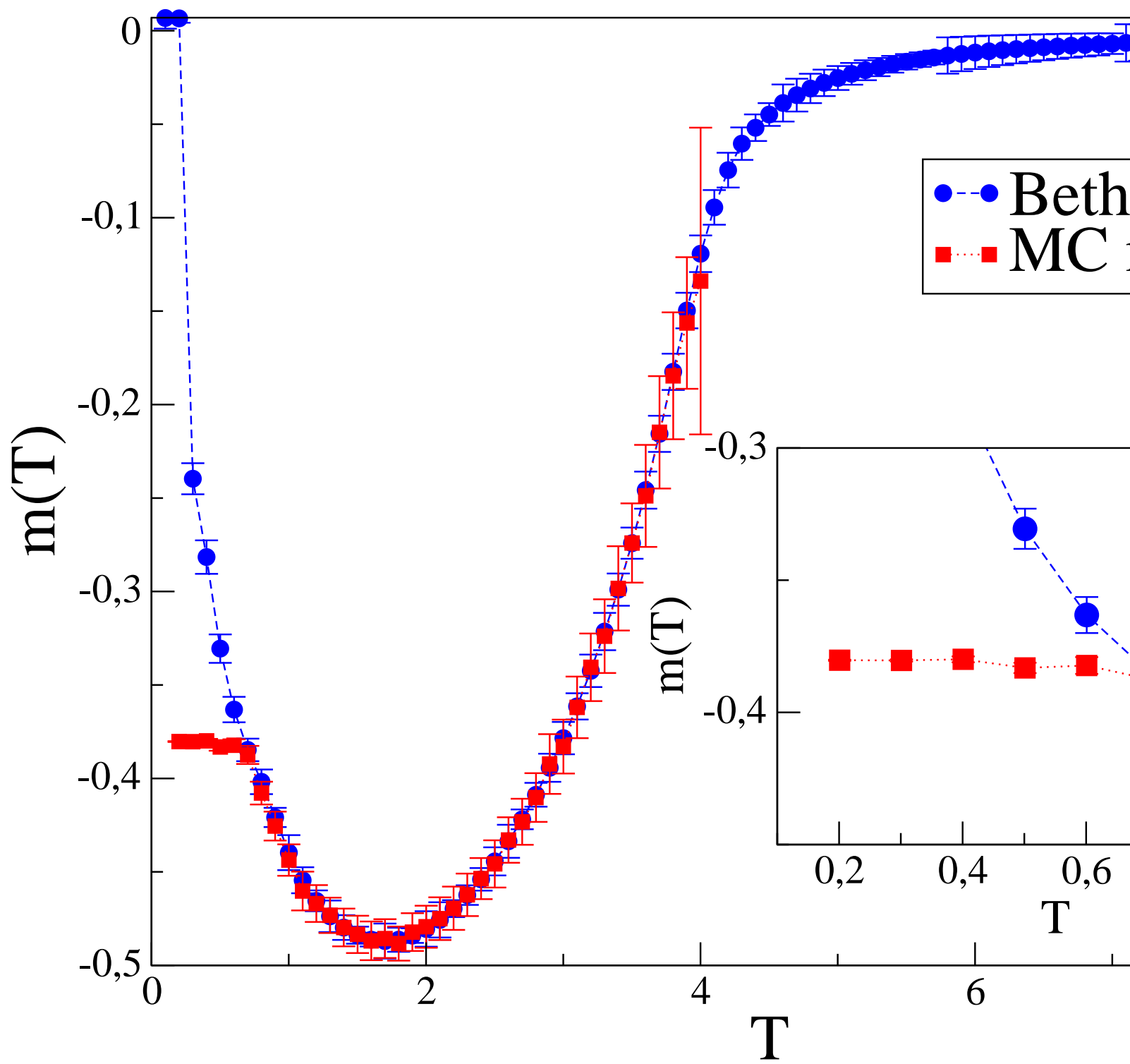
- [55] C.Toninelli and G.Biroli J.Stat.Phys., vol 126 no. 4 (2007)
- [56] FH Stillinger, PG Debenedetti, TM Truskett J. Phys. Chem. B, 2001
- [57] N.Schupper and N.M.Shnerb, Phys. Rev. E 72, 046107 (2005)
- [58] T Narayanan, A Kumar, Physics Reports, 249 (3). pp. 135-218 (1994)
- [59] C.S.Hudson Z.Phy.Chem.47, 113 (1905)
- [60] J.Hirschfelder,D.Stevenson and H.Eyring J.Chem.Phys. 5 (1937)
- [61] J.C.Wheeler J.Chem.Phy. 62,433 (1975)
- [62] G.Tammann Kristallisieren und schmelzen 26-46 (1903)
- [63] S Rastogi, GWH Hohne, A Kellers, Macromolecules, 32 (26) (1999)
- [64] M. Blume Phys. Rev. 141, 517524 (1966)
- [65] J.Park and M.E.J.Newmann, Phys. Rev. E 70, 066117 (2004)
J.D.Noh, Phys. Rev. E 76, 026116 (2007)
- [66] A.Crisanti and L.Leuzzi, Phys. Rev. Lett. 95, 087201 (2005)
- [67] G Bianconi, M Marsili J. Stat. Mech. (2005) P06005
- [68] JP Sethna, KA Dahmen, CR Myers, Nature 410, 242-250 (2001)
- [69] S Sabhapandit, P Shukla, D Dhar,J.Stat.Phys. 98 (2000)
- [70] D.De Martino, S.Bradde, L.Dall'Asta and M.Marsili, *in preparation*
- [71] R.Bruinsma *Phys.Rev B*, vol 30, n 1 (1984)
- [72] P.Ball *Complexus* **1** 190 (2003)
- [73] F.Vega-Redondo *Complex social networks* Cambridge university press (2007)
- [74] H. P. Young *The Journal of Economic Perspectives*, **10**, 105-122, (Spring, 1996)
- [75] Topa, G., Rev. Ec. Studies **68**, 261 (2001).
- [76] M.E.J. Newman, PNAS, vol 101, 5200, (2004)
- [77] J.W.Grossman, Congressum Numerantium, **158** 202-212 (2002)
- [78] M.Girvan and M.E.J. Newman, PNAS, vol 101, 5200, (2004)
- [79] C Castellano, S Fortunato, V Loreto, Rev. Mod. Phys. 81, 591646 (2009)
- [80] M.Granovetter, Am. J. Sociol. **91**, 481 (1985)

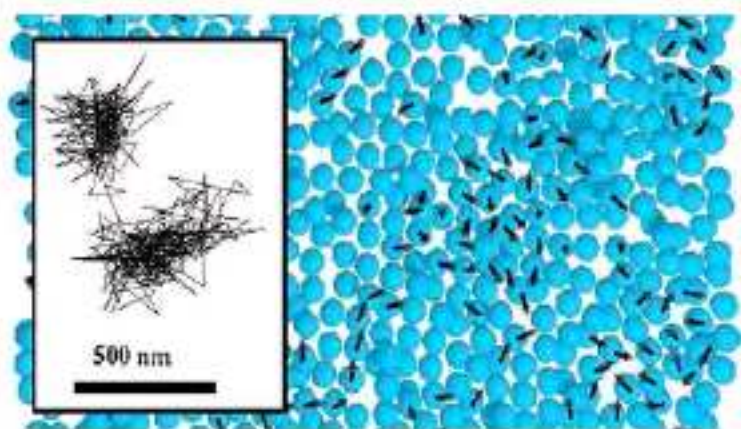
- [81] C. Nardini, B. Kozma, A. Barrat, Rev. Lett. **100**, 158701 (2008); F. Vazquez, V.M. Eguiluz, M. San Miguel, Phys. Rev. Lett. **100**, 108702 (2008).
- [82] T. Gross and B. Blasius, J. R. Soc. Interface **5**, 259 (2008).
- [83] J.Crane, Am. J. Sociol. **96**, 1226 (1991)
- [84] S.Goyal, M.J.van der Leij, J. L. Moraga-Gonzales, J. Polit. Econ. **114**, 403 (2006)
- [85] J.Hagedoorn, Research policy **31**, 477 (2002)
- [86] A.Saxenian, *Regional Advantage: culture and competition in Silicon Valley and route 128* (Harvard university press, Cambridge,MA, 1994)
- [87] Y.Benkler, Yale Law Journal **112** 369 (2002)
- [88] J.Davidsen, H.Ebel and S.Bornholdt, Phy.Rev.Lett. **88**, 12, 128701 (2002)
- [89] M.Marsili, F.Vega-Redondo and F.Slanina, Proc.Natl.Acad.Sci. U.S.A. **101**, 1439 (2004)
- [90] G.Ehrhardt, M.Marsili and F.Vega-Redondo, Phy.Rev. E **74**, 036106 (2006)
- [91] D.De Martino and M.Marsili Eur. jour. phy. B **65** 595-600 (2008)

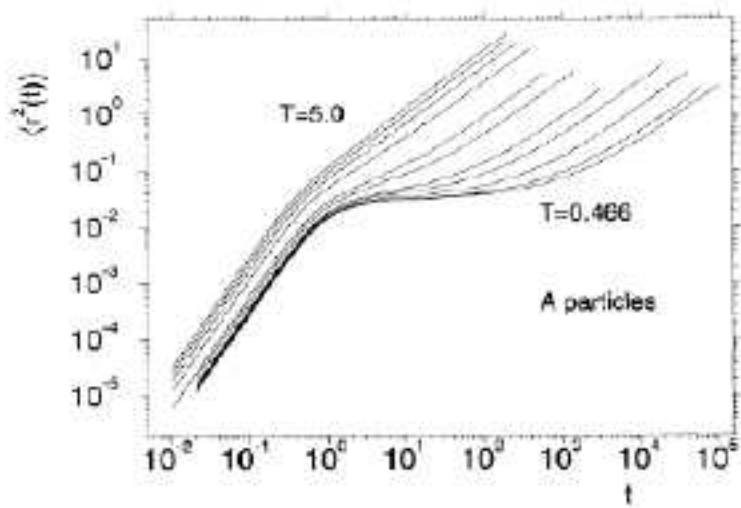


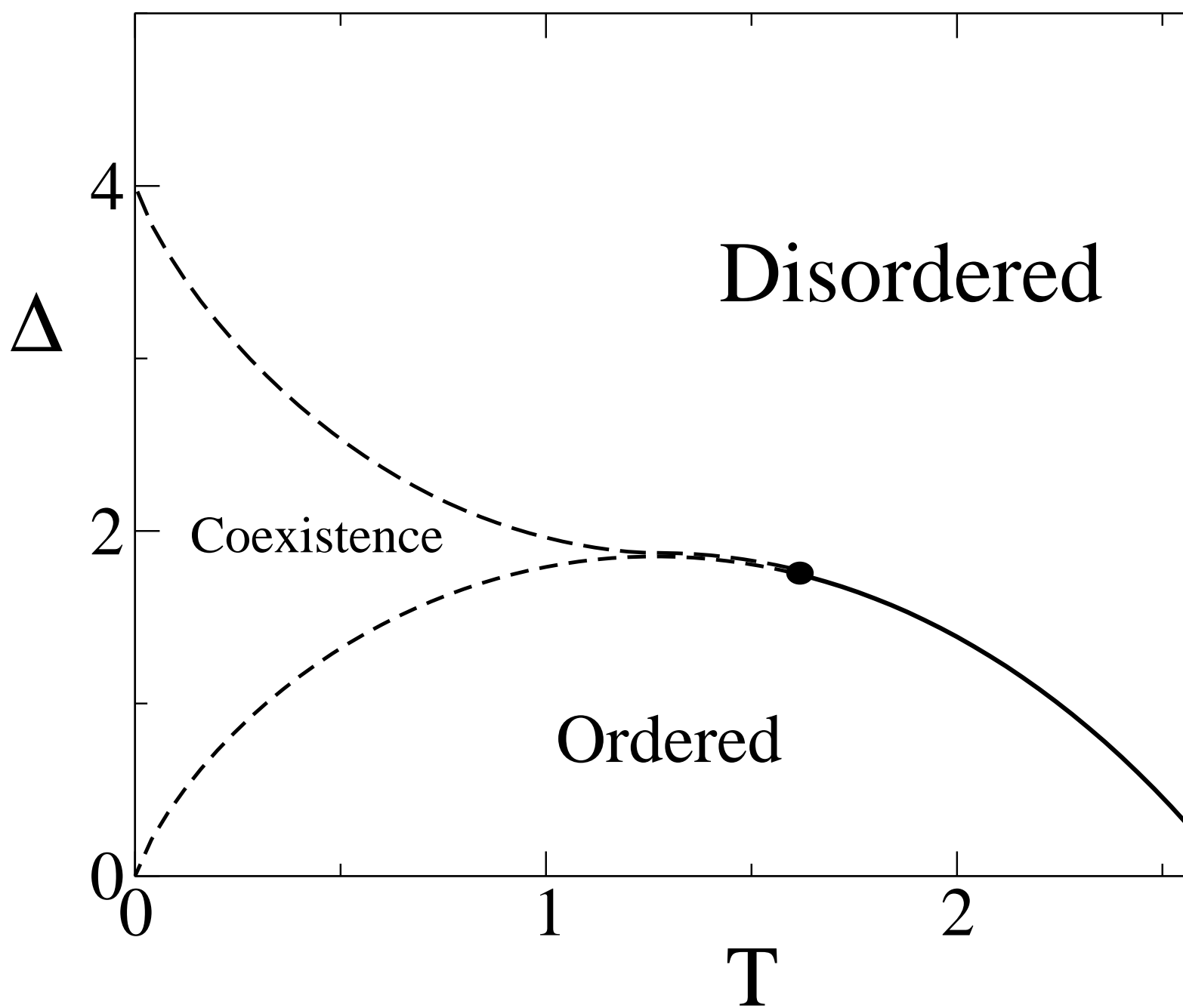


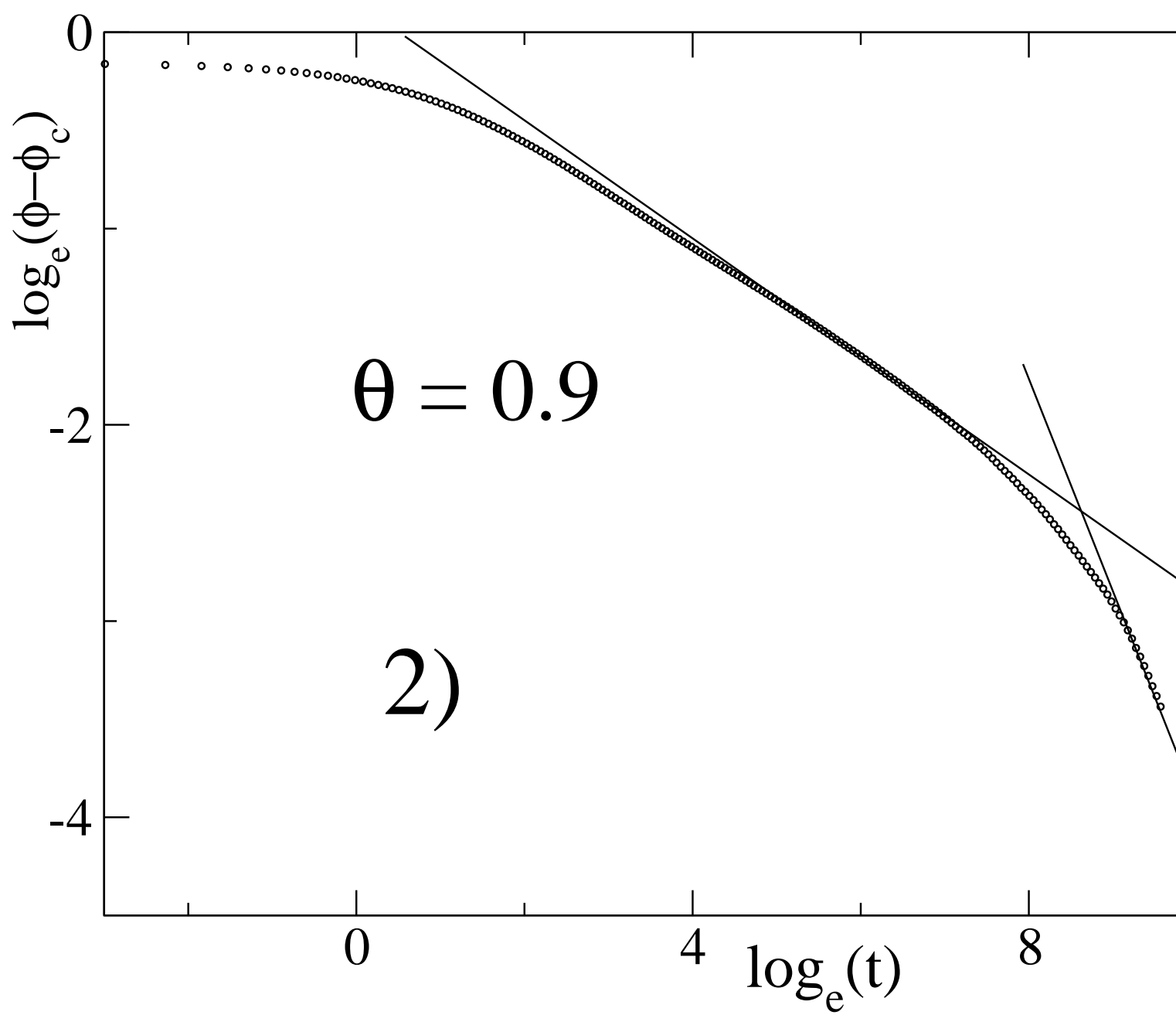


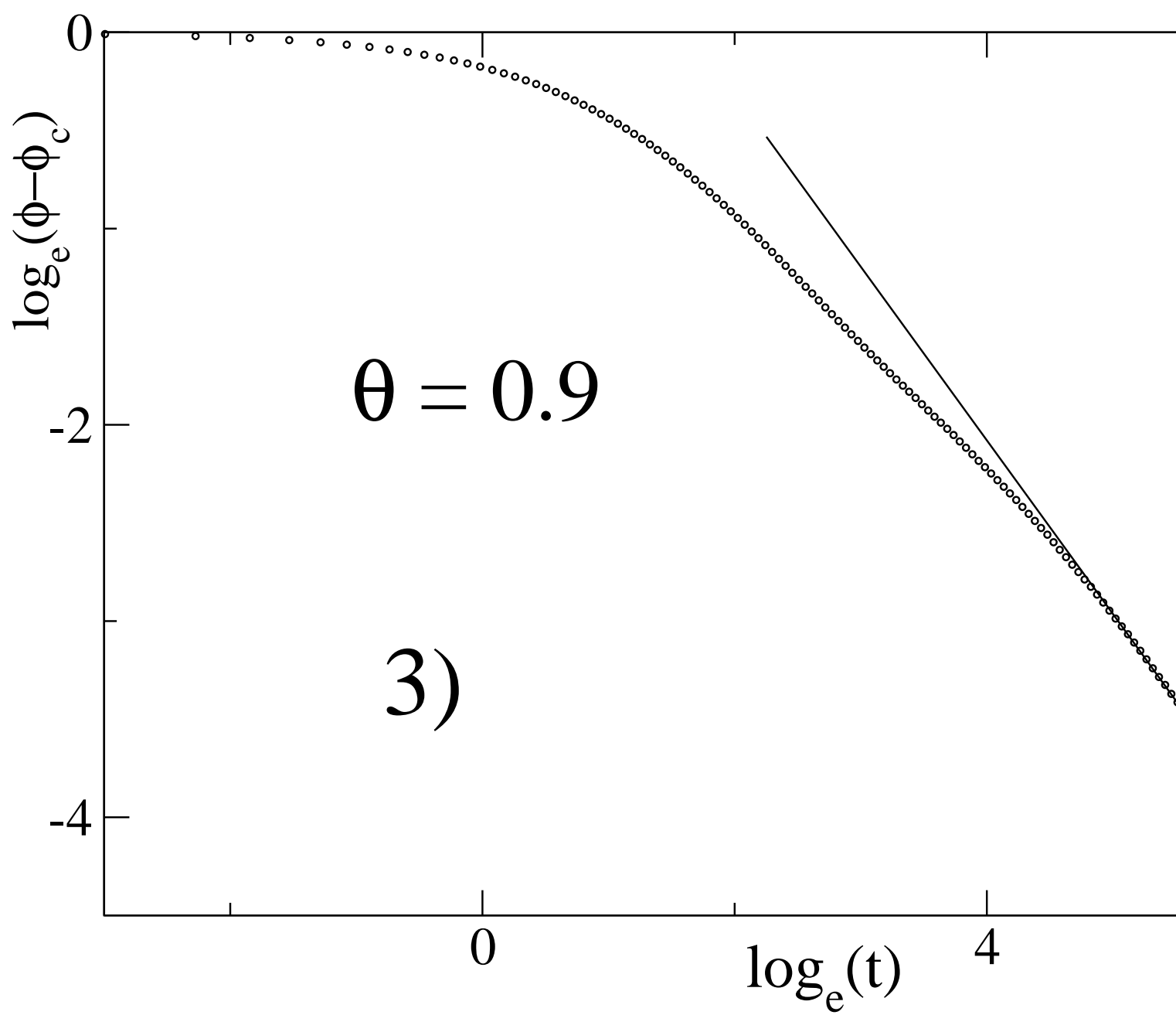


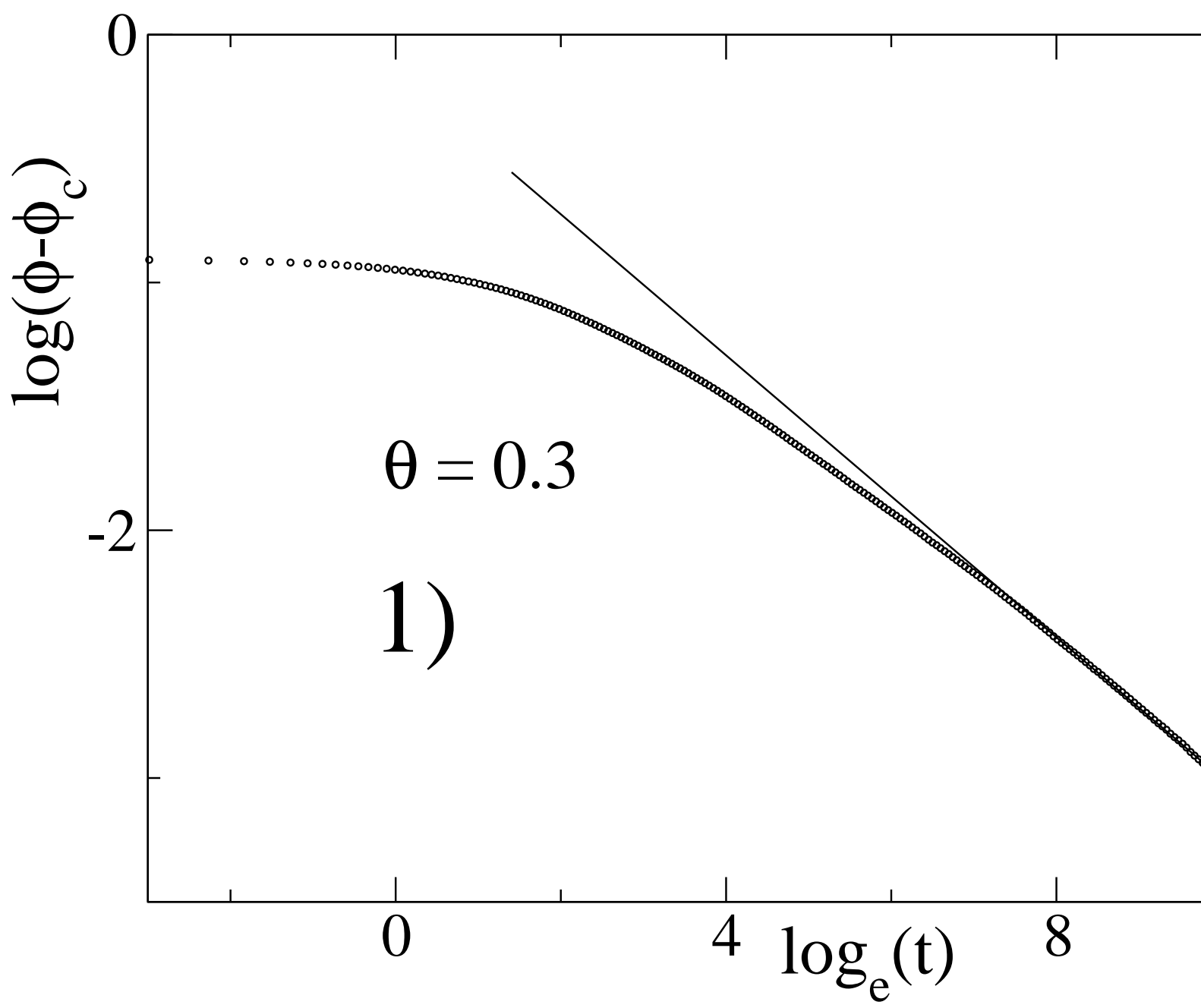


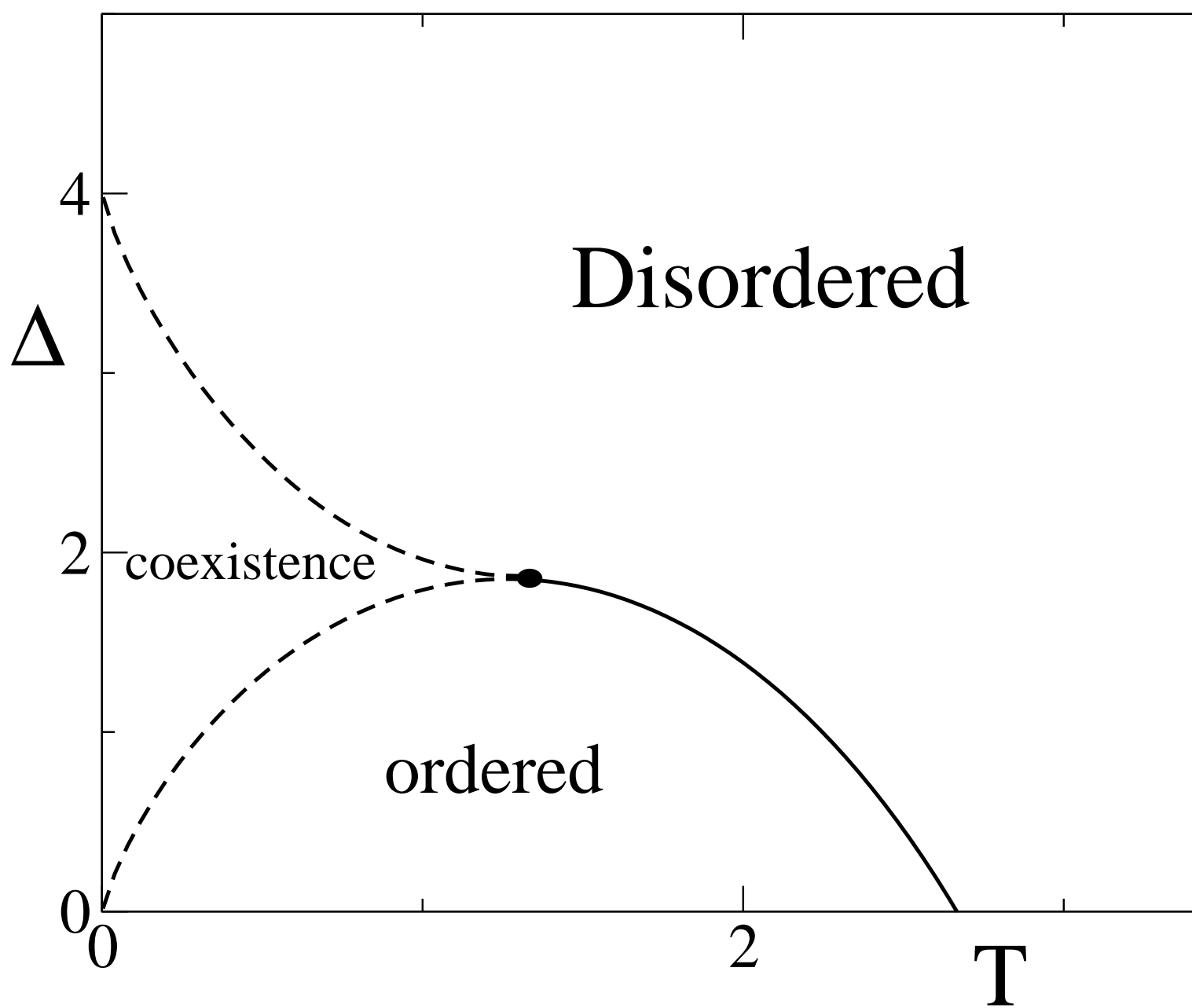


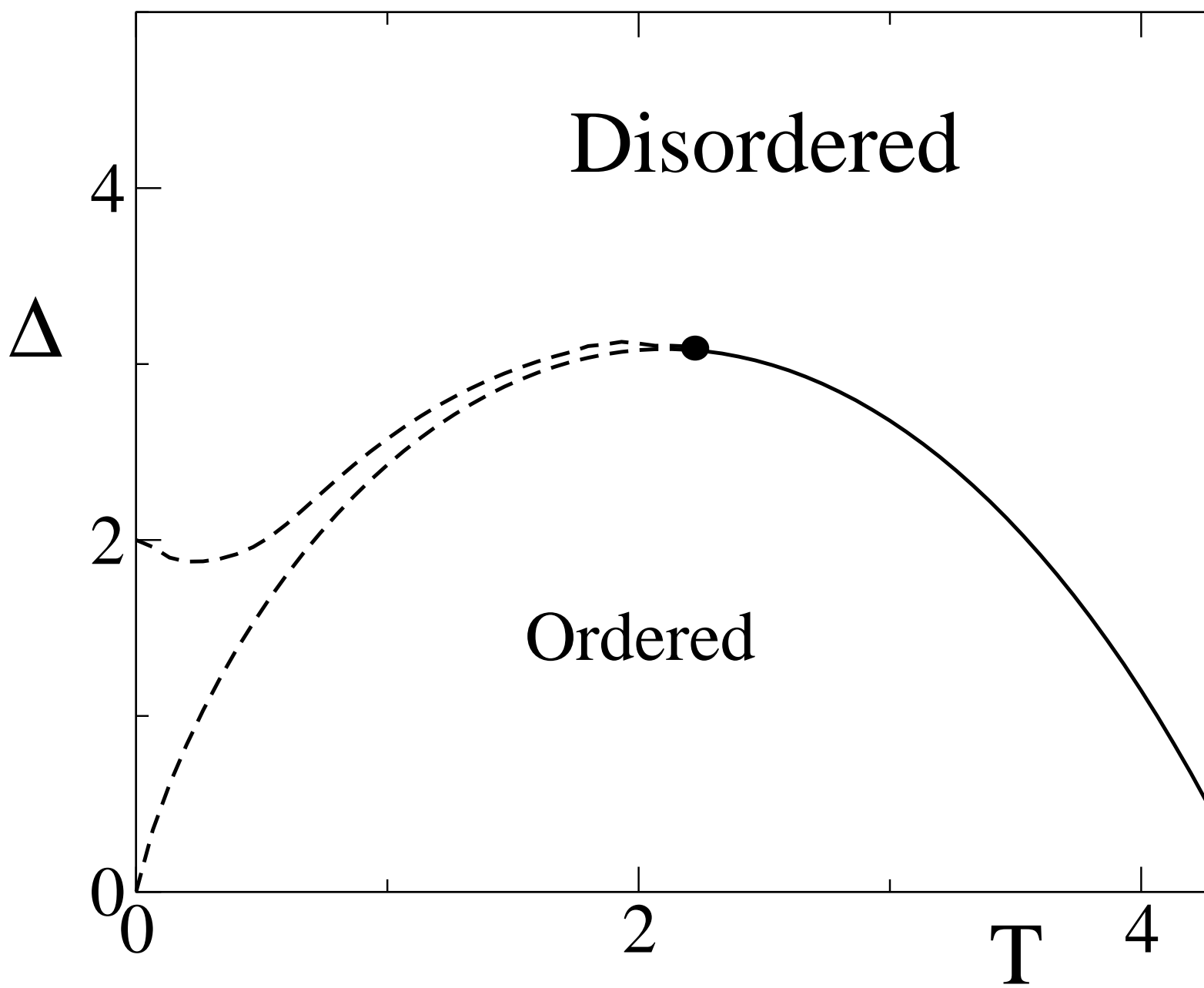


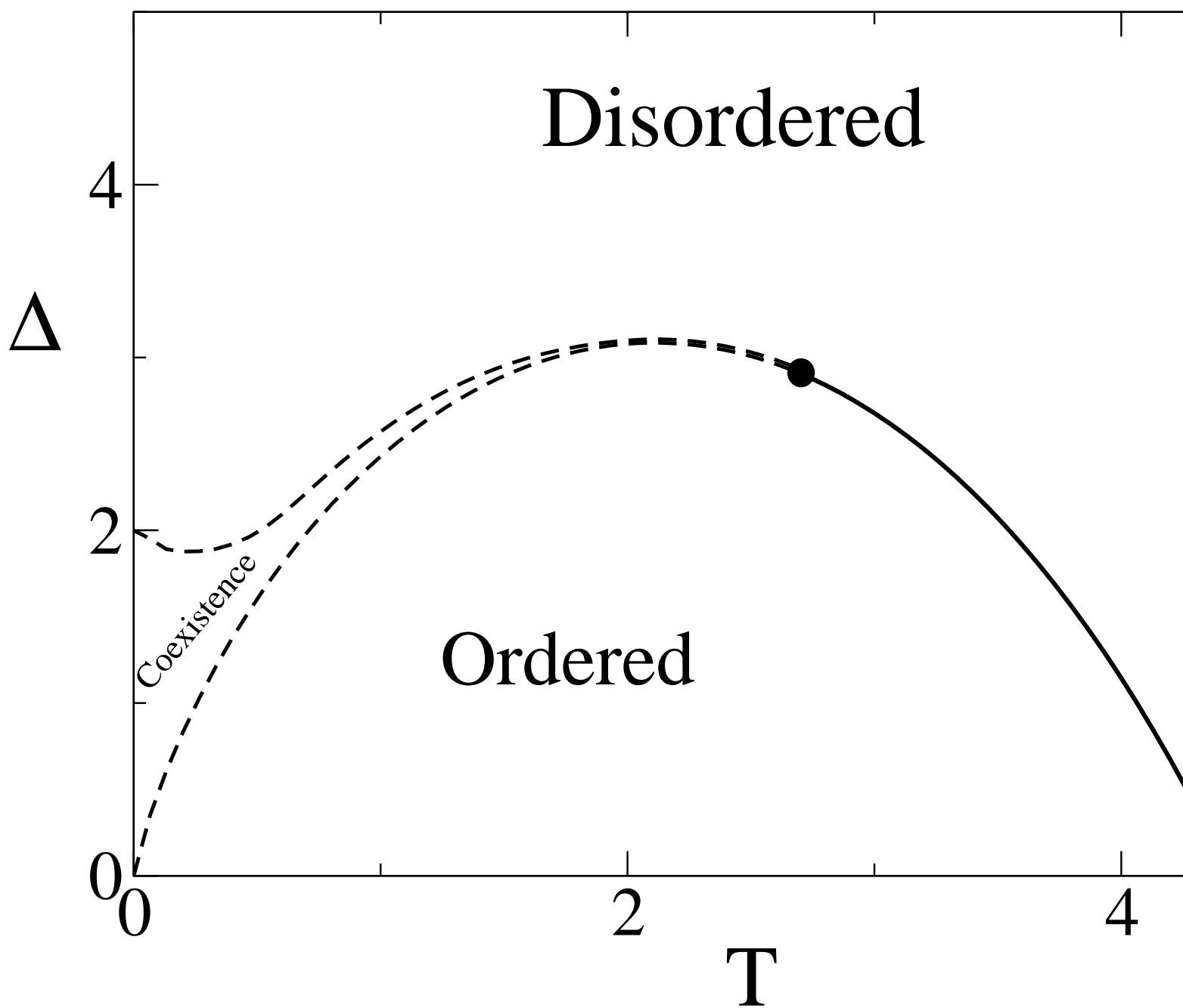


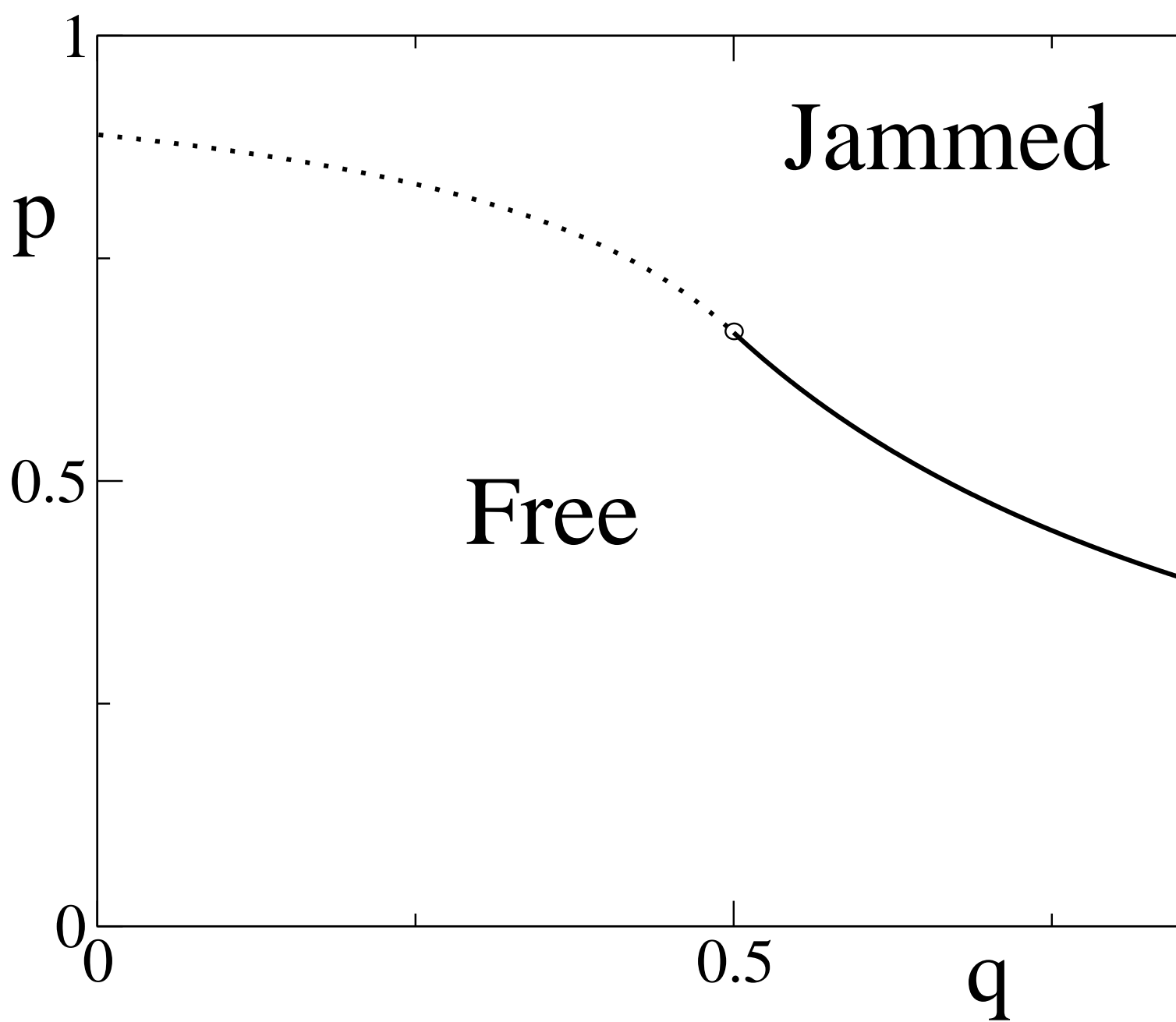


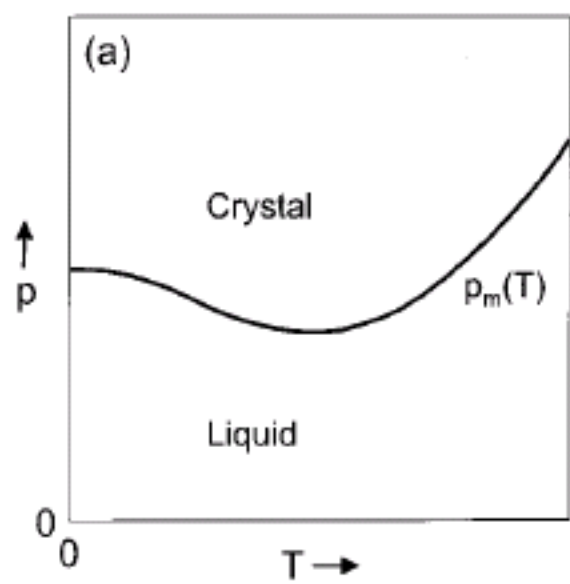


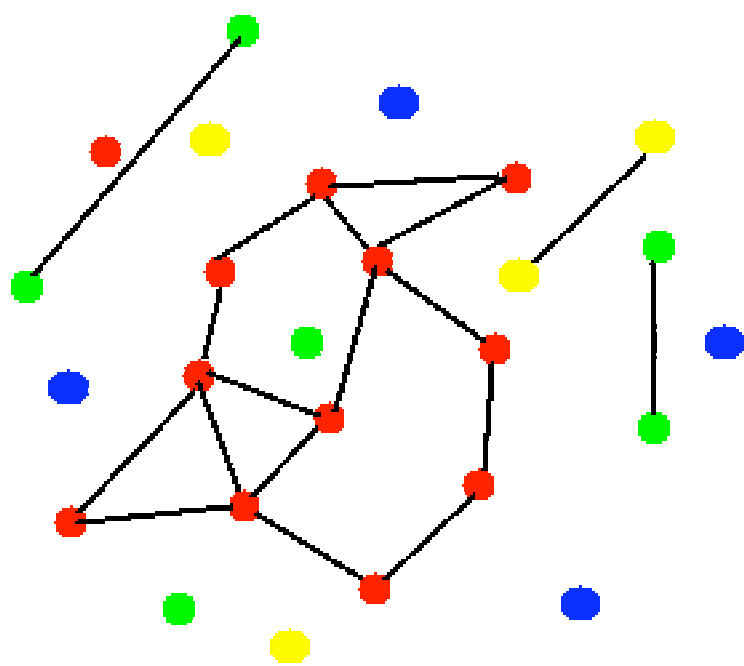












1978-1985

Largest
Group:
40

Authors:
88

Central
Node:
12
(20 links)

1986-1992

Largest
Group:
32

Authors:
201

Central
Nodes:
131, 58,
68, 46, 187
(8 links)

1993-1999

Largest
Group:
138

Authors:
419

Central
Node: 58
(15 links)

2000-2006

Largest
Group:
206

Authors:
776

Central
Node: 343
(18 links)

